MOLECULAR RESPONSES OF *GIARDIA LAMBLIA* TO GAMMA-IRRADIATION

Except where reference is made to the work of others, the work described in this dissertation is my own or was done in collaboration with my advisory committee. This dissertation does not include proprietary or classified information.

_____
Scott Lenaghan

Certificate of Approval:

_____	_____
R. Curtis Bird Professor Pathobiology	Christine A. Sundermann, Chair Professor Biological Sciences
_____	_____
Nannan Liu Associate Professor Entomology	James T. Bradley Mosley Professor Biological Sciences
_____	_____
Michael E. Miller Research Fellow IV AU Research and Instrumentation Facility	Christine C. Dykstra Associate Professor Pathobiology

_____
Joe F. Pittman
Interim Dean
Graduate School

MOLECULAR RESPONSES OF *GIARDIA LAMBLIA* TO GAMMA-IRRADIATION

Scott Lenaghan

A Dissertation

Submitted to

the Graduate Faculty of the

Auburn University

in Partial Fulfillment of the

Requirements for the

Degree of

Doctor of Philosophy

Auburn, Alabama
August 9, 2008

MOLECULAR RESPONSES OF *GIARDIA LAMBLIA* TO GAMMA-IRRADIATION

Scott Lenaghan

_____
Signature of Author

_____
Date of Graduation

DISSERTATION ABSTRACT

MOLECULAR RESPONSES OF *GIARDIA LAMBLIA* TO GAMMA-IRRADIATION

162 pages

Scott Lenaghan

Doctor of Philosophy, August 9, 2008
(B.S., University of Miami, 2000)

Directed by Christine A. Sundermann

Giardia lamblia (*syn intestinalis, syn duodenalis*) is an important human pathogen and the etiological agent of giardiasis, the most common gastrointestinal disease in the world. Since its discovery in 1681, *Giardia* has been extensively studied; however, much of the basic biology of this organism still remains a mystery. The goal of this dissertation was to determine the molecular responses of *Giardia lamblia* trophozoites to gamma (γ)-irradiation, a means of disinfection. Dose-response curves were determined for the *Giardia lamblia* WB isolate trophozoites after γ-irradiation using a Cobalt-60 source. Microscopic observation of trophozoites, along with direct observation of subcultures was used to determine the dosing levels that gave 10, 37 and 90% killing. Dose/Response curves for 4 additional isolates from assemblages A and

B were also generated in order to determine if differing sensitivities to γ-irradiation existed among isolates of importance to human disease. In addition, dose/response curves were generated using methyl methane sulfonate (MMS), an alkylating agent that mimics damage induced by radiation. MMS was used to determine whether it induced a similar alteration in gene expression to γ-irradiation. A high-throughput method for quantitating trophozoite killing by both MMS and γ-irradiation using 96 well-plates was tested against the laborious method of manually counting viable cells with a hemacytometer.

In order to evaluate changes in gene expression for genes commonly involved in DNA damage repair due to γ-irradiation and MMS, real-time (RT) PCR using primers designed to amplify ~60 known repair genes was conducted. Profiles generated indicate whether or not the gene of interest is upregulated, downregulated, or remains the same as the untreated control cells. Comparisons between MMS and γ-irradiation were then made to determine whether there were differences between expression profiles between the two treatments. The results of this study indicated that there were statistically different responses between isolates of *Giardia lamblia*. Different sensitivities also existed between isolates when MMS and γ-irradiation treatments were compared. The lethal dose of γ-irradiation required to inactivate *Giardia lamblia*, isolate WB, trophozoites was found to be 10.0 kGy, while the recovery doses ranged from 0.25-1 kGy. Doses below 0.25 kGy were ineffective at inactivating any of the trophozoites. It was determined decreased use of media, time, and allowed for a higher-throughput screening of toxic agents.

Journal used: Journal of Applied and Environmental Microbiology

Computer software used: Microsoft Office

TABLE OF CONTENTS

LIST OF FIGURES

LIST OF TABLES

CHAPTER 1

LITERATURE REVIEW

INTRODUCTION

The prevalence of drug resistant strains in a variety of eukaryotic and prokaryotic pathogens has necessitated the need for further study into alternative means of disinfecting that have the potential to be more effective than current disinfection options. One way that has been used for disinfection of spices from a variety of insect pests in Europe and throughout the world is the use of gamma (γ)-irradiation. This method of disinfection has proven effective in reducing the number of pests in spices, has also been used for sterilization of medical equipment, and to sterilize food in the Armed Services for years in the United States. *Giardia lamblia* (*syn intestinalis, syn duodenalis*) is one of the most common waterborne pathogens of humans in the U.S. according to recent CDC surveillance reports and has been linked to both chronic and acute forms of disease. Even with the high level of wastewater disinfection throughout the U.S. and other developed nations, *Giardia*

still remains an extremely important pathogen. In underdeveloped countries the instance of giardiasis, the gastrointestinal disease caused by *Giardia* infection, is of increased importance, as infection often leads to increased malnutrition and potentially death. By examining the effects of γ-irradiation on *Giardia* there exists the potential to develop a new means of disinfection that leaves no residue and could cause toxicity to the consumer.

THE BIOLOGY OF *GIARDIA*

Taxonomy

Before delving into the complex biology of *Giardia,* a definition of *Giardia* is necessary. In scientific terms, there is some controversy in answering the question, "what is *Giardia*?" There are currently two main schools of thought as to the phylogenetic classification of *Giardia*. The classical view is based on rRNA sequences that generally place *Giardia* at the root of the eukaryotic branch of the tree of life ([1], Figure 1). Through this classification scheme, *Giardia* has been placed under the domain Eukarya, kingdom Protozoa, subkingdom Archezoa, subphylum Eopharyngia, class Trepomonadea, subclass Diplozoa, and order Giardiida [2]. For many years this system of classification had been accepted since *Giardia* appears to be a more "minimal" eukaryote, lacking several common eukaryotic organelles, such as nucleoli, smooth endoplasmic reticulum, peroxisomes, a Golgi apparatus, and most importantly to evolutionary biologists, mitochondria. The morphological evidence seems to support the rRNA phylogenetic

Figure 1. Classical evolutionary tree created using small subunit rRNA.

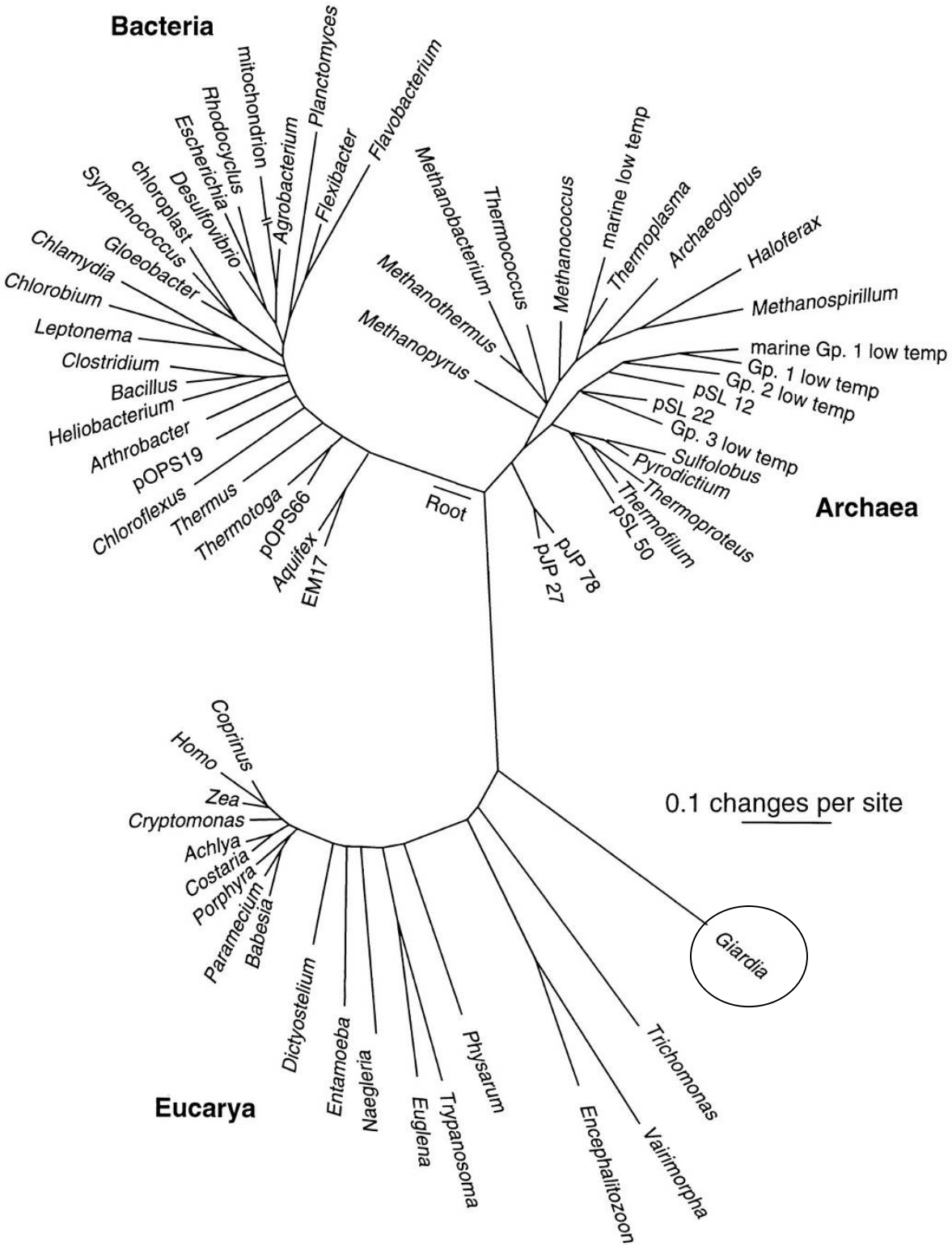

Figure 1. Classical evolutionary tree created using small subunit rRNA. The position of *Giardia* was indicated by a circle, and demonstrates its position at the base of the eukaryotic tree.

analysis that suggested that *Giardia* be classified early in the domain Eukarya. In addition to rRNA data, analysis of actin genes, HSP70, and cathepsin B genes indicated an early diverging position of *Giardia* [2]. However, an alternative classification system has recently emerged based on a comparison of both small and large subunit rRNA. The combination of both small and large subunits is believed by some to provide better clarification of the placement of many protozoa. This classification system, however, is not compatible with older models, and rearranges the classifications into 5 “supergroups”, Excavata, Rhizaria, Plantae, Unikonts, and Chromalveolates (*[3]*, Figure 2).

Figure 2. Classification based on rRNA as well as morphological features.

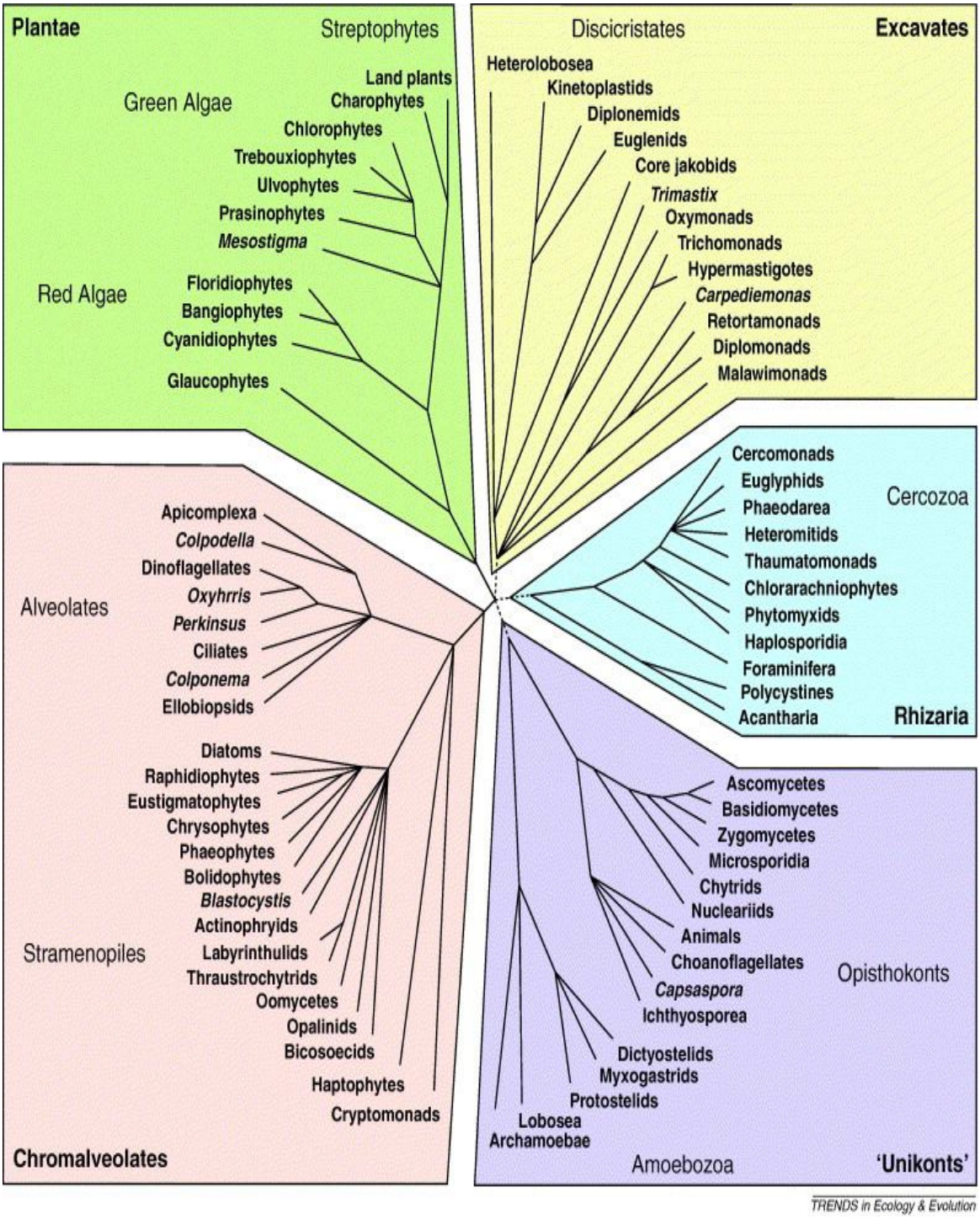

Figure 2. Classification based on rRNA as well as morphology. Note the 5 distinct supergroups currently proposed based on this data [3]. In this system *Giardia*, a member of the Diplomonads, was grouped with the Excavates and does not represent an ancestral eukaryote.

Within this new system of supergroups, *Giardia* falls within the supergroup Excavata and is no longer placed at the base of the eukaryotic tree, but instead takes its place further up on the evolutionary ladder (*[4]*, Figure 3). This system of classification directly competes with the so-called "crown systematics" that places a higher emphasis on metazoans and thus imparts a bias that places humans at the top of the evolutionary tree ([5]). Evidence that *Giardia* may simply have a reductionist strategy and lost organelles previously believed to be acquired later in evolution has recently begun to surface, strengthening their classification with the Excavata. Researchers recently discovered that *Giardia* encodes proteins homologous to yeast krr1 and fibrillarin protein, which are involved in pre-rRNA processing and ribosomal assembly, are localized to the nucleolus in other eukaryotes. In addition, genes encoding nearly half of all nucleolus-localized proteins can be found in *Giardia* genome [6]. This provides evidence that the anucleolate condition of *Giardia* is the result of a secondary evolutionary condition, and does not represent a primitive feature of the organism. Similar evidence exists for the amitochondriate condition of *Giardia*. A recent report has shown that *Giardia* possesses a mitochondrial-like organelle, the mitosome, that contains double membranes with function in iron-sulphur protein maturation [7]. In addition, *Giardia* possesses a large number of nuclear genes with mitochondrial ancestry [7]. However, not all of the "mystery" of *Giardia* can be elucidated by molecular approaches. Researchers noted that microscopically, encysting trophozoites possess a Golgi-like structure, and encystation-specific vesicles (ESVs) are capable

Figure 3. Classification of *Giardia* into the supergroup Excavata based on rRNA ([4]).

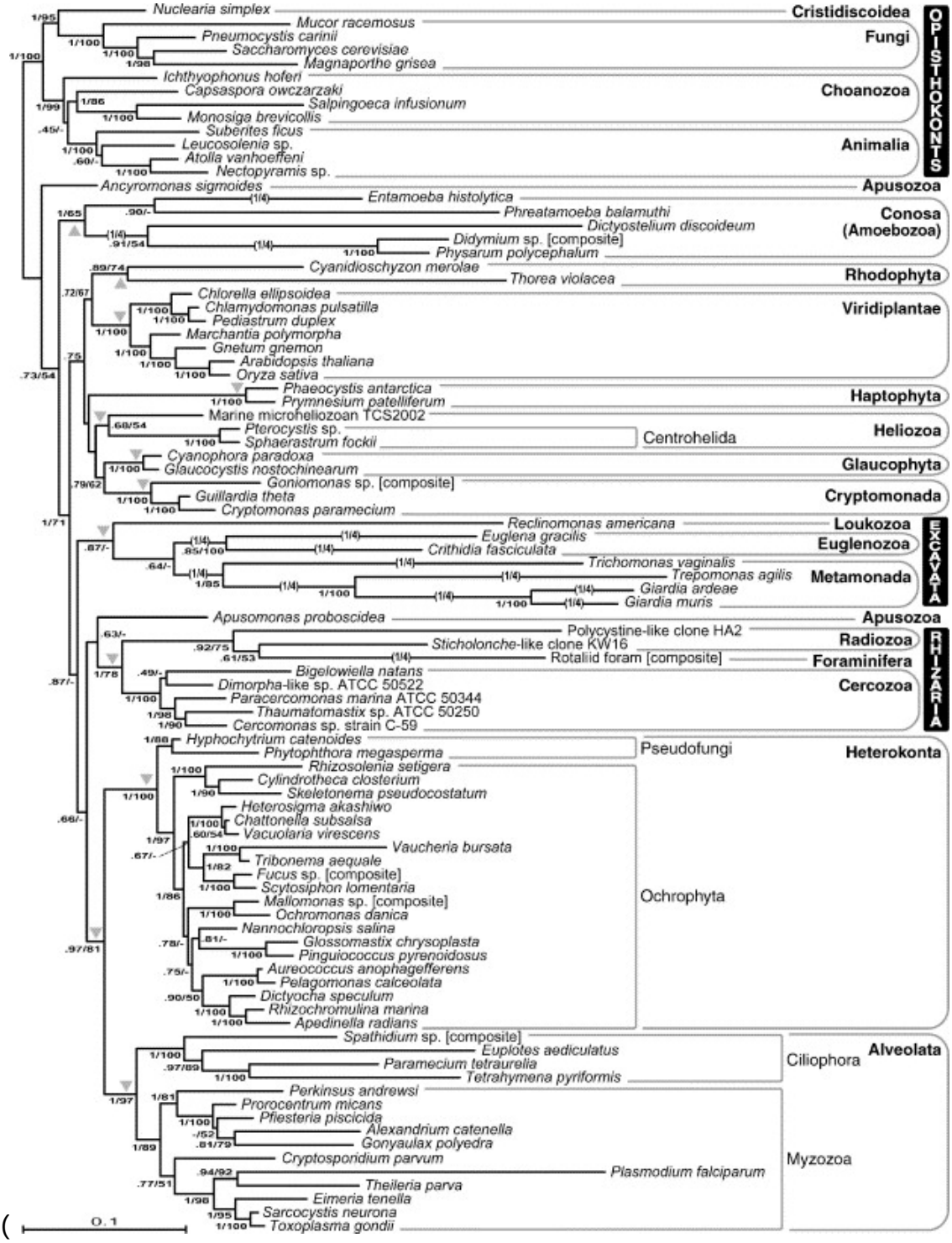

Figure 3. Classification of *Giardia* into the supergroup Excavata based on rRNA ([4]). This tree is derived from small and large subunit rRNA and the placement of *Giardia* lies with Excavata, specifically the Metamonads. This system provides support for the theory that *Giardia* represents a reductionist organism and not an ancestral eukaryote.

of carrying out some Golgi-like functions [8]. These vesicles have similar secretory properties to “normal” eukaryotic Golgi apparatus, and share some biochemical characteristics found in Golgi cisternae. Further study revealed that although some of the biochemical characteristics were similar to the Golgi, ESVs represent a unique and ancestral secretory system suggesting a convergent evolution mechanism for this structure [9].

So far an emphasis in the review has been on the complexities of classifying *Giardia* at the genus level. Now, an exploration of the difficulties with further separating *Giardia* into species and subspecies will be described. Presently, there are 5 recognized species of *Giardia* based on morphological differences in the structure of the trophozoite and cyst: *lamblia*, *agilis*, *ardeae*, *muris*, and *psittaci* (Table 1, Figure 4). Originally, species were described based on the host that the parasite was isolated from; leading to the description of many “new” species that were later discovered to be identical. Despite the fact that there are large differences in the morphology of the currently recognized species, recent molecular data indicates that actually more species may exist with morphology identical to that of *G. lamblia*. This area of research has been of great interest to researchers within the past decade, and several molecular techniques have been developed to clarify the distinctions within this species. As early as the late 1970’s there was a shift to use molecular techniques to identify species of *Giardia*, apart from morphological analysis alone. The first attempt in this direction was the to use isozyme analysis to separate *Giardia lamblia*

subpopulations, mainly for the purposes of screening either humans or animals in a clinical setting [15-20].

Table 1. Recognized species of *Giardia*.

Species	Isolated From:	Morphology	Trophozoite Length (µm)	Trophozoite Width (µm)	Reference
agilis	Tadpole	Slender trophozoites with club shaped median bodies	20-21	4-5	[10]
ardeae	Heron	Rounded shape with characteristic notch in ventral disc and incomplete caudal flagella. Median bodies vary in shape.	10	6.5	[11]
lamblia	Human	Teardrop shaped with claw shaped median bodies	12-15	6-8	[12]
muris	Mouse	Rounded shape with round median bodies	9-12	5-7	[13]
psittaci	Budgerigars [14]	Teardrop shaped with claw shaped median bodies, no ventrolateral flange	14	6	[14]

Analysis of the zymodemes generated by using isozyme analysis showed that there was a wide variety of genetic diversity within the species *G. lamblia*, and this represented the first evidence that it may exist as a “species complex”. Due to the poor isozyme analysis sensitivity, and the requirement of a large sample size, that

Table 1. Recognized species of *Giardia* based on a variety of morphological characters. Shape of adhesive disc, along with the general shape of the trophozoite, can lead to identification of species. Different species vary widely in size, but retain all morphological characters, including the median body.

Figure 4. Morphological comparison of three species of *Giardia* trophozoites, A) *G. agilis*, B) *G. muris*, C.) *G. lamblia* [21].

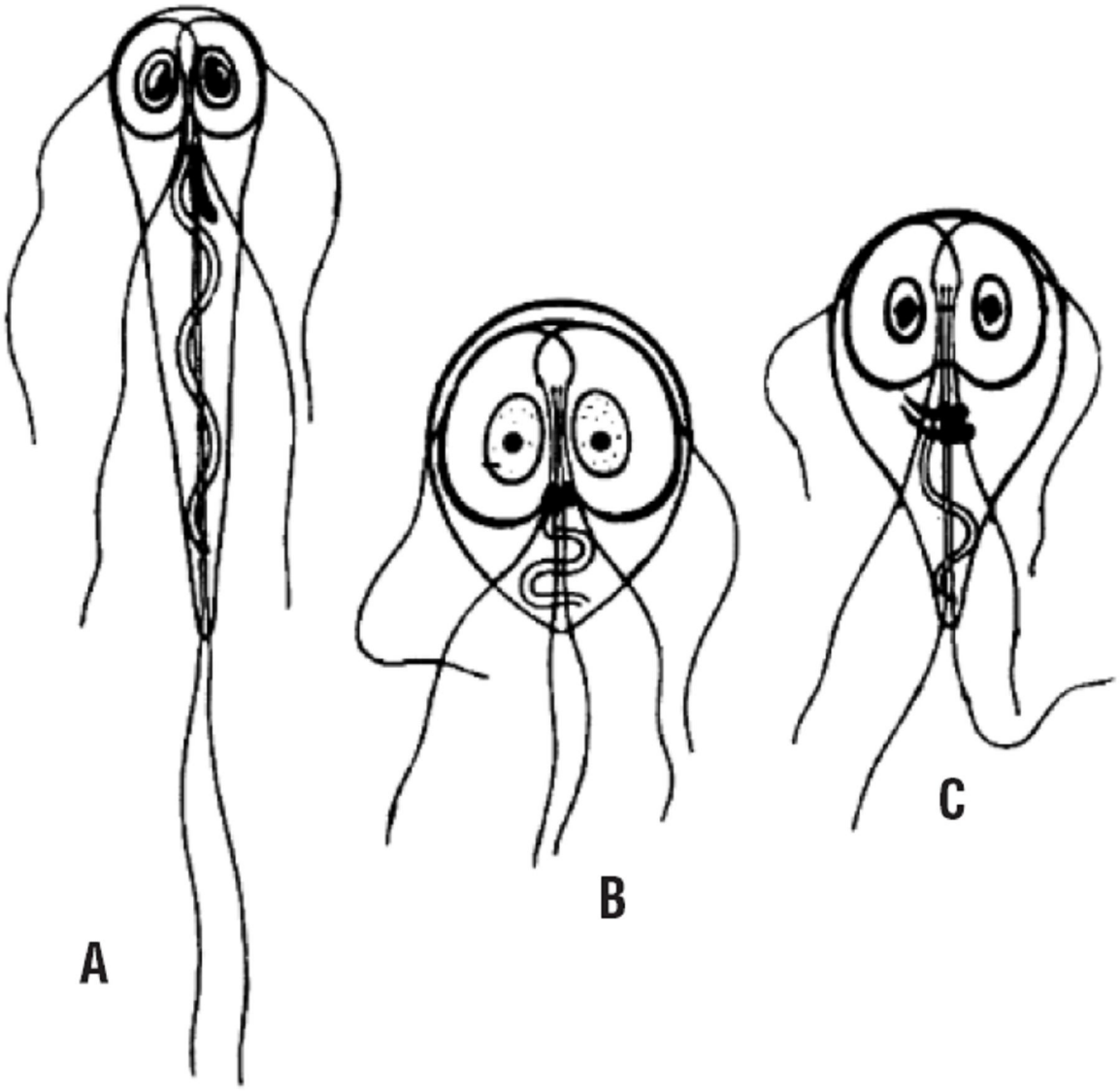

Figure 4. Morphological comparison of 3 known species of *Giardia.* A) Demonstrates the slender appearance of *G. agilis*, B) Shows the smaller and rounder *G. muris*, and C) Shows the normal teardrop shape of *G. lamblia*. Note that all trophozoites have the same key morphological features.

resulted in a bias toward culturable strains, a movement was made to use more sensitive PCR based techniques. Nash was one of the first to pioneer the use of PCR based techniques to distinguish between isolates, by using the 18S rRNA gene differences for the analysis. Nash separated the isolates into 3 groups, aptly named groups 1, 2, and 3 [22]. Optimization of this technique led to the ability to detect DNA from only one cell for amplification and subsequent typing. Further evidence for the relationships generated by the use of the 18S rRNA gene was found later by analyzing differences between variant-specific surface proteins (VSPs) and the GL^{ORF-C4} gene [23]. At the same time that Nash was pioneering the use of PCR based diagnosis in North America, researchers in Australia were asking the same question, but used different markers. Monis et al. used a housekeeping gene sequence, glutamate dehydrogenase to separate *G. lamblia* isolates into what they termed assemblages A and B. Recent molecular evidence has confirmed that Nash groups 1/2 and 3 are equivalent to assemblages A and B of the Australian researchers [24]. As more samples are analyzed more assemblages have been described. Presently, assemblages from A to G are recognized with varying host specificities defined by the assemblages (Table 2). Only assemblages A and B have been isolated from humans, although a variety of assemblages have been isolated from companion animals, leading to questions as to whether or not giardiasis represents a zoonosis. There is a strong emphasis worldwide on identifying the *Giardia lamblia* assemblage infecting a wide variety of animals, both companion and otherwise in order to further shed light on this issue [25-29]. Much research

remains before a conclusive location of *Giardia* in the evolutionary tree can be set and the resolution of new species based on molecular and morphological data.

Table 2. Assemblages of *Giardia lamblia* and its host specificity.

Assemblage	Host	Reference
A	Mammal	[30]
B	Mammal	[30]
C + D	Dog	[31]
E	Livestock	[32]
F	Cat	[30]
G	Rodent	[30]

Key features of the *Giardia* morphology and life cycle

Giardia can best be described as a single-celled eukaryotic parasite that infects the gastrointestinal tract of mammals, birds, and amphibians. Trophozoites, the vegetative stage, consist of two nuclei, 8 flagella, a microtubular adhesive disc for attachment to intestinal epithelial cells, and a median body of unknown function. Peripheral vesicles with lysosomal activity are localized to the periphery of the inner cell membrane, and vary in size and number between individuals. Upon receiving a signal to encyst in the distal portion of the small intestine, the teardrop shaped trophozoites begin to form round to oval cysts that are double walled, and contain 4 nuclei. The cysts are

Table 2. Assemblages of *Giardia* and their host specificity. As observed, host specificity varies widely between the assemblages, from narrow as in the case of C-G, to wide ranging such as A and B.

environmentally resistant and can withstand a variety of disinfecting agents. The cyst is also the infectious stage, ingested by the host, and upon entry into the duodenum, the cysts excyst and a quadrinucleated excyzoite emerges and attaches to the intestinal epithelium. The excyzoite divides without DNA replication to generate 2 binucleated trophozoites. The trophozoites then multiply through binary fission until the numbers are high enough to physically block the absorption of nutrients through the intestine (Figure 5). A recent advance allowing the synchronization of the trophozoite cell cycle *in vitro* using aphidicolin will allow studies investigating many questions about the mechanisms behind *Giardia* reproduction that have not been possible before [33]. Studies using *Giardia* must still contend with several unusual morphological features including two nuclei, a lack of mitochondria, a median body of unknown function, and an adhesive disc needed for attachment to surfaces.

Binucleate Condition

One of the most interesting features of *Giardia* is the presence of two nuclei. Morphologically the two nuclei are identical, always appearing in the anterior portion of the trophozoite on either side of the ventral flagella. The relative distance between the two nuclei is also of a consistent length, varying only between species. Kabnick and Peattie (1990) demonstrated that the nuclei remained in the same planes even after replication, the resulting daughter nuclei remaining in the same plane as their parent before cytokinesis. Until relatively recently, the number of chromosomes per nucleus remained a mystery. In 1988

chromosomes from six isolates of *Giardia lamblia* were separated by pulse field gel electrophoresis (PFGE) and revealed that the chromosomes were similar in size between isolates [34]. Four major chromosomes and several minor

Figure 5. Life cycle of *Giardia*. (Public health library, Center for Disease Control)

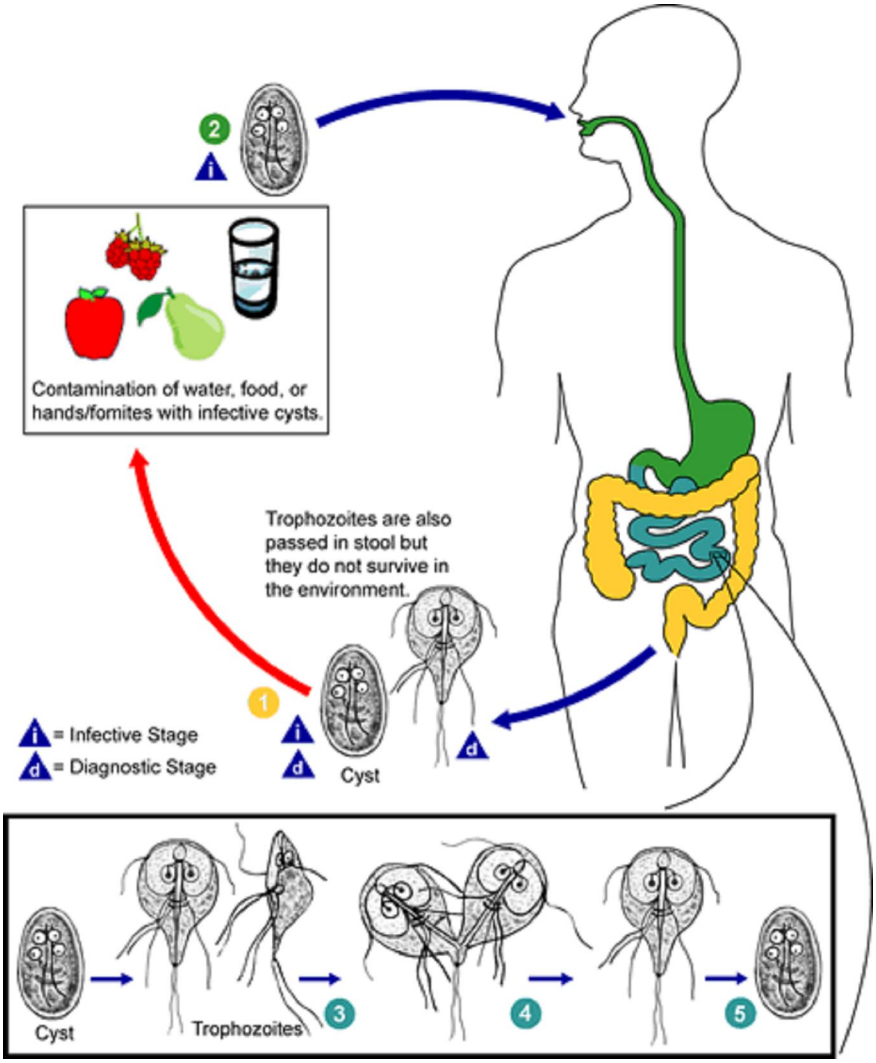

chromosomes were identified. In the JH isolate, however a fifth major band was found. A comparison of *Not* I restriction enzyme fragments revealed common-

Figure 5. Life cycle of *Giardia* demonstrating normal course of infection from the fecal-oral route. The infective cysts are ingested and then excyst in the small intestine into 2 trophozoites that attach, and begin division.

sized DNA fragments. It was thus determined that *Giardia lamblia* had five chromosomes [34]. This data matched other PFGE experiments as well as microscopic observations. The chromosome sizes were determined to be 1.6, 1.6, 2.3, 3.0, and 3.8 Mb totaling 12.0 Mb. This data was in agreement with densitometric analysis of the *Not* I digests of total *Giardia lamblia* DNA suggesting 10.6-11.9 Mb. This data contrasted with C_oT data which could be explained by levels of repetitive DNA [35]. Yet to be determined is an evaluation of potential differences in chromosomes between the two nuclei, whether there is genetic recombination between the two nuclei at any point in the life cycle, or why two nuclei are maintained.

This new information on the number and size of chromosomes in each nucleus led to a new debate over the ploidy, not only of each nucleus, but the entire cell. Early work that elucidated the chromosome numbers indicated that each nucleus was haploid and that the two nuclei would make the organism diploid [34]. A study in 2001 using flow cytometry and fluorescence microscopy elucidated the ploidy for the entire life cycle of the *Giardia lamblia* isolate WB-C6. This isolate has the standard five chromosomes, however, reports of aneuploidy in other strains of *Giardia* have been reported [36]. It was determined that during vegetative growth, each nucleus cycles through a 2N and 4N genome, resulting in a cellular ploidy of 4N to 8N. Therefore, during encystation, the cellular ploidy can reach 16N due to four nuclei per one cyst (Figure 6). This ploidy is very different than first hypothesized. In fact, there is no haploid stage in the life cycle. Quantitative data

Figure 6: *Giardia lamblia* life cycle stages . Cell ploidy at each stage is indicated in bold numbers and nuclear ploidy is indicated in parentheses [36]

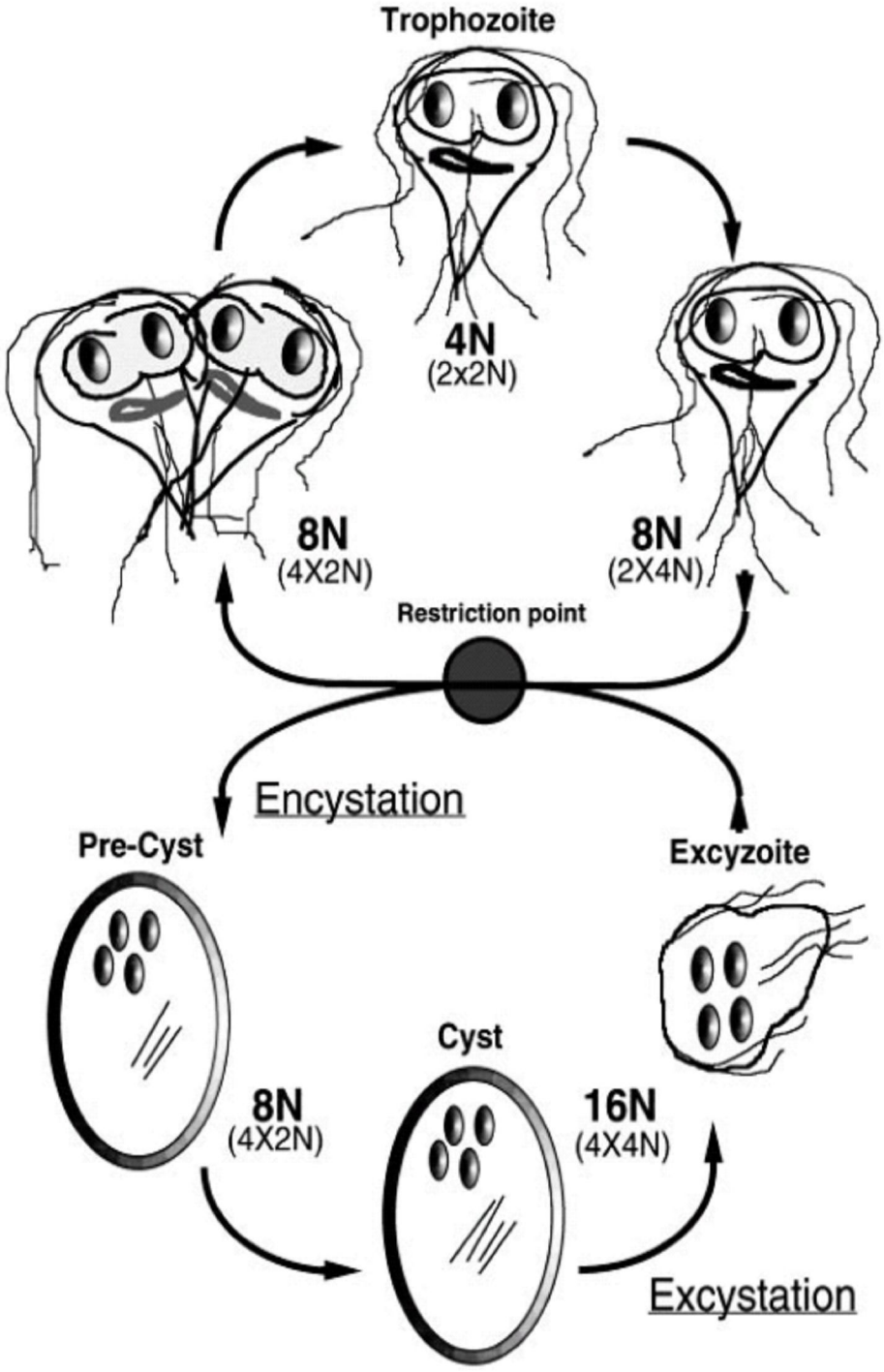

Figure 6. *Giardia lamblia* life cycle stages . Cell ploidy at each stage is indicated in bold numbers and nuclear ploidy is indicated in parentheses [36].

comparing the total amount of genomic DNA (1.34 X 10^8 bp) to the average size of an individual chromosome (2.36 X 10^6 bp) estimated a ploidy of 12N per trophozoite. PFGE experiments predicted a ploidy ranging from 6-10N based on the numbers each chromosome copy 30-60 [35]. Both of these studies match the actual ploidy values that range from 4-16N depending on the stage of the life cycle. The physical structure of the two nuclei has been clearly defined, each containing 4-6 chromosomes and a ploidy of 2-4N. But yet to be addressed was whether or not the two nuclei are distinct. Kabnick and Peattie in 1990 set out to determine the identity of each nucleus. They found that both nuclei contained equal amounts of DNA by staining with DAPI and quantitating the fluorescence intensity photometrically. The DAPI staining also demonstrated that the two nuclei are synchronized during mitosis. Condensed structures were visible in both or neither nuclei but never in one nucleus and not the other. That the two nuclei are synchronized was further evaluated microscopically using DAPI stained trophozoites that were found to have either two or four nuclei, never three. The four nuclei-stained trophozoites were believed to have completed karyokinesis but not cytokinesis. Unlike cells with a macronucleus and micronucleus, such as *Tetrahymena*, where replication can take place at different times, it has been shown that replication of *Giardia* nuclei are coordinated and take place at the same time [37]. *In situ* hybridization using the entire rDNA complex of *G. lamblia* was used to probe nuclear DNA. Hybridization was always seen in both nuclei and based on the hybridization pattern, it was determined that each nucleus contained the rDNA in the same order, making the

two nuclei genetically identical. To prove that each nuclei transcribes RNA at equivalent rates, an autoradiographic technique using [H^3]uridine incorporation was employed showing that the two nuclei transcribed RNA at the same rate [37]. In another fluorescence *in situ* hybridization experiment researchers discovered that genes from each of the five chromosomes were found in both nuclei [38]. Thus the two nuclei of *Giardia lamblia* are identical in transcription rate, genetic content, and are synchronized in respect to the cellular cycle.

Elmendorf in 2000 developed a technique that gives researchers the ability to localize foreign proteins to the two nuclei of Giardia lamblia using the SV40 T-antigen nuclear localization signal (NLS) [39]. The SV40 NLS has been shown to rearrange proteins from the cytoplasm to the nucleus and can be used in conjunction with the green fluorescent protein (GFP) or the tetracycline repressor (TetR) labels. This work showed that both nuclei accumulate proteins containing the signals at the same rate permitting the targeting of proteins from the cytoplasm to the nucleus. This method has the potential to elucidate any possible differences between the two nuclei and thus far, none have been reported.

Kabnick and Peattie discussed that further studies focusing on the physical removal of one nucleus could provide further information on the importance of the binuclear system. Unfortunately there is very little evidence of studies that have used ablation of one of *Giardia's* nuclei to study of the effects nuclear loss might have on the cell's survival. Hypothetically, if the two nuclei are truly identical, then the cell should survive if one of the nuclei is removed.

Assuming that the two nuclei act as a redundancy system, then removal of one of the nuclei would make the cell more susceptible to injury from sources such as UV or γ-irradiation. However, the remaining nucleus would still be 2 or 4 N, leaving templates available for recombinational repair systems to easily repair the damage. Insults from these sources also lead to increased mutation rates within the genome, affecting gene function crucial to cell survival and replication. If negative mutations occurred in only one nucleus, then there is potential for the other nucleus to compensate for these mutations. This redundancy could also have some effect on the cell's ability to survive in microaerophilic environments. Damaging reactive oxygen species could be created and cause damage to the cellular DNA. By having two nuclei working in concert it is possible that the cell is more effective at removing these damaging agents. It has been reported that there is very little difference between alleles in the two nuclei and a surprising level of homozygosity between the two [37]; thus it is unlikely that genes in one nucleus represent a positive adaptation against some stress compared to the other nucleus. Assuming that having two nuclei acts as a redundant, backup system, it would be evolutionarily advantageous for the cell to maintain two nuclei despite the higher energy cost.

Another interesting question regarding *Giardia lamblia* is the question of how the binucleate condition first arose and persists to this day. As mentioned above, in order for the condition to persist a positive adaptive advantage over *Giardia* cells with one nucleus is expected to exist. Kabnick and Peattie proposed several theories on how the binucleate condition could have first

arisen. In other binucleate organisms such as *Tetrahymena* and *Paramecium* it is believed that the macronucleus gave rise to the micronucleus, slowly losing some of its genes on the way [37]. It is possible that the binucleate condition arose in *Giardia* as a result of a malfunction that allowed karyokinesis, but delayed cytokinesis. In this theory the nucleus was allowed to replicate, however, cellular division was delayed leaving two copies of the same nucleus in one cell. The delay in cytokinesis could have allowed another round of nuclear replication before cytokinesis, resulting in two nuclei per cell. This malfunction would most likely not originate in the genome, otherwise the same process would occur again leading to giant multinucleate cells. Instead this could have resulted from a one time malfunction of a protein. This theory is supported by the genetic similarity between the two nuclei and the synchronicity of their cellular processes. Another theory could be derived from the endosymbiont hypothesis. If the nucleus, as an organelle, was first the result of endosymbiosis then the possibility exists that the first *Giardia* cells internalized two ancient bacterial cells that were daughter cells and were incorporated through evolution into the nuclei that exist today. If the bacterial cells were replicates of one another then their genomes would be homologous. This theory could also potentially explain the lack of development of the mitochondrion. The internalization of two large bacterial cells could have provided enough energy at some point in evolutionary history that internalization of the mitochondrial precursor was not necessary. Slowly throughout evolutionary history the energetic potential of these bacterial cells could have become reduced resulting in the amitochondriate cells seen today.

This would still fit in with recent research elucidating the presence of the mitosome, and genes of mitochondrial origin. Perhaps someday light will be shed on the binucleate position, but until that time the large amount of speculation will have to suffice.

Adhesive Disc

It has long been known that the adhesive, or ventral, disc functions in attachment of *Giardia* to the intestinal epithelium, but more recently the role of the adhesive disc throughout the entire *Giardia* life cycle has been studied. Due to the fact that the adhesive disc is crucial for the parasite-host cell attachment and resulting infection, the microtubular structure of the disc has long remained a popular drug target. Nocodazole, colchicine, albendazole, and mebendazole all work by inhibiting tubulin polymerization and microtubule assembly and have been proven effective at treating infection with *Giardia* [40]. In 2005 researchers were able to determine that the adhesive disc was broken down into four components in encysting cells and reassembled quickly upon excystation into the 2 adhesive discs used by the emerging trophozoites [41]. Some evidence exists indicating that the breakdown of the adhesive disc into its four microtubular components may allow it to participate in the process of karyokinesis [42]. The structure of the adhesive disc itself represents a unique set of proteins termed giardins that have been shown through immunolabeling to localize to the ventral disc. There are 3 major types of giardins, ά-, β-, and γ-giardins [43]. These proteins are structurally members of the annexin family and are believed to

provide a structural framework along with tubulin, that allows the adhesive disc to function in intestinal epithelium attachment [44]. It has also been hypothesized that giardins are involved in the dismantling of the adhesive disc during the process of encystation, and then aids in its reassembly during excystation. Although it is well established that an intact adhesive disc is crucial to attachment and subsequent infection, the structural makeup and processing of this structure is not clearly defined, and more research is need to truly understand how this structure functions.

Median Body

The least defined of the unique microtubular structures of *Giardia* is the median body (MB). The median body has been a subject of much debate, and its function remains unknown. What little is known about the median bodies, indicate that it is of microtubular origin, and that it reacts with a variety of tubulin, giardin, and centrin antibodies [45-47]. A recent publication made an attempt to explore the structure and function of the median body using a variety of microscopic techniques. Researchers determined that median bodies were not composed of one or two structures as earlier described, and varied in number, shape, and position [48]. This is an interesting finding, since early researchers, and still some today use the median bodies as a key factor in separating some species from each other. Contradicting previous reports, the median bodies were observed in both mitotic and interphase stage trophozoites, and by immunoanalysis, were observed in 80% of trophozoites. The median bodies

were not structurally “free-floating” within the cytoplasm, but were anchored either to the adhesive disc, plasma membrane, or the caudal flagella. Perhaps of most interest is the observation that the median bodies can protrude through the cell surface [48].

Giardiasis

After covering the classification of *Giardia* and understanding some of the complex problems that researchers face when working with this organism, we must ask, “What other reasons exist for studying Giardia?” We have briefly touched on the fact that *Giardia* is the etiological agent for giardiasis, the most common protozoal gastrointestinal disease in the world [49]. Within the United States *Giardia* is the most commonly identified intestinal parasite, with 4,600 individuals hospitalized annually. The NIAID categorizes *Giardia* as a Category B priority pathogen, with potential to become a bioterrorism agent. Giardiasis has also been classified by both the CDC and NIAID as an emerging infectious disease that requires significant monitoring and surveillance. Worldwide giardiasis poses an even greater risk, as it can increase the severity of starvation conditions, exacerbate malnutrition, and chronic giardiasis has even been linked to growth retardation [50]. Despite considerable efforts to improve water disinfection practices through a variety of physical and chemical means, giardiasis outbreaks continue to occur even within developed nations [51-53]. In addition to infection by contaminated water, giardiasis is recognized as a food-borne disease [54, 55] and outbreaks commonly occur in day-care settings [56,

57]; [58]. The need for new methods of disinfection has led to research into alternatives to the current practices of physical removal via filtration or flocculation, and chemical inactivation using chlorination, bromination or iodination. The current shift is toward safer, cheaper, and potentially more reliable disinfection, such as radiation (low-dose ionizing irradiation or ultraviolet irradiation) or non-residue producing treatments such as peroxidation and ozone.

GAMMA-IRRADIATION

In 1900 a new type of radiation was discovered by the French physicist Paul Ulrich Vilard. This new radiation was more energetic than the previously discovered alpha and beta particles and was capable of penetrating solids including the human body. In 1914 Rutherford and Andrade were able to prove that these new “wavelengths” were in fact different from the previously discovered X-rays and were even more energetic. The main difference between X-rays and gamma-rays is determined by the radiation source, outside of the nucleus in the case of X-rays and within the nucleus in the case of gamma-rays [59]. Given the limits of instrumentation at the times, it was difficult to ascertain the biological effect of various types of radiation particles, so a “quality factor” (QF) was assigned to each type of particle based on the relationship between the mass of the particle and its ionizing energy (Table 1). A larger QF equals a greater its biological impact. At first glance, it would appear that gamma-radiation particles are among the least destructive to biological tissues; however,

it must be realized that alpha particles due to their large mass, cannot penetrate skin. Their high QF requires radiation source internalization, and even in this circumstance, the effects are not be spread over the entire body, but are limited to tissues in the vicinity of the source. Gamma radiation, penetrates the entire body, passing through organs, tissues, and even bone. Thus, although the QF is lower for gamma-radiation, the entire body is affected by one point source.

Table 1. Types, quality factors associated with each, and common sources of radiation.

Type of Radiation	Quality Factor (QF)	Source of Radiation
X-ray	1	Electromagnet
γ-ray	1	Co^{60}, Cs^{137}
β-particle	1	I^{131}, P^{32}, Sr^{90}
α-particle	20	Ur^{238}, Pu^{239}
Thermal neutrons	3	Nuclear Reactors
“Fast” neutrons	10	Nuclear Reactors
Fission fragments	>20	Fission Reactors

Applications for this new type of radiation were readily apparent to the scientific community, since in the absence of the source, there was no residual radioactivity present with gamma-radiation. There are currently 4 major gamma-radiation uses regulated by the FDA: food preservation, food sterilization, sprouting and ripening control, and insect control in fruits and vegetables. The

Table 1. Types of radiation and the QF associated with each. The higher the QF, the greater the biological impact of the particle. It is important to note that although larger particles have a higher QF, it is more difficult for them to penetrate into the body.

first approved use was in 1963 when the FDA approved gamma-radiation use in insect control for wheat and wheat powder. Although it was not actually used for U.S. products, Europe and Russia gamma-irradiated a large amount of imported wheat. The first use of gamma-radiation in the U.S. was in 1964 when it was approved to extend the shelf life of white potatoes by inhibiting sprouting. In the 1970's NASA used gamma irradiation to sterilize meat for astronauts to eat in space (www.epa.gov). This was the first time that large-scale food irradiation was used in the U.S. and has served as the template for current meat sterilization protocols. This long term space use by has helped to allay safety concerns. Despite NASA efforts to promote the use of gamma irradiation, it was not until 1997 that the FDA approved gamma radiation use for red meat, mainly to control parasites and pathogens, and in 2000 the U.S. Department of Agriculture's Food Safety and Inspection Service (FSIS) approved the irradiation of beef. The U.S. is one of the most conservative countries when it comes to the use of radiation to control pathogens, as demonstrated in Table 2 [60]. It is important to note that the FDA strictly regulates the doses of gamma radiation allowed for each type of food product, and not all food products are suitable for gamma radiation. Dairy products and some fruits, such as peaches and nectarines, have undesirable flavor changes after gamma radiation (Table 3).

One of the requirements for foods that have been irradiated in the U.S. is that the Radura symbol must be placed on product packaging if they are sold in stores (Figure 7). However, customer notification is not required for irradiated foods sold in restaurants.

Table 2. Maximum doses allowed for the control of microbial pathogens in poultry in various countries [60].

Country	Item	Date (year)	Dose max. (kGy)
Bangladesh	Chicken	1983	7
Brazil	Poultry	1985	7
Chile	Chicken	1985	7
China	Chicken (spiced)	1994	8
Costa Rica	Chicken	1994	7
Croatia	Poultry (fresh)	1994	3
	Poultry (frozen)	1994	7
France	Chicken	1990	5
	Chicken meat (mech. separated)	1985	5
Israel	Poultry	1987	7
Mexico	Chicken (fresh or frozen) and chicken products	1995	7
Netherlands	Poultry	1992	10.5
Pakistan	Poultry (fresh, frozen)	1996	5
South Africa	Poultry	1989	10
Syria	Chicken	1986	7
Thailand	Chicken	1986	7
United Kingdom	Poultry	1991	7
USA	Poultry (fresh or frozen)	1992	3
	Poultry meat	1992	3
	Red meats (fresh)	1997	4.5
	Red meats (frozen)	1997	7

Table 2. Maximum doses allowed for the control of microbial pathogens in poultry in various countries [60]. No global standards currently exist for the control of microbial pathogens on food and the allowable dose greatly depends on the country.

Table 3. Radiation doses that produce detectable “off-flavor”.

Food Type	Dose (kGy)
Turkey	1.5
Pork	1.75
Beef	2.5
Chicken	2.5
Shrimp	2.5

Figure 7. Radura is the international symbol for radiation and must be placed on all foods irradiated by gamma radiation.

Table 3. Examples of levels of radiation that produce flavor changes in a variety of foods.

Figure 7. Radura is the international symbol for radiation and must be placed on all foods irradiated by gamma radiation

The effects of γ-radiation against pathogens has been the main focus of most research. The most widely studied organisms are bacterial pathogens known to cause food borne illnesses in humans. Pathogenic parasites have also been a common target for inactivation studies (Table 4). Pathogen inactivation doses on a wide variety of foods have been examined since the discovery of γ-radiation (Table 5). In recent years, research on viruses known to cause foodborne diseases has increased. Interestingly, the radiation dose required to inactivate viruses requires more radiation than for bacterial and parasitic diseases (Table 4). In addition, as early as 1978 it was observed that prions had a high level of resistance to γ-radiation [61]. More recently it was shown that it took a dose of 50 kGy to inactivate scrapie at a level of 1.5 log (95%) [62].

Table 4. Radiation doses that control parasites on foods.

Parasite	Dose (kGy)	Stage Tested	Reference
Toxoplasma gondii	0.5	Oocysts	[63]
Chlonorchis sinensis	0.015	Metacercaria	[64]
Encephalitozoon cunniculus	2.0	Spores	[65]
Trichinella spirallis	0.3	Adult	[60]
Taenia solium	0.3	Cysticercosis	[66]
Giardia lamblia	7.0	Trophozoites	[67]
Trichomonas vaginalis	1.8	Trophozoites	[68]

Table 4. Radiation doses used to control parasites on fruits and vegetables. A variety of parasites have been researched to determine the dose required to inactivate them on fruits and vegetables. Both single cellular and multicellular parasites have been tested, and doses are listed.

Table 5. Control of bacterial and viral pathogens on foods by gamma radiation.

Pathogen	Dose (kGy)	Food Product	Inactivation	Reference
Salmonella typhimurum	0.57-0.74	Chicken	1 log	[69]
Vibrio parahaemolyticus	1.0	Oysters	4 log	[70]
Bacillus subtilis	25.0	Honey	1 log	[71]
E. coli O157:H7	1.5	Romaine Lettuce	4 log	[72]
Campylobacter jejuni	0.175-0.235	Ground Beef	1 log	[73]
E. coli O157:H7	0.36	Ready-to-eat meal	1 log	[74]
Salmonella spp.	0.61	Ready-to-eat meal	1 log	[74]
Listeria monocytogenes	0.47	Ready-to-eat meal	1 log	[74]
Coxsackievirus B-2	7.5	Ground Beef	1 log	[75]
Feline calcivirus (model norovirus)	0.5	Water	3 log	[76]
Canine calcivirus (model norovirus)	0.3	Water	3 log	[76]
Porcine parvovirus	50	Cultured virus	3 log	[62]

Table 5. Common pathogens and the dose and level of inactivation achieved with γ-radiation.

ULTRAVIOLET RADIATION

Ultraviolet radiation (UV) has long been associated with mutagenic and genotoxic effects. The damage and the mechanisms of damage depends both on the type of UV and the dose that the organism receives. The most energetic (hence penetrating) wavelength is UV-C (100-290 nm) with UV-B (290-320 nm) and finally UV-A (320-400 nm) being less and less energetic. The mechanisms involved in UV damage and the effects of each UV class are evaluated.

UV-A

This least energetic wavelength causes indirect DNA damage through two distinct pathways. Type I damage results from one electron oxidation of a nucleo-tide base, resulting in the formation of a cationic radical. The primary type I damage target is guanine, followed by adenine, thymine and cytosine. The type I damage mechanism is due to the absorption of a photon from UV-A by an endogenous photosensitizer. The energy from this photon causes the abstraction of one electron from guanine to create an 8-oxo-7,8-dihydroguanyl radical. This radical is highly reactive and is quickly converted to 2,6-diamino-4-hydroxy-5-formamidopyrimidine (FapyGua). The extra amino and hydroxyl groups of FapyGua favor crosslinking between the mutated base and an amino acid such as proline or lysine, producing a bulky adduct. Another fate of the reactive base is tandem lesions resulting from adjacent base mutations, preferably when a pyrimidine is next to the reactive guanine [77]. Singlet oxygen

formed by the transfer of an electron from a photosensitizer, such as a porphyrin, to molecular oxygen induces the formation of 8-oxoGuanosine, a hallmark reactive oxygen species (ROS).

UV-B

By being more energetic than UV-A, UV-B radiation more directly affects DNA. Photons from UV-B radiation are absorbed by pyrimidines. Cyclobutane pyrimidine dimers (CPDs) are the most common photoproducts. Unrepaired CPDs most often result in frameshift mutations. UV-C radiation however, has the potential to split the cyclobutane ring of CPDs converting them back into pyrimidines. Two other common UV-B adducts are, pyrimidine (6-4) pyrimidone adducts and cytosine photoproducts that result in a CC-TT mutation (Figure 8). The rate of CPD formation is approximately one lesion per 10^7 bases per J m^{-2} UV-B, while formation of 6-4 pyrimidone lesions is 2-8 fold lower. 8-oxo-2′-deoxyguanosine (8-oxodGuo) formation is two more orders of magnitude lower [77].

UV-C

UV-C radiation has the highest energy and causes the same types of damage as described above for UV-B, but to a greater extent at an equivalent dose. The rate of CPD formation from UV-C is 2-10 lesions/10^6 bases per J m^{-2} UV-C [77]. UV-C radiation also induces single and double-stranded DNA breaks which if unrepaired, results in cell death.

Figure 8. Chemical structure of cyclopyrimidine dimers (CPD) and 6-4 pyrimidine pyrimidone photodimers. (www.medicalecology.org)

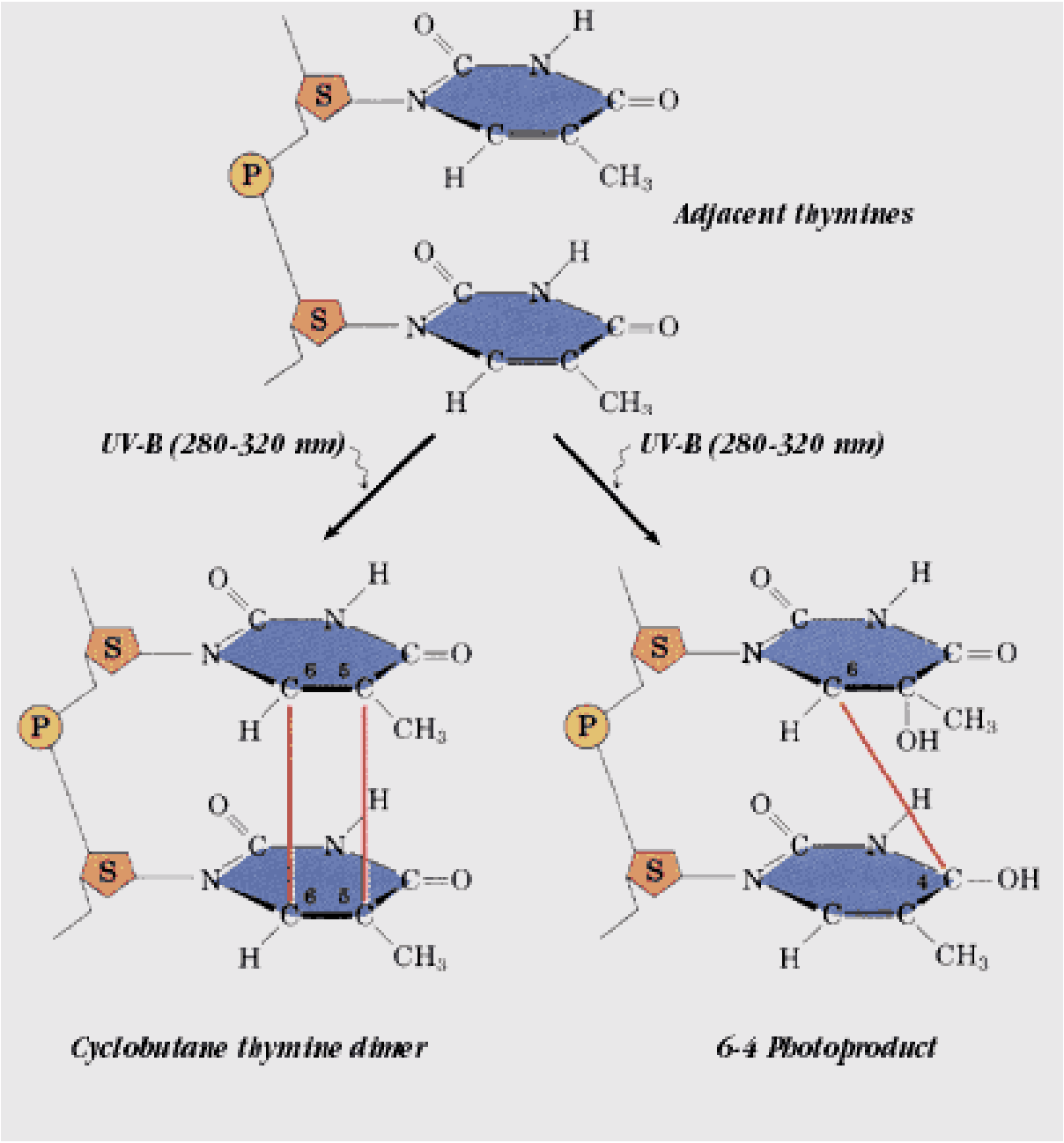

Figure 8. Chemical structure of cyclopyrimidine dimers (CPD) and 6-4 pyrimidine pyrimidone photodimers. These 2 lesions represent the most common lesions associated with UV damage. (www.medicalecology.org)

Transcription Effects

A key way that UV initially damages a cell is by interference with transcription. The presence of CPDs and other photo-adducts halt RNA polymerase elongation along DNA and thus inhibit gene expression. In addition, most DNA polymerases cannot bypass UV-induced lesions, eventually leading to cell death. However, the so called “SOS” repair DNA polymerase, DNA polymerase η has the unique ability to bypass UV lesions, however, it always inserts an adenine opposite the lesion, often leading to C to T transition mutations, but permitting cell survival.

Other Cytotoxic effects

ROS also cause lipid photo-oxidation leading to cell membrane disruption and cell death [78]. Some diseases such as Xeroderma Pigmentosa (XP) give individuals a hypersensitivity to UV resulting from a DNA repair mechanism defect in this case the nucleotide excision repair (NER) pathway. Mutations in the XP family of genes (XPA-D, ERCC4-6. and Pol η) confer sensitivity to ultraviolet light increasing the risk of skin cancers and more aggressive cancers. Such defects drastically increase the amount of damage caused by UV due to repair defects.

Ultraviolet Irradiation Equipment

The design of an experiment with UV radiation as a method of water disinfection depends on the scale of the application. For designing a bench-scale disinfection study, medium or low pressure mercury lamps are the most commonly used. The mercury gas in the medium pressure lamps are under a pressure of 1000 Torr, increasing the intensity of the radiation, but they emit broader wavelengths (185 nm to 1367 nm). A low pressure lamp, as the name implies, pressurizes the mercury gas at < 10 Torr and emits a single monochromatic wavelength of 254 nm [79]. Most early research was conducted using low pressure lamps, hence the 254 nm wavelength has been termed the "germicidal" wavelength. Comparative research using *Klebsiella pneumoniae*, *Citrobacter diversus*, *Citrobacter freundii*, and bacteriophage ΦX174 showed that germicidal efficiency against one bacterial or virus species can be directly correlated to the responses of other species by medium pressure UV irradiation (Giese 2000). Another consideration when choosing a lamp is that the dose is easily calculated with a low pressure lamp using a radiometer but, calculating doses with a medium pressure lamp involves complicated formulas and standardization to allow pressure lamp. For this reason, most bench scale studies utilize low pressure lamps, however these lamps are not suitable for commercial scale operations which require less energy demanding medium pressure lamps to be financially feasible.

After choosing a lamp, the UV beam must be modified to make it uniform. In order to achieve this uniformity, a collimated beam apparatus must be used.

The collimated beam apparatus consists of a reflective housing for the UV lamp, a mechanism to adjust the height of this housing to vary the dose, and a collimating tube for concentrating the light. The advantage of a collimated beam system is that the UV light is concentrated and the operator can place a sample directly under the UV lamp. Without this system, the UV lamp will emit UV from 360^0 around the lamp and the sample would be irradiated from many different angles instead of one direct angle. Collimated beam apparatuses have been used successfully for disinfection studies of a wide variety of organisms including *Giardia lamblia, Giardia muris, Cryptosporidium parvum, Encephalitozoon intestinalis, Escherichia coli, and Streptococcus faecalis* ([80]; [65]; [81]; [82]; [83]; [84]).

The bench-scale collimated beam apparatus choice depends on what method is planned for determining the UV radiation dose to be applied to the target. The choice is either a digital or chemical radiometer. Digital radiometers are expensive, but accurately determine UV radiation doses over time, radiation strength at any given point in the sample, and are usually calibrated for a wide range of wavelengths. Chemical radiometers, also known as actinometers, are less expensive than digital instruments, but are just as accurate. The most common chemical radiometer is the Rahn actinometer. The Rahn actinometer uses iodide and iodate. When excited by the UV light, they are converted to triiodide crystals that can be measured by a spectrophotometer at a wavelength of 352 nm [85]. The formation of triiodide crystals at 254 nm is linear with increasing doses of UV. An advantage of the chemical system is that it

measures the accumulated UV dose over the entire field, rather than for a particular point. The Rahn actinometer has previously been used for UV disinfection experiments with *Giardia lamblia* [65].

Many large-scale water treatment facilities use flow-through reactors designed to irradiate water passing through a series of clear tubes in contact with a bank of UV lamps. These systems are expensive to install but not to operate and rapidly irradiate large water volumes.. In essence, they are equivalent to a large collimated-beam system with tubing that permits constant water flow through the UV light beam.

UV damage DNA repair pathways

Photoreactivation

Photoreactivation is non-mutagenic process by which many organisms are able to repair damage from both cyclobutane dimers and 6-4 photoproducts in the presence of 300 nM (blue) light. Photolyase catalyzes photoreactivation and are known to be present in the microsporidian *Antonospora locustae*, bacteria such as *Legionella pneumophila* and *Escherichia coli*, the marsupial *Monodelphis virginianus*, and the alga *Chlamydomonas reinhardtii* ([86]; [87]; [88]; [89]). Mammals are the only group reported to have entirely lost the ability to use photolyase. A mammalian enzyme cryptochrome (*CRY*), with structural properties similar to photolyase is not used as a photolyase, but as a blue light photoreceptor involved in the regulation of circadian rhythms [90]. Expression of

a marsupial photolyase in mammalian Xeroderma pigmentosa (XP) cells and subsequent exposure to visible light produced a significant increase in cyclobutane dimer repair. An increased UV-irradiated XP cell survival was also found [88]. This suggests that perhaps the cryptochrome enzyme could act as a fall back photolyase, but that its normal function is in circadian rhythm control.

The photoreactivation mechanism is well understood. All photolyases contain a non-covalently bound flavin adenine dinucleotide (FAD) cofactor, which is necessary for photolyase binding to damaged DNA. The FAD also serves as a chromophore by absorbing the energy from UV-A (320-400nm) light and blue (400-500nm) light. FAD is reduced to $FADH^-$ by the energy. $FADH^-$ then donates an electron to the CPD or 6-4 photoadduct and the negative charge induces splitting of the cyclobutane ring. [90]. Two chromophores are known to be involved in the absorption of low-energy photons permitting cleavage of the cyclobutane ring, metheyltetrahydrafolate and 8-hydroxy-5-deazaflavin [91]. In *E. coli* a *phr* mutation at Trp-277 leads to excitation by photons in the far UV range, and splitting of the cyclobutane ring without a chromophore [91]. After ring breakage, an electron is transferred back to the FADH* resulting in a net electron exchange of zero. Upon damage recognition, photolyase catalyzes DNA bending (approximately 50^o around the lesion) exposing its active site and the FAD molecule to the lesion [92]. After repair, the photolyase detaches from the DNA releasing the restored dinucleotide. The photoreactivation catalyzed by photolyase is extremely efficient and error free. Complete CPD and 6-4 photoadduct repair takes an hour for *Legionella pneumophila* and several hours

for *E. coli* [87]. Because energy is received from visible light, the process is energetically favorable, requiring no energy from the cell. For these reasons this pathway should function in cells that are otherwise dormant. Examples of this are the spores of the microsporidian *Antonospora locustae.* The spores of these cells are the only stages of the life cycle that are exposed to the environment; the other stages proceed in an animal host. It was discovered that although these spores are dormant from all other cellular processes, they are still capable of light induced repair using photolyase [86].

Photoreactivation, is a crucial pathway for repair from UV damage, but its true importance to humans involves the increased ability of the photoreactivated cells to withstand further UV damage. UV disinfection of drinking water has grown in popularity and is currently used worldwide to purify water supplies for human consumption. The water after treatment is released into the environment and exposed to blue light and UV-A, both of which can induce photoreactivation. Without photoreactivation, fecal coliforms are inactivated by 5.2 mW s/cm^{-2}, however, after photoreactivation 24 mW s/ cm^{-2} is required for the same level of inactivation [93]. *E. coli* and *S. faecalis* are 2-8 times more resistant to UV after photoreactivation has occurred (Harris 1987). What are the mechanisms that make these photoreactivated organisms more resistant to UV radiation? Although no clear answer currently exists there are several hypotheses that could explain this phenomenon.

One hypothesis is that the initial photoreactivation process primes the photolyase pathway and allows it to proceed simultaneously while the cell is

being irradiated with further UV. As mentioned earlier photolyase uses the energy from light to carry out its repair processes, thus it could possibly use the damaging UV light to initiate repair, as demonstrated with the Trp-277 mutation in *E. coli* discussed earlier. This is especially true in the case of medium pressure UV lamps that emit a wide variety of wavelengths, including the UV-A wavelengths used by photolyase. The variable wavelengths are not as evident with low pressure monochromatic UV lamps. Activation of the photoreactivation pathway upregulates other repair pathways. Normally nucleotide excision repair (NER) is also involved in the repair of CPDs and 6-4 photoadducts. This is not as energetically favorable as photolyase and requires an investment of ATP by the cell, but is generally also a non-mutable pathway. Both repair pathways working in concert would be able to repair many lesions quickly. Examination of this hypothesis could be easily conducted by looking at expressed protein profiles during photoreactivation. No matter the actual increased resistance mechanism to UV radiation after photoreactivation is, it is of crucial importance when evaluating drinking water safety before using ultraviolet light as a disinfection method.

EUKARYOTIC MECHANISMS OF DNA REPAIR

The repair of DNA is a crucial process to the survival of cell, not only to correct for endogenous errors, but also to correct for damage resulting from a variety of environmental factors that cells are exposed to every day. Ultraviolet radiation, electromagnetic radiation, normal DNA metabolism, and a variety of

chemicals cause damage to DNA on a daily basis through a variety of mechanisms including alkylation, oxidation, and other base modifications, double and single strand breaks, and cross-linking of DNA strands. Without efficient error correction, no cell would be able to survive the constant assault of its own environment. DNA repair mechanisms ensure that fewer than 1 in 10^6 mutations result in a permanent mutation in a cell. Only germ cells can pass this change to the next generation, so DNA repair is even more efficient in germ cells. There are five major DNA repair pathways: direct repair, base excision repair, nucleotide excision repair, non-homologous end joining, and homologous recombination. In addition, there are highly mutagenic pathways that utilize non-templated copying by repair DNA polymerases so that cell survival (with a high mutation rate) is at least possible should damage not be repairable.

Direct (non-mutagenic) Repair

The two most common enzymes involved in direct repair are photolyase and O^6-methylguanine DNA methyltransferase (O^6-MGMT). Photolyase is found in a wide variety of prokaryotic and eukaryotic organisms, but is lacking in others, such as placental mammals. The function of photolyase is to remove UV induced cyclobutane pyrimidine dimers (CPD) and (6-4) photoproducts. These bulky products prevent the replication machinery from traveling down DNA resulting in stalled or aborted DNA replication. Since nearly all organisms come into contact with UV radiation in the photolyase plays a crucial role in maintaining normal function in the cell as was described in the previous section.

O^6-MGMT specifically targets repair of a methylated guanine residue. O^6-MGMT forms a loose association with DNA and scans the DNA for any methylated guanine residues, and if it comes into contact with the residue, the O^6MeGua "flips out" into the active site of the enzyme, where the methyl group is transferred to a cysteine in the active site. O^6-MGMT then dissociates from the DNA, however, because the C-S bond of methylcysteine is stable, the enzyme is only capable of one methyl transfer before it becomes inactivated. This is unusual for an enzyme, therefore, O^6-MGMT has been termed a suicide enzyme.

Base Excision Repair (BER)

Base excision repair uses DNA glycosylases to recognize a specific altered base and catalyze its removal. Glycosylases recognize oxidized/reduced bases, alkylated bases, deaminated bases, and base mismatches. Organisms usually have glycosylases specific for each modified base. In the case of eukaryotes, uracil-DNA glycosylase, methyl-purine glycosylase, and homologs of *E. coli* endonuclease III, Fapy glycosylase, and 8-oxoguanine glycosylase detect and repair modified bases. Should the glycosylase not repair the modified bases, there are two sub-pathways involved in BER, the very short-patch repair pathway and the short-patch repair pathway. The very short-patch repair pathway also known as the single nucleotide replacement pathway occurs when the glycosylase lacks lyase activity, leaving an abasic sugar at the site. A 5' incision is made by AP endonuclease I and the resulting abasic sugar is removed

by DNA polymerase β (polβ). DNA polymerase β plus DNA ligase III-XRCC1 fills the 1-nucleotide gap formed after the cleavage. In the short-patch repair pathway the first step is removal of the altered base by a lyase mechanism leaving a 5'-phosphomonoester and a 3'-unsaturated sugar phosphate residue. AP endonuclease I recognizes the gap, makes a 5' incision and then DNA Polδ/ε, PCNA, and FEN1 displace the strand 3' to the nick producing a flap of 2-10 nucleotides. The flap is cut by FEN1 at the transition between the single and double-strand DNA, the gap is filled in by DNA Polδ/ε with the aid of PCNA, and the nick is ligated by DNA ligase I.

Damage detection for BER occurs in the same manner as direct repair by a loose association with DNA and the recognition of slight distortions in the DNA backbone by any altered bases. When an altered base is recognized by the glycosylase, the base is sometimes "flipped out" of the helix into the active site of the enzyme and the repair process is begun. Unfortunately a price that must be paid by glycosylases that have a wide affinity for substrates is that normal bases will occasionally be attacked by the repair mechanism which gives a chance for mutations.

Nucleotide Excision Repair (NER)

The nucleotide excision repair pathway repairs bulky lesions using a multienzyme complex that scans DNA. An "excision nuclease" makes dual incisions after identification of the lesion, creating a 24-32 nucleotide oligomer spanning the bulky lesion. A DNA helicase activity then removes the incised

strand. The recognition of the damaged DNA strand is accomplished by a series of factors including XPA, RPA, and XPC, which all bind to DNA close to the replication fork and scan in a processive manner for lesions. When these factors, in combination with each other, stop moving along the DNA, this serves as a signal to additional repair proteins to begin DNA repair. This is often coupled with transcription to ensure that a faithful copy of the DNA is available for transcription. In this case, TFIIH is recruited by these recognition factors and has both a 3' to 5' and a 5' to 3' helicase activity activated by the recruitment of XPB and XPD. Once TFIIH has been recruited, the PIC1 (preincision complex 1) is formed. Approximately 20 bp of newly synthesized DNA is then unwound at the site of damage. If the complex happens to stop on normal DNA, ATP hydrolysis leads to disassembly of the repair enzyme complex. If the complex binds at a damaged site, XPG replaces XPC, which has a higher affinity for unwound DNA and forms PIC2. Endouclease activity in PIC2 makes a 3' incision, creates a nick recognized by XPF-ERCC1, which which then produces a second incision on the other side of the lesion releases the oligomer. The single stranded DNA gap is filled by DNA Polδ/ε with the aid of PCNA, RFC and DNA ligase IV.

Non-Homologous End-Joining (NHEJ)

Perhaps one of the easiest of the repair mechanisms to understand is non-homologous end-joining. This mechanism is involved in double-strand break DNA repair, which if left unrepaired results in lethality. This mechanism is the most error prone of the repair mechanisms, as this repair pathway results in the

deletion of bases in order to ligate the broken strands together. Ku binds to DNA ends, essentially randomly brings them together, and recruits DNA-PKCs and DNA ligase4-XRCC4 which ligates the broken strands together. Nucleotide loss due to nucleases usually occurs before the end joining reaction can begin, but survival of the cell is paramount. This mechanism can also result in DNA translocations when two unrelated strands become ligated together.

Homologous Recombination (HR)

Another important pathway in the cell is homologous recombination. As opposed to NHEJ, HR accurately repairs double-strand breaks in DNA by using the matching daughter strand that is near replication fork. This permits templated DNA repair of essentially any lesion without loss of bases resulting in high mutation rates since a template is used for accurate replacement of the damaged region. HR also functions to repair mistakes at stalled replication forks, which is crucial since mistakes resulting in stalled replication forks occur during every round of DNA replication. The first step in the processing of the double-strand break is the exonuclease activity on the broken ends in a 5' to 3' direction by a complex of Mre11/RAD50/NBS1. At the completion of this step, which results in single stranded DNA tails, RAD52 binds to the modified termini and recruits RAD51 to the single stranded DNA, which then initiates strand invasion of the nearby homologous donor DNA. Because RAD51 has multiple binding sites, it can efficiently bind single and double-stranded DNA to form a heteroduplex. RAD51, in cooperation with BRCA1 and BRCA2, then induces branch migration

along the homologous DNA producing a gap that is filled in by DNA polymerases. The resulting duplex DNA still has a crossover of the two strands (Holiday junction or cruciform structure) and this structure is resolved by Mus81-MMS4 endonuclease/religation .

Mismatch Repair (MMR) or Long-Patch Repair

Mismatch repair, as the name implies, is a means by which cells correct for incorrect nucleotide pairings and extra-helical loops. Cells with mutations in MMR genes have up to a 1000 fold increased mutation rates [94]. MMR loss results in repeated sequence modification, termed microsatellite instability (MSI), and resistance to DNA methylating agents. The first step in MMR is the recognition of incorrect nucleotide pairings or loops by MutSα (MSH2/MSH3 or MSH2/MSH6), or in the case of larger loops MutSβ [95]. The next step is transformation of the MutS complex to a sliding clamp that can leave the mismatch site and slide along DNA. This is MSH6-dependent. The next step is binding of MutLα (MLH1 and PMS1), triggering excision of the newly synthesized DNA strand containing the error. MutLα stimulates the translation of MutS along DNA and recruitment of the UvrD helicase, DNA polymerase α, and DNA ligase to finish the repair process [96, 97].

DNA REPAIR IN PARASITIC EUKARYOTES

Much of the DNA repair machinery in unicellular eukaryotic parasites, such as *Trypanosoma*, *Leishmania*, and *Plasmodium*, varies from that of their

multicellular eukaryotic cousins. Even less is known about DNA repair in *Giardia lamblia*, but it is hypothesized that most *Giardia* repair pathways will function similarly to other unicellular eukaryotic parasites with a similar physiology. This section will focus on the function and identification of DNA repair genes in unicellular eukaryotic parasites, to aid insight into the potential function of similar *Giardia lamblia* genes.

Trypanosoma

Trypanosomes are responsible for significant human disease in both South America and Africa. *Trypansoma cruzi* is the etiological agent for Chagas disease in South America and is vectored by triatomids endemic to the area. Chagas is a disfiguring disease that has significant human implications throughout South America. *Trypanosoma cruzi* and *Trypanosoma brucei* are parasites afflicting the African continent, causing African sleeping sickness in humans, and Nagana in cattle respectively. These parasites are vectored by the Tsetse fly and are extremely prevalent throughout the continent. Research conducted on the DNA repair mechanisms of these pathogens has been focused mainly on evaluating DNA repair genes as potential drug targets, and to explain how these genes are important for host immune evasion. Genes involved in several DNA repair pathways have been studied and are described below.

Homologous Recombination Genes

The *recA* homolog, *Rad51* was studied in *T. cruzi* and found to be present in all life cycle forms based on mRNA detection, but was expressed 2-fold higher

in amastigotes. Like most other eukaryotes, *T. cruzi* has multiple paralogs of *RAD51* including *RAD51-3,4,5,6* and *DMC1*. It was hypothesized that functional RAD51 was what allowed the parasite to survive in excess of 1 kGy of ionizing radiation. This was confirmed by an induction of *RAD51* mRNA after ionizing radiation and increased resistance to zeomycin, an agent known to cause DNA double strand breaks. Overexpression of *RAD51* led to increased recovery kinetics after ionizing radiation, whereas disruption of *RAD51* led to increased double strand breaks and cell death [98]. In *T. brucei, RAD51* was found to be crucial to antigenic variation allowing for recombination and the switching of variant surface glycoproteins (VSGs) [99]. It has also been hypothesized that efficient DNA recombination and repair by *RAD51* has led to the decreased heterozygosity found in most *T. cruzi* genomes. Heterologous expression of TcRAD51 in mammalian cells led to increased recombination rates [99].

A second paralog of *RAD51*, *DMC1*, was studied in order to determine its role in *T. brucei* DNA repair. In yeast it is known that *Dmc1*$^{-}$ mutants typically go into cell cycle arrest during meiosis, and that *DMC1* co-localizes with *RAD51 [100]*. It was determined that *T. brucei DMC1* has no role in recombination, VSG switching, or DNA repair. *Dmc1*$^{-/-}$ mutants also had no increased methyl methane sulfonate (MMS) sensitivity. In fact, *Dmc1*$^{+/-}$ and *Dmc1*$^{-/-}$ mutants had increased resistance to MMS at a dose of 0.0004% [100]. Unlike *RAD51*, *DMC1* was expressed only in the bloodstream stage. There is peripheral evidence that genetic exchange occurs in *T. cruzi* and it is possible that *DMC1* is involved

during this process, but the function of *DMC1* in trypanosomes remains unknown.

MRE11 is another gene that is important to homologous recombination and was studied in *T. brucei* in order to ascertain its function. A green fluorescent protein (GFP)-MRE11 fusion was found to localize to the nucleus of both bloodstream and procyclic stages. In vertebrates, *MRE11* is essential for the survival of the cell, but in yeast, loss of *MRE11* leads to increased DNA damaging agent sensitivity, poor growth, and an increased rate of spontaneous recombination. *MRE11* null mutants generated in *T. brucei* had lower rates of homologous recombination, reduced growth, and increased sensitivity to MMS and ionizing radiation [101]. These results were similar to the findings in yeast. It was further determined that *MRE11* has no role in VSG switching.

Genes involved in Mismatch Repair (MMR)

Both *T. cruzi* and *T. brucei* possess a complete set of mismatch repair pathway genes [102]. Interestingly, different *MSH2* isoforms were found in *T. cruzi*, but not in *T. brucei*, with a wide variation in MMR rates after treatment with genotoxic agents between the *T. cruzi* strains. Surprisingly, it was found that the *T. cruzi* MSH2 protein was not functional in *T. brucei*, suggesting that the two species are more divergent than other studies have suggested. In *T. cruzi msh2* knockout mutants, an increased sensitivity to hydrogen peroxide was observed, and the sensitivity could be reduced by reintroduction of the *T. cruzi MSH2* protein. *MSH1* deletion mutants were not sensitive to hydrogen peroxide,

indicating that *MSH2* is crucial for oxidative damage repair. Peculiarly, the *T. cruzi MSH2* gene did not complement the MMR pathway as assessed by a microsatellite instability assay or a MNNG tolerance assay. This indicated a potential role for *MSH2*-regulated oxidative repair outside of the confines of the typical MMR pathway [103]. This differs from mammals, where *MSH2* only acts in the MMR pathway. From this evidence, it appears that *MSH2* in trypanosomes functions differently than any other previously studied eukaryotes.

Another protein involved in MMR functioning differently than what was previously observed in mammalian genes is uracil DNA glycosylase (*UNG*). This enzyme in trypanosomes initiates the short patch repair pathway of MMR and is responsible for repairing mismatched uracil resulting from the deamination of cytosine. The substrate preference of TcUNG was determined to be ssU>U:G>U:A with no U:T activity. Heterologous expression of *TcUNG* in *ung*$^{-}$ *E. coli* restored the mutants to the WT phenotype [104]. Unlike human *UNG*, which has a 10-fold increased activity in 10 mM Mg^{++}, TcUNG was 85% inhibited in the presence of 10 mM Mg^{++}, suggesting that some other cofactor may be necessary for the function of this gene in *T. cruzi* [104].

Genes involved in Non-Homologous End Joining (NHEJ)

Two genes involved in eukaryotic NHEJ, Ku70 and Ku80, were found in the *T. brucei* genomic analysis. In other eukaryotes, NHEJ is dependent on Ku70/Ku80 binding to the broken DNA ends . It was determined that end joining in *T. brucei* was independent of Ku70 and Ku80, and since there are no DNA

ligase IV or *XRCC4* (genes crucial to NHEJ) it was suggested that this pathway is not active in *T. brucei* [105]. However, DNA end joining was observed in *T. brucei* and it was determined that this end joining was a result of microhomology mediated end joining (MMEJ) [105]. More confounding was the observation that that MMEJ was found to act independently of ATP, normally essential for DNA ligase activity. This suggests that the DNA end joining repair pathway in trypanosomes functions far differently from other known eukaryotes.

A final gene of interest is involved in several different repair pathways is the transcription factor: (PARP-1). PARP-1was one of the first transcription factors found to recognize DNA lesions and is involved in histone removal, allowing repair machinery access to a lesion. In *T. cruzi* it was determined that nicked DNA enhanced the activity of PARP-1, and that histones purified from *T. cruzi* increased this activity *in vitro.* Covalent binding of PARP-1 to histones was observed ([106]). Poly ADP-ribose (PAR) synthesis was increased in response to the addition of DNA damaging agents, as expected, indicating that PARP-1 functions similarly to other eukaryotic systems ([106]). Trypanosome gene expression differs from other eukaryotic gene expression by an absence of transcription initiation sites, a polycistronic transcription process, and a decreased number of known transcription factors. It was hypothesized that chromatin remodeling by protein modification, including PAR ribosylation may be important in overall regulation of gene expression in these parasites ([106]).

Leishmania

Leishmania affects over 12 million people worldwide, and as many as 2 million new cases occur each year. Of further concern is the fact that children are often the ones afflicted with these terrible diseases. Cutaneous and visceral forms of the disease are present throughout the world, and the only appproved treatments are pentavalent antimony compounds. These compounds are extremely toxic to the host and drug resistant strains have emerged to the most common methods of treatment. The DNA repair pathways of this organism have become focal points for the design of novel therapeutics, since many of the genes are highly dissimilar to their mammalian homologs and are essential. Another aim for studying the DNA repair pathways from this parasite, is to determine how the parasites respond to DNA damage induced by host cells, specifically macrophages. It is hypothesized that macrophage-induced oxidative damage may lead to increased mutation frequencies, and thus increase drug resistance selection.

Homologous Recombination

RAD51, as mentioned earlier, is a key component of homologous DNA recombinational repair, and a *RAD51* homolog was found to exist in *Leishmania major*. In exponentially growing cultures, *RAD51* was expressed at below the level of detection, however, after exposure to phleomycin, a DNA damaging agent, *RAD51* mRNA and protein were readily detectable [107]. Similar to other known RAD51 proteins, LmRAD51 was found to bind to DNA and exhibited DNA-

stimulated ATPase activity *in vitro*. It has been hypothesized that RAD51 may have a key role in the parasite's defense against oxidative destruction from macrophages. The potential exists that RAD51 may provide drug resistance in the form of gene amplification. *RAD51* was the first component of the homologous recombination pathway to be reported from *Leishmania*, and has been reported from both *L. donovani* and *L. major* to date [107].

Another homologous DNA recombination gene closely associated with *RAD51* was discovered in *L. donovani, BRCA2* (*BRH2*) [108]. BRH2 binds to RAD51 *in vitro* and is thought to stimulate the initiation of DNA strand transfer and provide support, or scaffolding for the RAD51-DNA association. Surprisingly, comparison of known *BRH2* genes showed that *LdBRH2* was more closely related with mammalian *BRH2* than to yeast and plant *BRH2* [108]. Discovery of this second gene provides further evidence for a homologous DNA recombination pathway in *Leishmania*.

Base Excision Repair

Based on genomic searches, a gene with homology to DNA polymerase β, a DNA repair polymerase important in short patch DNA repair, was discovered in the genome of *Leishmania infantum* [109]. This gene was overexpressed in *E. coli*, and it was discovered that it had intrinsic DNA polymerase activity. Increased levels of both DNA polymerase β mRNA and protein were detected during the infective stage of the parasite and during the intracellular stage of the amastigote. The increased levels at these stages were believed to result from

increased DNA damage resulting from host cell defenses. Unlike *C. fasciculata*, a closely related Trypanomastid, the LiPol β was found to localize to the nucleus instead of the mitochondria [109]. In contrast to mammalian DNA Pol β, LiPol β was strongly activated by Mn^{++}, not Mg^{++}. LiPol β was found to be capable of normal eukaryotic Pol β functions including gap filling, gap tailoring, and ATP-dependant DNA polymerase activity [109]. The discovery of this gene indicates the presence of a short-patch DNA repair pathway, which most likely helps in the defense against attack by components of parasitized macrophages.

An AP endonuclease gene is another gene involved in BER discovered in *Leishmania major*. AP endonuclease is responsible for repairing abasic sites (AP) that commonly occur in DNA. AP sites commonly occur as a result of oxidative damage, or the misincorporation of dUTP. It was demonstrated that AP endonuclease from *L. major* (APLM) expressed in *E. coli* conferred resistance to both MMS and hydrogen peroxide [110]. It was also discovered that APLM was able to repair damage from methotrexate, a drug that causes massive mis-incorporation of dUTP and results in DNA fragmentation Overexpressing APLM conferred increased resistance to methotrexate, and led researchers to hypothesize that this system may function to help repair oxidative damage from macrophages [111].

Plasmodium

One of the most important human parasites in the world, *Plasmodium* species cause a variety of malarial diseases. Malaria infects between 300-500

million people a year and drug resistant strains are constantly emerging. *Plasmodium* is a member of the Apicomplexans and Apicomplexans, in general represent an important group of pathogens infecting a wide variety of food animals and humans. Understanding the mechanisms they use to repair DNA damage is essential to our understanding of these complex parasites.

Homologous Recombination

Similar to the other organisms studied thus far, *RAD51* was the first homologous recombination gene discovered in *Plasmodium* or any other Apicomplexan because it is so conserved throughout evolution. First discovered by a homology search of the *P. falciparum* genome, *PfRAD51* was shown to have 66-77% identity with the catalytic region of yeast, human, *Trypanosoma*, and *Leishmania RAD51*. Researchers also discovered that there was an increase in *RAD51* mRNA and protein after treating the intracellular stage of the organism with MMS *in vivo* [112]. Oddly, the *PfRAD51* gene is more similar to human *RAD51* than to yeast, *Trypanosoma,* or *Leishmania RAD51*. This finding was counterintuitive considering that *Plasmodium* is more closely related phylogenetically to *Trypanosoma* and *Leishmania*. Genome searches have revealed that *RAD54*, another member of the RAD family complex, was also present in the *P. falciparum* genome. With characterization of *PfRAD51* activity, a mechanism has been proposed that could explain the drug resistance that commonly emerges within *Plasmodium* species. Recombinational events in the *PfMdr1* gene on chromosome 5, and spontaneous recombination in the *var*

cluster of genes on chromosome 12 have been linked to drug resistance [113, 114].

Base Excision Repair (BER)

Analysis of the *P. falciparum* genome revealed homologous sequences for genes involved in the entire long-patch DNA repair pathway of BER. Homologs for *FEN1*, DNA ligase I, Pol δ and Pol ε have all been identified in *P. falciparum* Researchers have hypothesized that the long-patch DNA repair pathway is the major pathway involved in BER, despite the fact that in most eukaryotes, the short-patch repair pathway is responsible for 80% of BER repair. Only a Pol β-like enzyme has been indentified for the short-patch repair pathway, and attempts to find homologous sequences to DNA ligase III and XRCC2 have failed.

The *FEN1* gene from *P. falciparum* and *P. yoelii* was cloned and expressed in *E. coli* to assess the biochemical activity of FEN1 protein from *Plasmodium* species. Recombinant PfFEN1 and PyFEN1 demonstrated 5' to 3' exonuclease activity and DNA structure-specific flap endonuclease in *E. coli* similar to FEN1 from other eukaryotes. PfFEN1 and PyFEN1 both had an extended C-terminal domain, but had high homology to other eukaryotic FEN1 proteins in the N-terminal region [115]. PfFEN1 generated a nicked DNA substrate that was ligated by DNA ligase I using an *in vitro* repair assay. It was discovered that C-terminal truncated mutants, with up to 230 amino acids removed, had an endonuclease activity ~130 times greater *in vivo*. The increased

endonuclease activity without this region, may lead to increased mutation frequency due to less specificity. Without *FEN1* the long-patch repair pathway would not be able to repair flap substrates, and thus would not be able to repair the damage.

A second gene involved in BER is DNA ligase I. This DNA ligase was found to be ATP dependent, bound specifically to a singly nicked substrate, and had gap filling functions, similar to other eukaryotic DNA ligase Is. In order to make sure Pf DNA ligase I was not involved in the short-patch repair pathway, the ability of Pf DNA ligase I to join RNA-DNA, a function of DNA ligase III, was tested [115]. It was determined that Pf DNA ligase I had no RNA-DNA joining capacity. The final evidence for the long-patch repair pathway was the characterization of Pf polymerases ά, δ, and ε, with polymerase ά and δ having been fully cloned and sequenced [116].

The only protein discovered thus far in *Plasmodium* implicated in the short-patch repair pathway is a Pol β-like enzyme. A Pol β-like enzyme was isolated from crude extracts and partially purified, despite genome searches that showed no homologous sequences to known Pol β. This enzyme was able to repair 3-5 nucleotides, but was not able to repair 1 nucleotide, indicating that this polymerase may have a role in long-patch repair. To test ability of the Pol β-like enzyme to repair a UG mismatch, the extract was incubated with a 28-mer with a UG mismatch located in the middle of the sequence. Repair started after 15 minutes, with Pf Pol β-like enzyme showing low processivity up to 10 bp, while Pb Pol β-like enzyme was able to repair 100 bp. Unlike mammalian Pol β, the Pf

Pol β-like enzyme was more resistant to aphidicolin and showed increased resistance to inhibition by dTTP [116]. Mammalian Pol β was extremely sensitive to inhibition by dTTP, whereas Pf Pol β-like enzyme was greater than 10-fold more resistant. Evidence thus far points to a potential role of Pf Pol β-like enzyme in long-patch repair, despite the fact that Pol β in other eukaryotes is generally involved only in short-patch repair [116].

Mismatch Repair

Two homologs of *MSH2*, *Plasmodium bergheri MSH2-1* and *MSH2-2*, were discovered by genome analysis. Mutants deficient in *Pbmsh2-2* were found to be more prone to mutations using a dominant mutator assay [117]. *PbMSH2-2* was not essential to any stage of the parasite life cycle. In addition to *MSH2*, homologs were found to *MSH6*, *PMS1*, and *MLH1* [117]. The discovery of these genes provides evidence for an intact mismatch repair in *Plasmodium* species.

A gene encoding *UvrD*, a helicase used in DNA mismatch repair, was found by probing the *Plasmodium* genome for sequences encoding functional domains similar to known helicases. *PfUvrD* had only 15% similarity to human *UvrD*. UvrD-catalyzed unwinding generally increases in the presence of *MutL in vitro*. A *MutL* homolog, *MSH2* has already been identified as mentioned earlier. By itself UvrD helicase can unwind 20-50 bp, but in the presence of MutL can unwind 1-2 kb. In other eukaryotes, *UvrD* is essential, but this has yet to be tested for PfUvrD.

Conclusions

Although *Giardia* has been studied since the early 1600's much of the basic biology of *Giardia* remains unknown. In order to ensure that disinfection methods are appropriate to control this pathogen it is necessary to understand how this organism repairs from a variety of damaging agents. It is also crucial that disinfection studies are designed to account for the potential of *Giardia* to repair from potential disinfecting agents. By understanding the repair pathways that *Giardia* uses to repair damage it will be possible to design more efficient methods of disinfection, and to provide potential targets for novel drugs. With the lack of residual radiation, γ-radiation may provide a novel means of disinfecting *Giardia* on fruits and vegetables.

LITERATURE CITED

1. Pace, N.R., *A molecular view of microbial diversity and the biosphere.* Science, 1997. **276**(5313): p. 734-40.
2. Adam, R.D., *Biology of Giardia lamblia.* Clin Microbiol Rev, 2001. **14**(3): p. 447-75.
3. Keeling, P.J., et al., *The tree of eukaryotes.* Trends Ecol Evol, 2005. **20**(12): p. 670-6.
4. Moreira, D., et al., *Global eukaryote phylogeny: Combined small- and large-subunit ribosomal DNA trees support monophyly of Rhizaria, Retaria and Excavata.* Mol Phylogenet Evol, 2007. **44**(1): p. 255-66.
5. Dacks, J.B., G. Walker, and M.C. Field, *Implications of the new eukaryotic systematics for parasitologists.* Parasitol Int, 2008. **57**(2): p. 97-104.
6. Xin, D.D., et al., *Identification of a Giardia krr1 homolog gene and the secondarily anucleolate condition of Giaridia lamblia.* Mol Biol Evol, 2005. **22**(3): p. 391-4.
7. Tovar, J., et al., *Mitochondrial remnant organelles of Giardia function in iron-sulphur protein maturation.* Nature, 2003. **426**(6963): p. 172-6.
8. McCaffery, J.M., G.M. Faubert, and F.D. Gillin, *Giardia lamblia: traffic of a trophozoite variant surface protein and a major cyst wall epitope during growth, encystation, and antigenic switching.* Exp Parasitol, 1994. **79**(3): p. 236-49.
9. Marti, M. and A.B. Hehl, *Encystation-specific vesicles in Giardia: a primordial Golgi or just another secretory compartment?* Trends Parasitol, 2003. **19**(10): p. 440-6.
10. Feely, D.E. and S.L. Erlandsen, *Morphology of Giardia agilis: observation by scanning electron microscopy and interference reflexion microscopy.* J Protozool, 1985. **32**(4): p. 691-3.
11. Erlandsen, S.L., et al., *Axenic culture and characterization of Giardia ardeae from the great blue heron (Ardea herodias).* J Parasitol, 1990. **76**(5): p. 717-24.
12. Gillin, F.D., D.S. Reiner, and S.E. Boucher, *Small-intestinal factors promote encystation of Giardia lamblia in vitro.* Infect Immun, 1988. **56**(3): p. 705-7.
13. Friend, D.S., *The fine structure of Giardia muris.* J Cell Biol, 1966. **29**(2): p. 317-32.
14. Erlandsen, S.L. and W.J. Bemrick, *SEM evidence for a new species, Giardia psittaci.* J Parasitol, 1987. **73**(3): p. 623-9.
15. Meloni, B.P., A.J. Lymbery, and R.C. Thompson, *Isoenzyme electrophoresis of 30 isolates of Giardia from humans and felines.* Am J Trop Med Hyg, 1988. **38**(1): p. 65-73.
16. Upcroft, J.A. and P. Upcroft, *Two distinct varieties of Giardia in a mixed infection from a single human patient.* J Eukaryot Microbiol, 1994. **41**(3): p. 189-94.

17. Bertram, M.A., et al., *A comparison of isozymes of five axenic Giardia isolates.* J Parasitol, 1983. **69**(5): p. 793-801.
18. Andrews, R.H., et al., *Additional enzymes for the genetic characterization of Giardia from different host species.* Parasitol Res, 1993. **79**(4): p. 337-9.
19. Moss, D.M., et al., *Isoenzyme comparison of axenic Giardia lamblia strains.* J Protozool, 1992. **39**(5): p. 559-64.
20. Meloni, B.P., A.J. Lymbery, and R.C. Thompson, *Genetic characterization of isolates of Giardia duodenalis by enzyme electrophoresis: implications for reproductive biology, population structure, taxonomy, and epidemiology.* J Parasitol, 1995. **81**(3): p. 368-83.
21. Olson, M.E., *Giardia and Giardiasis: A zoonotic threat.* Suppl. Compend Contin Educ Pract Vet, 2002. **24**(5): p. 1-15.
22. Weiss, J.B., H. van Keulen, and T.E. Nash, *Classification of subgroups of Giardia lamblia based upon ribosomal RNA gene sequence using the polymerase chain reaction.* Mol Biochem Parasitol, 1992. **54**(1): p. 73-86.
23. Nash, T.E. and M.R. Mowatt, *Identification and characterization of a Giardia lamblia group-specific gene.* Exp Parasitol, 1992. **75**(4): p. 369-78.
24. Monis, P.T., et al., *Molecular genetic analysis of Giardia intestinalis isolates at the glutamate dehydrogenase locus.* Parasitology, 1996. **112 (Pt 1)**: p. 1-12.
25. Trout, J.M., M. Santin, and R. Fayer, *Detection of Assemblage A, Giardia duodenalis and Eimeria spp. in alpacas on two Maryland farms.* Vet Parasitol, 2008. **153**(3-4): p. 203-8.
26. Geurden, T., et al., *Mixed Giardia duodenalis assemblage A and E infections in calves.* Int J Parasitol, 2008. **38**(2): p. 259-64.
27. Coklin, T., et al., *Prevalence and molecular characterization of Giardia duodenalis and Cryptosporidium spp. in dairy cattle in Ontario, Canada.* Vet Parasitol, 2007. **150**(4): p. 297-305.
28. Lebbad, M., et al., *Dominance of Giardia assemblage B in Leon, Nicaragua.* Acta Trop, 2008. **106**(1): p. 44-53.
29. Leonhard, S., et al., *The molecular characterisation of Giardia from dogs in southern Germany.* Vet Parasitol, 2007. **150**(1-2): p. 33-8.
30. Monis, P.T., et al., *Molecular systematics of the parasitic protozoan Giardia intestinalis.* Mol Biol Evol, 1999. **16**(9): p. 1135-44.
31. Hopkins, R.M., et al., *Ribosomal RNA sequencing reveals differences between the genotypes of Giardia isolates recovered from humans and dogs living in the same locality.* J Parasitol, 1997. **83**(1): p. 44-51.
32. Ey, P.L., et al., *Genetic analysis of Giardia from hoofed farm animals reveals artiodactyl-specific and potentially zoonotic genotypes.* J Eukaryot Microbiol, 1997. **44**(6): p. 626-35.
33. Reiner, D.S., et al., *Synchronisation of Giardia lamblia: Identification of cell cycle stage-specific genes and a differentiation restriction point.* Int J Parasitol, 2008. **38**(8-9): p. 935-44.

34. Adam, R.D., T.E. Nash, and T.E. Wellems, *The Giardia lamblia trophozoite contains sets of closely related chromosomes.* Nucleic Acids Res, 1988. **16**(10): p. 4555-67.
35. Adam, R.D., *The Giardia lamblia genome.* Int J Parasitol, 2000. **30**(4): p. 475-84.
36. Bernander, R., J.E. Palm, and S.G. Svard, *Genome ploidy in different stages of the Giardia lamblia life cycle.* Cell Microbiol, 2001. **3**(1): p. 55-62.
37. Kabnick, K.S. and D.A. Peattie, *In situ analyses reveal that the two nuclei of Giardia lamblia are equivalent.* J Cell Sci, 1990. **95 (Pt 3)**: p. 353-60.
38. Yu, L.Z., C.W. Birky, Jr., and R.D. Adam, *The two nuclei of Giardia each have complete copies of the genome and are partitioned equationally at cytokinesis.* Eukaryot Cell, 2002. **1**(2): p. 191-9.
39. Elmendorf, H.G., S.M. Singer, and T.E. Nash, *Targeting of proteins to the nuclei of Giardia lamblia.* Mol Biochem Parasitol, 2000. **106**(2): p. 315-9.
40. Mariante, R.M., et al., *Giardia lamblia: evaluation of the in vitro effects of nocodazole and colchicine on trophozoites.* Exp Parasitol, 2005. **110**(1): p. 62-72.
41. Palm, D., et al., *Developmental changes in the adhesive disk during Giardia differentiation.* Mol Biochem Parasitol, 2005. **141**(2): p. 199-207.
42. Benchimol, M., *Participation of the adhesive disc during karyokinesis in Giardia lamblia.* Biol Cell, 2004. **96**(4): p. 291-301.
43. Nohria, A., R.A. Alonso, and D.A. Peattie, *Identification and characterization of gamma-giardin and the gamma-giardin gene from Giardia lamblia.* Mol Biochem Parasitol, 1992. **56**(1): p. 27-37.
44. Bauer, B., et al., *Functional identification of alpha 1-giardin as an annexin of Giardia lamblia.* FEMS Microbiol Lett, 1999. **173**(1): p. 147-53.
45. Crossley, R., et al., *Immunocytochemical differentiation of microtubules in the cytoskeleton of Giardia lamblia using monoclonal antibodies to alpha-tubulin and polyclonal antibodies to associated low molecular weight proteins.* J Cell Sci, 1986. **80**: p. 233-52.
46. Soltys, B.J. and R.S. Gupta, *Immunoelectron microscopy of Giardia lamblia cytoskeleton using antibody to acetylated alpha-tubulin.* J Eukaryot Microbiol, 1994. **41**(6): p. 625-32.
47. Correa, G., J.A. Morgado-Diaz, and M. Benchimol, *Centrin in Giardia lamblia - ultrastructural localization.* FEMS Microbiol Lett, 2004. **233**(1): p. 91-6.
48. Piva, B. and M. Benchimol, *The median body of Giardia lamblia: an ultrastructural study.* Biol Cell, 2004. **96**(9): p. 735-46.
49. Wolfe, M.S., *Giardiasis.* Clin Microbiol Rev, 1992. **5**(1): p. 93-100.
50. Farthing, M.J., *Giardiasis.* Gastroenterol Clin North Am, 1996. **25**(3): p. 493-515.
51. Robertson, L.J., et al., *Demographics of Giardia infections in Bergen, Norway, subsequent to a waterborne outbreak.* Scand J Infect Dis, 2007: p. 1-4.

52. Isaac-Renton, J.L., et al., *A second community outbreak of waterborne giardiasis in Canada and serological investigation of patients.* Trans R Soc Trop Med Hyg, 1994. **88**(4): p. 395-9.
53. Slifko, T.R., H.V. Smith, and J.B. Rose, *Emerging parasite zoonoses associated with water and food.* Int J Parasitol, 2000. **30**(12-13): p. 1379-93.
54. Smith, H.V., et al., *Cryptosporidium and Giardia as foodborne zoonoses.* Vet Parasitol, 2007. **149**(1-2): p. 29-40.
55. Dawson, D., *Foodborne protozoan parasites.* Int J Food Microbiol, 2005. **103**(2): p. 207-27.
56. Nunez, F.A., M. Hernandez, and C.M. Finlay, *Longitudinal study of giardiasis in three day care centres of Havana City.* Acta Trop, 1999. **73**(3): p. 237-42.
57. Harris, L.F., *Enterococcal endocarditis: recent experience.* Ala Med, 1988. **57**(7): p. 26-32.
58. Rodriguez-Hernandez, J., A. Canut-Blasco, and A.M. Martin-Sanchez, *Seasonal prevalences of Cryptosporidium and Giardia infections in children attending day care centres in Salamanca (Spain) studied for a period of 15 months.* Eur J Epidemiol, 1996. **12**(3): p. 291-5.
59. L'Annunziata, M.F., *Radioactivity: Introduction and History*. 2007: Elsevier Science. 632.
60. Farkas, J., *Irradiation as a method for decontaminating food. A review.* Int J Food Microbiol, 1998. **44**(3): p. 189-204.
61. Gibbs, C.J., Jr., D.C. Gajdusek, and R. Latarjet, *Unusual resistance to ionizing radiation of the viruses of kuru, Creutzfeldt-Jakob disease, and scrapie.* Proc Natl Acad Sci U S A, 1978. **75**(12): p. 6268-70.
62. Miekka, S.I., et al., *Inactivation of viral and prion pathogens by gamma-irradiation under conditions that maintain the integrity of human albumin.* Vox Sang, 2003. **84**(1): p. 36-44.
63. Dubey, J.P., et al., *Effect of gamma irradiation on unsporulated and sporulated Toxoplasma gondii oocysts.* Int J Parasitol, 1998. **28**(3): p. 369-75.
64. Quan, F.S., et al., *Resistance to reinfection in rats induced by irradiated metacercariae of Clonorchis sinensis.* Mem Inst Oswaldo Cruz, 2005. **100**(5): p. 549-54.
65. Campbell, A.T. and P. Wallis, *The effect of UV irradiation on human-derived Giardia lamblia cysts.* Water Res, 2002. **36**(4): p. 963-9.
66. Flores-Perez, I., et al., *Apoptosis induced by gamma irradiation of Taenia solium metacestodes.* Parasitol Res, 2003. **90**(3): p. 203-8.
67. Lenaghan, S. and C. Sundermann, *Effect of varying cobalt-60 doses on survival and growth of Giardia lamblia trophozoites.* J Eukaryot Microbiol, 2003. **50 Suppl**: p. 701.
68. Daly, J.J., et al., *The effect of ionizing radiation on the viability of Trichomonas vaginalis.* Comp Biochem Physiol A, 1991. **98**(2): p. 259-63.

69. Kohler, B., H. Hubner, and M. Krautschick, *[The use of ionizing radiation for the decontamination of salmonella-containing slaughtered broiler chickens and powdered eggs].* Z Gesamte Hyg, 1989. **35**(11): p. 665-8.
70. Jakabi, M., et al., *Inactivation by ionizing radiation of Salmonella enteritidis, Salmonella infantis, and Vibrio parahaemolyticus in oysters (Crassostrea brasiliana).* J Food Prot, 2003. **66**(6): p. 1025-9.
71. Postmes, T., A.E. van den Bogaard, and M. Hazen, *The sterilization of honey with cobalt 60 gamma radiation: a study of honey spiked with spores of Clostridium botulinum and Bacillus subtilis.* Experientia, 1995. **51**(9-10): p. 986-9.
72. Niemira, B.A., *Irradiation sensitivity of planktonic and biofilm-associated Escherichia coli O157:H7 isolates is influenced by culture conditions.* Appl Environ Microbiol, 2007. **73**(10): p. 3239-44.
73. Clavero, M.R., et al., *Inactivation of Escherichia coli O157:H7, salmonellae, and Campylobacter jejuni in raw ground beef by gamma irradiation.* Appl Environ Microbiol, 1994. **60**(6): p. 2069-75.
74. Sommers, C.H. and G. Boyd, *Radiation sensitivity and postirradiation growth of foodborne pathogens on a ready-to-eat frankfurter on a roll product in the presence of modified atmosphere and antimicrobials.* J Food Prot, 2006. **69**(10): p. 2436-40.
75. Sullivan, R., et al., *Gamma radiation inactivation of coxsackievirus B-2.* Appl Microbiol, 1973. **26**(1): p. 14-7.
76. De Roda Husman, A.M., et al., *Calicivirus inactivation by nonionizing (253.7-nanometer-wavelength [UV]) and ionizing (gamma) radiation.* Appl Environ Microbiol, 2004. **70**(9): p. 5089-93.
77. Ravanat, J.L., T. Douki, and J. Cadet, *Direct and indirect effects of UV radiation on DNA and its components.* J Photochem Photobiol B, 2001. **63**(1-3): p. 88-102.
78. Misra, R.B., et al., *Effect of solar UV radiation on earthworm (Metaphire posthuma).* Ecotoxicol Environ Saf, 2005. **62**(3): p. 391-6.
79. Zimmer, J.L., R.M. Slawson, and P.M. Huck, *Inactivation and potential repair of Cryptosporidium parvum following low- and medium-pressure ultraviolet irradiation.* Water Res, 2003. **37**(14): p. 3517-23.
80. Mofidi, A.A., et al., *The effect of UV light on the inactivation of Giardia lamblia and Giardia muris cysts as determined by animal infectivity assay (P-2951-01).* Water Res, 2002. **36**(8): p. 2098-108.
81. Craik, S.A., et al., *Inactivation of Cryptosporidium parvum oocysts using medium- and low-pressure ultraviolet radiation.* Water Res, 2001. **35**(6): p. 1387-98.
82. Rochelle, P.A., et al., *Irreversible UV inactivation of Cryptosporidium spp. despite the presence of UV repair genes.* J Eukaryot Microbiol, 2004. **51**(5): p. 553-62.
83. John, D.E., et al., *Development and optimization of a quantitative cell culture infectivity assay for the microsporidium Encephalitozoon*

intestinalis and application to ultraviolet light inactivation. J Microbiol Methods, 2003. **52**(2): p. 183-96.
84. Huffman, D.E., et al., *Low- and medium-pressure UV inactivation of microsporidia Encephalitozoon intestinalis.* Water Res, 2002. **36**(12): p. 3161-4.
85. Rahn, R.O., *Use of potassium iodide as a chemical actinometer.* Photochem Photobiol, 1993. **58**(6): p. 874-80.
86. Slamovits, C.H. and P.J. Keeling, *Class II photolyase in a microsporidian intracellular parasite.* J Mol Biol, 2004. **341**(3): p. 713-21.
87. Oguma, K., H. Katayama, and S. Ohgaki, *Photoreactivation of Legionella pneumophila after inactivation by low- or medium-pressure ultraviolet lamp.* Water Res, 2004. **38**(11): p. 2757-63.
88. Asahina, H., et al., *Expression of a mammalian DNA photolyase confers light-dependent repair activity and reduces mutations of UV-irradiated shuttle vectors in xeroderma pigmentosum cells.* Mutat Res, 1999. **435**(3): p. 255-62.
89. Vlcek, D., S. Podstavkova, and E. Miadokova, *Interactions between photolyase and dark repair processes in Chlamydomonas reinhardtii.* Mutat Res, 1995. **336**(3): p. 251-6.
90. Weber, S., *Light-driven enzymatic catalysis of DNA repair: a review of recent biophysical studies on photolyase.* Biochim Biophys Acta, 2005. **1707**(1): p. 1-23.
91. Kim, S.T., Y.F. Li, and A. Sancar, *The third chromophore of DNA photolyase: Trp-277 of Escherichia coli DNA photolyase repairs thymine dimers by direct electron transfer.* Proc Natl Acad Sci U S A, 1992. **89**(3): p. 900-4.
92. Thoma, F., *Repair of UV lesions in nucleosomes--intrinsic properties and remodeling.* DNA Repair (Amst), 2005. **4**(8): p. 855-69.
93. Tosa, K.a.H., T., *Photoreactivation of enterohemorrhagic Escherichia coli following UV disinfection*
Water Res, 1998. **33**(2): p. 361-366.
94. Limpaiboon, T., et al., *Promoter hypermethylation is a major event of hMLH1 gene inactivation in liver fluke related cholangiocarcinoma.* Cancer Lett, 2005. **217**(2): p. 213-9.
95. Hernandez-Pigeon, H., et al., *hMutS alpha is protected from ubiquitin-proteasome-dependent degradation by atypical protein kinase C zeta phosphorylation.* J Mol Biol, 2005. **348**(1): p. 63-74.
96. Jiricny, J., *Mediating mismatch repair.* Nat Genet, 2000. **24**(1): p. 6-8.
97. Borgdorff, V., et al., *Spontaneous and mutagen-induced loss of DNA mismatch repair in Msh2-heterozygous mammalian cells.* Mutat Res, 2005. **574**(1-2): p. 50-7.
98. Regis-da-Silva, C.G., et al., *Characterization of the Trypanosoma cruzi Rad51 gene and its role in recombination events associated with the parasite resistance to ionizing radiation.* Mol Biochem Parasitol, 2006. **149**(2): p. 191-200.

99. McCulloch, R. and J.D. Barry, *A role for RAD51 and homologous recombination in Trypanosoma brucei antigenic variation.* Genes Dev, 1999. **13**(21): p. 2875-88.
100. Proudfoot, C. and R. McCulloch, *Distinct roles for two RAD51-related genes in Trypanosoma brucei antigenic variation.* Nucleic Acids Res, 2005. **33**(21): p. 6906-19.
101. Tan, K.S., S.T. Leal, and G.A. Cross, *Trypanosoma brucei MRE11 is non-essential but influences growth, homologous recombination and DNA double-strand break repair.* Mol Biochem Parasitol, 2002. **125**(1-2): p. 11-21.
102. El-Sayed, N.M., et al., *Comparative genomics of trypanosomatid parasitic protozoa.* Science, 2005. **309**(5733): p. 404-9.
103. Machado-Silva, A., et al., *Mismatch repair in Trypanosoma brucei: heterologous expression of MSH2 from Trypanosoma cruzi provides new insights into the response to oxidative damage.* Gene, 2008. **411**(1-2): p. 19-26.
104. Pena-Diaz, J., et al., *Trypanosoma cruzi contains a single detectable uracil-DNA glycosylase and repairs uracil exclusively via short patch base excision repair.* J Mol Biol, 2004. **342**(3): p. 787-99.
105. Burton, P., et al., *Ku heterodimer-independent end joining in Trypanosoma brucei cell extracts relies upon sequence microhomology.* Eukaryot Cell, 2007. **6**(10): p. 1773-81.
106. Fernandez Villamil, S.H., et al., *TcPARP: A DNA damage-dependent poly(ADP-ribose) polymerase from Trypanosoma cruzi.* Int J Parasitol, 2008. **38**(3-4): p. 277-87.
107. McKean, P.G., et al., *Identification and characterisation of a RAD51 gene from Leishmania major.* Mol Biochem Parasitol, 2001. **115**(2): p. 209-16.
108. Misra, S., M. Hall, 3rd, and G. Chaudhuri, *Molecular characterization of a human BRCA2 homolog in Leishmania donovani.* J Parasitol, 2005. **91**(6): p. 1492-5.
109. Taladriz, S., et al., *Nuclear DNA polymerase beta from Leishmania infantum. Cloning, molecular analysis and developmental regulation.* Nucleic Acids Res, 2001. **29**(18): p. 3822-34.
110. Vidal, A.E., et al., *Crystal structure and DNA repair activities of the AP endonuclease from Leishmania major.* J Mol Biol, 2007. **373**(4): p. 827-38.
111. Gallego, C., et al., *Overexpression of AP endonuclease protects Leishmania major cells against methotrexate induced DNA fragmentation and hydrogen peroxide.* Mol Biochem Parasitol, 2005. **141**(2): p. 191-7.
112. Bhattacharyya, M.K. and N. Kumar, *Identification and molecular characterisation of DNA damaging agent induced expression of Plasmodium falciparum recombination protein PfRad51.* Int J Parasitol, 2003. **33**(12): p. 1385-92.
113. Triglia, T., et al., *Amplification of the multidrug resistance gene pfmdr1 in Plasmodium falciparum has arisen as multiple independent events.* Mol Cell Biol, 1991. **11**(10): p. 5244-50.

114. Deitsch, K.W., A. del Pinal, and T.E. Wellems, *Intra-cluster recombination and var transcription switches in the antigenic variation of Plasmodium falciparum.* Mol Biochem Parasitol, 1999. **101**(1-2): p. 107-16.
115. Buguliskis, J.S., et al., *Expression and biochemical characterization of Plasmodium falciparum DNA ligase I.* Mol Biochem Parasitol, 2007. **155**(2): p. 128-37.
116. Nunthawarasilp, P., S. Petmitr, and P. Chavalitshewinkoon-Petmitr, *Partial purification and characterization of DNA polymerase beta-like enzyme from Plasmodium falciparum.* Mol Biochem Parasitol, 2007. **154**(2): p. 141-7.
117. Bethke, L., et al., *The role of DNA mismatch repair in generating genetic diversity and drug resistance in malaria parasites.* Mol Biochem Parasitol, 2007. **155**(1): p. 18-25.
118. Belosevic, M., et al., *Studies on the resistance/reactivation of Giardia muris cysts and Cryptosporidium parvum oocysts exposed to medium-pressure ultraviolet radiation.* FEMS Microbiol Lett, 2001. **204**(1): p. 197-203.
119. Linden, K.G., et al., *UV disinfection of Giardia lamblia cysts in water.* Environ Sci Technol, 2002. **36**(11): p. 2519-22.
120. Betancourt, W.Q. and J.B. Rose, *Drinking water treatment processes for removal of Cryptosporidium and Giardia.* Vet Parasitol, 2004. **126**(1-2): p. 219-34.
121. Rand, J.L., et al., *A field study evaluation for mitigating biofouling with chlorine dioxide or chlorine integrated with UV disinfection.* Water Res, 2007. **41**(9): p. 1939-48.
122. Sauch, J.F., et al., *Propidium iodide as an indicator of Giardia cyst viability.* Appl Environ Microbiol, 1991. **57**(11): p. 3243-7.
123. Smith, A.L. and H.V. Smith, *A comparison of fluorescein diacetate and propidium iodide staining and in vitro excystation for determining Giardia intestinalis cyst viability.* Parasitology, 1989. **99 Pt 3**: p. 329-31.
124. Thompson, R.C. and P.T. Monis, *Variation in Giardia: implications for taxonomy and epidemiology.* Adv Parasitol, 2004. **58**: p. 69-137.
125. Andrews, R.H., et al., *Giardia intestinalis: electrophoretic evidence for a species complex.* Int J Parasitol, 1989. **19**(2): p. 183-90.
126. Mayrhofer, G., et al., *Division of Giardia isolates from humans into two genetically distinct assemblages by electrophoretic analysis of enzymes encoded at 27 loci and comparison with Giardia muris.* Parasitology, 1995. **111 (Pt 1)**: p. 11-7.
127. Monis, P.T., et al., *Genetic diversity within the morphological species Giardia intestinalis and its relationship to host origin.* Infect Genet Evol, 2003. **3**(1): p. 29-38.
128. Li, D., et al., *Comparison of levels of inactivation of two isolates of Giardia lamblia cysts by UV light.* Appl Environ Microbiol, 2007. **73**(7): p. 2218-23.

129. Keister, D.B., *Axenic culture of Giardia lamblia in TYI-S-33 medium supplemented with bile.* Trans R Soc Trop Med Hyg, 1983. **77**(4): p. 487-8.
130. Li, L., M. Story, and R.J. Legerski, *Cellular responses to ionizing radiation damage.* Int J Radiat Oncol Biol Phys, 2001. **49**(4): p. 1157-62.
131. King, D.A., M.W. Sheafor, and J.K. Hurst, *Comparative toxicities of putative phagocyte-generated oxidizing radicals toward a bacterium (Escherichia coli) and a yeast (Saccharomyces cerevisiae).* Free Radic Biol Med, 2006. **41**(5): p. 765-74.
132. Du, J. and J.M. Gebicki, *Proteins are major initial cell targets of hydroxyl free radicals.* Int J Biochem Cell Biol, 2004. **36**(11): p. 2334-43.
133. Li, L. and C.C. Wang, *A likely molecular basis of the susceptibility of Giardia lamblia towards oxygen.* Mol Microbiol, 2006. **59**(1): p. 202-11.
134. Campbell, J.D. and G.M. Faubert, *Comparative studies on Giardia lamblia encystation in vitro and in vivo.* J Parasitol, 1994. **80**(1): p. 36-44.
135. Peterson, D.G., B.W. Larson, and J.F. Barlow, *Thirteen month old Caucasian male admitted with extreme pallor.* S D J Med, 1984. **37**(10): p. 15-9.
136. Porter, J.D., et al., *Food-borne outbreak of Giardia lamblia.* Am J Public Health, 1990. **80**(10): p. 1259-60.
137. Robinson, R.D., et al., *Gastrointestinal parasitic infection in healthy Jamaican carriers of HTLV-I.* J Trop Med Hyg, 1991. **94**(6): p. 411-5.
138. Fraser, D., *Epidemiology of Giardia lamblia and Cryptosporidium infections in childhood.* Isr J Med Sci, 1994. **30**(5-6): p. 356-61.
139. Brodsky, R.E., H.C. Spencer, Jr., and M.G. Schultz, *Giardiasis in American travelers to the Soviet Union.* J Infect Dis, 1974. **130**(3): p. 319-23.
140. Black, R.E., *Epidemiology of travelers' diarrhea and relative importance of various pathogens.* Rev Infect Dis, 1990. **12 Suppl 1**: p. S73-9.
141. Okhuysen, P.C., *Traveler's diarrhea due to intestinal protozoa.* Clin Infect Dis, 2001. **33**(1): p. 110-4.
142. Lujan, H.D., et al., *Developmental induction of Golgi structure and function in the primitive eukaryote Giardia lamblia.* J Biol Chem, 1995. **270**(9): p. 4612-8.
143. Marti, M., et al., *The secretory apparatus of an ancient eukaryote: protein sorting to separate export pathways occurs before formation of transient Golgi-like compartments.* Mol Biol Cell, 2003. **14**(4): p. 1433-47.
144. Ghosh, S., et al., *How Giardia swim and divide.* Infect Immun, 2001. **69**(12): p. 7866-72.
145. McArthur, A.G., et al., *The Giardia genome project database.* FEMS Microbiol Lett, 2000. **189**(2): p. 271-3.
146. Jarroll, E.L., A.K. Bingham, and E.A. Meyer, *Effect of chlorine on Giardia lamblia cyst viability.* Appl Environ Microbiol, 1981. **41**(2): p. 483-7.
147. Leahy, J.G., A.J. Rubin, and O.J. Sproul, *Inactivation of Giardia muris cysts by free chlorine.* Appl Environ Microbiol, 1987. **53**(7): p. 1448-53.

148. Li, D., et al., *Survival of Giardia lamblia trophozoites after exposure to UV light.* FEMS Microbiol Lett, 2008. **278**(1): p. 56-61.
149. Labatiuk, C.W., et al., *Comparison of animal infectivity, excystation, and fluorogenic dye as measures of Giardia muris cyst inactivation by ozone.* Appl Environ Microbiol, 1991. **57**(11): p. 3187-92.
150. Wickramanayake, G.B., A.J. Rubin, and O.J. Sproul, *Inactivation of Giardia lamblia cysts with ozone.* Appl Environ Microbiol, 1984. **48**(3): p. 671-2.
151. Haas, C.N. and B. Kaymak, *Effect of initial microbial density on inactivation of Giardia muris by ozone.* Water Res, 2003. **37**(12): p. 2980-8.
152. Ramesh, M.A., S.B. Malik, and J.M. Logsdon, Jr., *A phylogenomic inventory of meiotic genes; evidence for sex in Giardia and an early eukaryotic origin of meiosis.* Curr Biol, 2005. **15**(2): p. 185-91.

CHAPTER 2

EFFECT OF VARYING COBALT-60 DOSES ON SURVIVAL AND GROWTH OF *GIARDIA LAMBLIA* TROPHOZOITES

INTRODUCTION

Giardia lamblia is a parasitic flagellate of the gastrointestinal tract of mammals and some birds. In humans in the United States, giardiasis is one of the most common intestinal diseases caused by a protozoan, and infection is even more prevalent in many developing countries [1,2]. Transmission occurs when cysts are accidentally ingested, and most outbreaks have been associated with contaminated drinking water and/or contaminated food such as fruits and vegetables [6,7]. Methods for chemical disinfection of drinking water aimed at cyst inactivation have been well studied. Methods utilizing ionizing radiation for food disinfection have received less attention. Gamma (γ) irradiation has previously been shown to inactivate a large number of bacterial pathogens that could potentially contaminate food, including *Campylobacter, Listeria, Salmonella, Shigella,* and *Staphylococcus* [3]. In addition, γ-irradiation has been shown to inactivate the oocysts of *Toxoplasma gondii* on fruits [4] and *Cryptosporidium parvum* in water [8]. The present study was undertaken to investigate the viability of *G. lamblia* trophozoites after exposure to low dose,

ionizing radiation from a cobalt-60 source and to investigate if evidence of cellular damage due to irradiation can be visualized with light microscopy.

MATERIALS AND METHODS

Trophozoites of *G. lamblia* WB strain were grown in glass culture tubes in modified Keister's medium at 37^0C [5]. Three days after inoculation, the cultures achieved maximum cell density ~$1.6x10^6$ cells/ml. At this time, the ratio of living:dead cells was determined microscopically, and the cultures were each then exposed a cobalt-60 irradiation source (Leach Nuclear Science Center, Auburn University). The doses, 0.25, 1.0, 7.0, and 10.0 kGy were calculated by using the known power of the radiation source times the exposure time. Control cultures were not irradiated (0 kGy). After irradiation, small aliquots were removed from each tube and examined by Nomarski interference contrast (NIC) microscopy. The first 600 cells were scored as either viable or dead in order to ascertain the percent of cells immediately killed by the radiation exposure. Cellular damage was noted during microscopic examination. Also, 0.2 ml of each sample was equally divided into two tubes of fresh Keister's medium and placed at 37^oC. The tubes were monitored daily for growth, and the time required for each culture to again reach maximum cell density. Each irradiation dose was characterized into three responses: (a) lethal with immediate visual cell death (b) debilitating in that not all cells were killed immediately but damaged cells could not recover and divide and (c) debilitating but cells could recover and divide and thus the culture and its subcultures recovered.

RESULTS AND DISCUSSION

In unirradiated controls, 30% of the trophozoites were dead. The control cultures returned to maximum cell density in one day, and subcultures, started immediately after irradiation, grew to a maximum density and then began to decline in 3–4 days based on observations of motile cells. Irradiation at 10.0 kGy caused immediate death of all cells. No motile cells were observed immediately after irradiation or several days later. NIC microscopy revealed that cell shapes were abnormal, membrane blebbing was pronounced, intact flagella were scarce, and nuclei were not identifiable in most cells (Figure 1).

Figure 1. NIC micrographs of *G. lamblia* trophozoites.

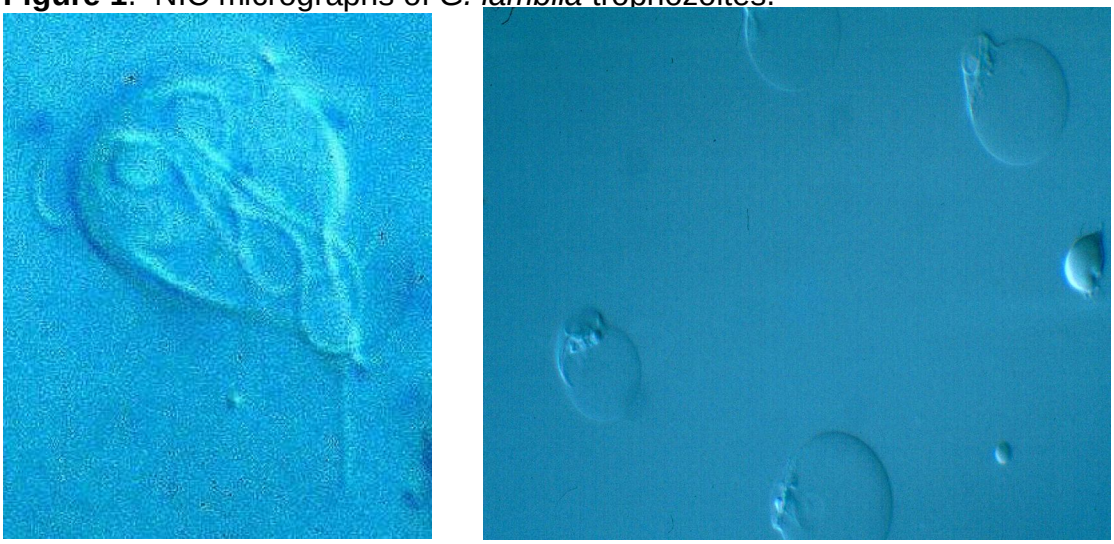

After the 7.0 kGy exposure, 79% of the cells were dead, and membrane blebbing was observed. The surviving cells could not divide, and no growth occurred in these cultures whether or not they were subcultured. After the1.0 kGy exposure, 61% of the cells were dead. Cellular damage was not visible by NIC microscopy and subcultures of the irradiated culture attained maximum density 14–21 days

Figure 1. Trophozoites of *Giardia lamblia* showing normal cellular morphology (left) and after 10 kGy of gamma-radiation, demonstrating membrane blebbing in a majority of the cells (right).

Table 1. Effects of varying doses on trophozoites of *Giardia lamblia*.

Dose (kGy)	**Gross Appearance**	**Microscopic Appearance**	**Immediate Subculturing**	**No subculture**	**Results**
Control	All Swimming or attached	Normal shape, all structures visible	Max. density achieved in 3-5 days	Population crashes in one day	Control Dose
0.25	80% still swimming, 20% attached	Normal shape, all structures visible	Max. density achieved in 5-7 days	Population crashes in 2-3 days	Recovery Dose
1	50% still swimming, none attached	Normal shape, all structure visible	Max. density achieved in 2-3 weeks	Population crashes in 4-8 days	Recovery Dose
7	No swimming	Normal shape,often lesion near nucleus	No growth recorded	No growth	Lethal Dose
10	No swimming	Cells appear to be melted, very few intact cells	No growth recorded	No growth	Lethal Dose

Table 1. Effects of varying doses of gamma-radiation on trophozoites of *Giardia lamblia.* Gross appearance of trophozoites on inverted microscope was observed, and attachment was measured. Microscopic appearance was determined using wet mounts and observing cells with NIC microscopy. Subculturing techniques were used to determine if the trophozoite population was able to recover.

after inoculation. The 0.25 kGy dose had similar numbers of dead cells to the negative controls, ~30%. These cultures reached maximum density in 2–3 days, and the subcultures required 6–7 days to reach maximum density (Table 1). It appears that cells were probably damaged at this dose in that the culture required more days to reach maximum density, but obviously some cells recovered and then divided. A similar trend was seen with trophozoites treated with 1.0 kGy, after 2-3 weeks the cultures recovered to achieve maximum density. Although the 7.0 kGy dose did not immediately kill all cells, survivors could not repair cellular damage and therefore could not divide, thus this dose was debilitating to trophozoites and eventually lethal to the culture. In order to guarantee that *Giardia lamblia* trophozoites are killed for the purposes for disinfection, it was determined that doses of 7 kGy and above must be used. Trophozoites treated with doses of 0.25-1 kGy were able to recover and regain the ability to grow *in vitro*. Continued research is necessary to ensure that doses of γ-irradiation chosen for disinfection are appropriate at effectively inactivating *Giardia lamblia*. With the emergence of new *Giardia lamblia* assemblages, a need to determine inactivation doses for both multiple isolates and the environmentally resistant cyst stage will be important.

LITERATURE CITED

1. Adam, R.D. 1991. The biology of *Giardia* spp. Microbiol. Rev., 55:706–732.
2. Adam, R.D. 2001. Biology of *Giardia lamblia*. Clin. Microbiol. Rev., 14: 447–475.
3. Clavero, M.R., Monk, J.D., Beuchat, L.R., Doyle, M.P. & Brackett, R.E. 1994. Inactivation of *Escherichia coli* O157:H7, *Salmonella* and *Campylobacter jejuni* in raw ground beef by gamma irradiation. Appl. Environ. Microbiol., 60:2069–2075.
4. Dubey, J.P., Thayer, D.W., Speer, C.A. & Shen, S.K. 1998. Effect of gamma irradiation on unsporulated and sporulated *Toxoplasma gondii* oocysts. Int. J. Parasitol., 28:369–375.
5. Keister, D.B. 1983. Axenic cultivation of Giardia lamblia in TYI-S-33 medium supplemented with bile. Trans. Royal Soc. Trop. Med. Hyg., 77: 487–488.
6. Mintz, E.D., Hudson-Wragg, M., Cartter, M.L. & Hadler, J.L. 1993. Foodborne giardiasis in a corporate office setting. J. Infect. Dis., 167:250–253.
7. Thompson, R.C.A. 2000. Giardiasis as a reemerging infectious disease and its zoonotic potential. Int. J. Parasitol., 30:1259–1267.
8. Yu, J.R. & Park, W.Y. 2003. The effect of gamma-irradiation on *Cryptosporidium parvum*. J. Parasitol., 89:639–642

CHAPTER 3

GIARDIA LAMBLIA TROPHOZOITE RADIATION RESISTANCE *IN VITRO*

ABSTRACT

New water treatment strategies under development include ultraviolet (UV) and gamma (γ) irradiation. Fruits and vegetables are also being irradiated with the advantage that there is no residue or toxic byproduct of disinfection by these processes. The *Giardia lamblia* trophozoite stage was found to be more resistant to ionizing radiation than the cyst form. The observed resistance levels for 5 different isolates are also higher than the current FDA standards for both UV and γ irradiation. While this stage is not as environmentally resistant as the cyst form, it can survive for some time, suggesting that the treatment dose levels require re-evaluation. A new, higher throughput method for generating statistically significant survival curves for *G. lamblia* is also described. It was also determined using both the traditional glass tube assay, and a 96 well plate assay, that the doses required for the same level of inactivation varied between the isolates and were different between MMS and γ–irradiation treatments. The D3 isolate was statistically, the most sensitive to γ-irradiation, while the GS-M isolate

was the most sensitive to MMS. No observable physical damage was observed with scanning electron microscopy, however by transmission electron microscopy, degranulation of cytoplasm and lamellar bodies was observed after lethal doses of 7 kGy and above. The 96 well plate assay proved an effective means of statistically determining inactivation levels, of a large sample size.

INTRODUCTION

Giardiasis is the most common gastrointestinal disease of protozoal etiology in the world [49]. Members of *Giardia sp.* are one of the most important enteric parasites in the world with species infecting a wide range of organisms including birds, reptiles, and mammals. Infection occurs through ingestion of environmentally stable cysts and the subsequent attachment of trophozoites to the intestinal mucosa.

Disinfection protocols aimed at *Giardia* inactivation in water supplies using ultraviolet irradiation are under development and on fruits and vegetables using γ-irradiation because of the low cost and lack of residue. Ultraviolet light at 254 nm has produced a greater than 3 log *Giardia lamblia* cyst inactivation at doses ranging from 3-40 mJ/cm^2 in a variety of delivery systems ([118],[65],[80],[119]). Combinations of chemical and ultraviolet irradiation have also been used by a variety of researchers to increase the potency ([120, 121]). Similarly, γ irradiation has been shown to inactivate cysts at 0.25 kGy (C. Sundermann, unpublished), and trophozoites at doses greater than 7 kGy [67]. Determination of the inactivation dose for all of the cyst studies used the Mongolian gerbil (*Meriones*

unguiculatus) *in vivo* infectivity assay. This method represents the "gold-standard" for determining cyst infectivity, but is not a quantitative assay. Other viability assays using fluorescent dyes and excystation frequencies have proven unreliable in quantitatively determining cyst viability [65, 122, 123]. Trophozoite inactivation is more easily directly measured by allowing treated cells to grow in media and determining the number of surviving cells that can attach and replicate over time. Our studies have found that trophozoites are more resistant to both γ and UV irradiation than cysts and depending on the isolate, often require doses 10-100 fold greater to achieve the same inactivation level . Therefore it seems logical to use the trophozoite form instead of cysts for inactivation studies. This would reduce costs, increase sensitivity and specificity, and omit animal use.

Inactivation studies of *Giardia lamblia* are further complicated by genotypic evidence that a minimum of 7 distinct assemblages (or subtypes) exist (currently distinguished by a variety of PCR techniques) [124]. These assemblages have varying levels of host-specificity, and potential virulence. Assemblages A and B and their subtypes are the only isolates originally from humans, although they have been isolated other mammals ranging from companion animals to whales. Researchers, through a variety of molecular techniques, have shown that the genetic distance separating these two assemblages exceeds that used to separate other species of protists, suggesting that perhaps the different assemblages should be classified as different species [125-127], [24]. Isolate comparisons in disinfection studies are not commonly reported, but if the different assemblages are very different genetically, it is likely that different sensitivities to

disinfection will be found. A recent study showed that there were differences in cyst infectivity between the WB and H3 isolates after treatment with UV light [128]. This finding emphasizes the need to re-evaluate common disinfection methods using multiple isolates.

The first goal of this study was to determine what types of damage to the cytoskeleton were caused by increasing doses of γ irradiation. The second goal of this study was to evaluate inactivation levels of five different *Giardia* isolates to methyl methane sulfonate (MMS), a commonly used radiomimetic that is also an alkylating agent, and to γ irradiation. The final goal was to optimize the method for determining trophozoite inactivation that is statistically significant, reproducible, and less time consuming than enumeration with a hemacytometer.

MATERIALS AND METHODS

Trophozoite cultivation and chemicals. The isolates used in this work (Table 1) were obtained from the American Type Culture Collection (ATCC).

Table 1. ATCC Isolates of *Giardia lamblia*

Name	**ATCC#**	**Source**	**Reference**
WB	30957	Human	Gillin 1983
WB-C6	50803	WB Clone	Reiner 1993
Portland-1 (P-1)	30888	Human female	Gillin 1980
GS-M	50580	Human	Nash 1985
D3	203334	Dog	Beverly Sheridan, pers. comm. 1986

Table 1. ATCC isolates of *Giardia lamblia* with the original reference and the source isolated from.

Trophozoites were grown axenically at 37^{o}C in 13 x 100 mm screw capped glass culture tubes in Modified Keister's Medium [129]. The cultures were passaged every 3-4 days by making a 1/10 dilution into fresh media after detachment of trophozoites from the glass by chilling on ice for 15 minutes. Parasite numbers were determined by counting 10 μl aliquots of the detached parasites in a hemacytometer. Chemicals were of reagent grade unless otherwise indicated. Methyl methane sulfonate (MMS) was purchased from Sigma-Aldrich Co.

γ Irradiation. Late, logarithmic stage cultures (75% confluence) were chilled, centrifuged, and resuspended in PBS at a concentration of 1x10^{6} cells/ml, aliquoted into sterile 1.5 ml microfuge tubes, and placed on ice. A cobalt 60 (Co^{60}) source was used to deliver various γ-radiation doses. The source output at the distance used for this work was 7,000 Rad/min or 70 Grey (Gy)/min. Doses were determined based on the time exposed to the source. Doses of 0, 78, 156, 312, 625, 1250, 2500, and 5000 Gy were chosen based on results from a previous study [67]. Trophozoites were kept on ice during irradiation and until all doses were completed. Each sample was then subcultured 1/9 into fresh medium, and survival was evaluated over time by counting viable parasites with a hemacytometer. All measurements were conducted in triplicate.

Transmission Electron Microscopy Trophozoites of the WB isolate ($1x10^7$) were concentrated by slow speed centrifugation at 1000 x g immediately after irradiation and resuspended in 100 ul of molten 1% low melting point agarose at 37^oC. The agarose mixture was then pipetted onto parafilm strips in 25 ul increments and allowed to solidify at 4^0C for 30 minutes. Primary fixation was with 2% glutaraldehyde in phosphate buffer for 1 hour (4^oC). Samples were then washed three times in 0.1M phosphate buffer with 5% sucrose. After primary fixation, the samples were placed in 1% osmium tetroxide in phosphate buffer for 1 hour and then washed with distilled water. The preparation was dehydrated through an ascending series of ethanols (55%-100%) and infiltrated with Spurr's resin using ascending concentrations of Spurr's in 100% ethanol, and finally infiltrated and embedded with 100% resin. The preparation was cured at 70^0C overnight. Thin sections (70nm) were stained with uranyl acetate and lead citrate and viewed with a Philips transmission electron microscope at 60kv.

Scanning Electron Microscopy. Trophozoites were concentrated as described previously and fixed in 2% glutaraldehyde. Cells were then pipetted into 30 µm microporous specimen capsules (EMS 0187-20); all subsequent procedures were carried out in these capsules. Dehydration used an increasing series of alcohols, and the samples were then dried in an EMS 850 Critical Point Dryer. After drying, samples were removed from the capsules and placed on aluminum stubs with double-sided carbon tape. Sputter coating was accomplished in a

Pelco SC-7 Sputter Coater. Samples were then analyzed on a Zeiss DSM 940 scanning electron microscope.

MMS. Parasites grown to a density of approximately 1 X 10^6 cells/ml were incubated on ice to detach the parasites and then centrifuged at 2,000 X g for 10 minutes. The medium was removed with a pipet and the trophozoites were resuspended in sterile phosphate buffered saline (PBS) to a density of 1x10^6 cells/ml and placed on ice. MMS was added to a sterile 1.5 ml microfuge tube to create an initial dilution of 1% in 100 μl PBS and then serially diluted 2-fold in PBS with a final volume of 100 μl in each dilution tube. After warming the MMS tubes to 37°C, 900 μl of the trophozoite suspension were added to create the final dilution series from 0.1 to 0.00156 % MMS. A tube with only PBS was the no MMS control tube. The tubes were then incubated for 10 minutes at 37°C. Sterile sodium thiosulfate (100 μl) was added to the tubes to a 0.5% final dilution and incubated for 10 minutes at room temperature to inactivate the MMS. This was conducted for each isolate in triplicate. Aliquots were then taken for the following assays.

96 Well Plate Assay

Plates were prepared prior to the start of MMS treatment by the addition of 200 μl of fresh media to each well. 10 μl of treated trophozoites (1 X 10^4) were added to the first well of each row and serially diluted 5-fold across 6 wells in quadruplicate for each dose with a multi-channel pippetor. The plates were then

placed individually into double layered quart sized Zip-Loc® freezer bags and sparged with N_2 gas at least 3 times, expelling the gas from the bag between each flush and finally maintaining a slight positive pressure before sealing. After incubating at 37°C for 72 hours, plates were scored by determining if any trophozoites were moving in each well. If trophozoites were moving, then a + was assigned to the well, and if no trophozoites were moving, a – was assigned. Movement was characterized by swimming trophozoites, or the movement of flagella in cells attached to the plastic. Survival frequencies were determined by the method of Reed and Muench (19) where the lowest dilution which had at least one survivor was counted as positive. The % control was determined by averaging the 4 values in comparison to the control wells.

Glass Tube Assay

The remainder of the treated parasites from each dose, approximately $1x10^6$ trophozoites, was added to fresh tubes of media and allowed to incubate at 37°C for 72 hours. After detachment by chilling, motile trophozoites were counted using a hemacytometer. The percent control was determined by dividing the total number of motile trophozoites in each tube by the total number of motile trophozoites in the control tubes.

RESULTS

Scanning Electron Microsopy.

At γ-radiation doses of 0.25 and 1-kGy, trophozoites maintained normal "teardrop" shape and had ultrastructural features similar to the unirradiated controls. The surface of the adhesive disc was uniform, without membrane blebbing. The only damage found on the adhesive disc was a C-shaped protrusion, an artifact of attachment also seen in control samples. In addition, the ventrolateral flange present on many trophozoites was of uniform size and shape. All flagella were in the proper location and were free from obvious damage. At a dose of 7-kGy, membrane blebbing was observed on the outer surface of the trophozoite on both the dorsal and ventral surfaces, and on the surface of the adhesive disc (Figure 1). No cell membrane breaks were observed. Flagella were in the proper location, and undamaged even at the 7-kGy dose (Figure 1).

Transmission Electron Microscopy. The γ-radiation doses ranged from 0.25-kGy to 7 kGy. Previous studies showed that 0.25 and 1 kGy doses were "recovery doses", where the parasite could recover and replicate (9). The 7 kGy and higher doses were found to be lethal to all cells. The ultrastructure of trophozoites receiving recovery doses differed little from that of non-irradiated, control trophozoites. The tubulin structure of the adhesive disc remained intact with normal spacing and number of microtubules. The bare region of the disc

Figure 1. Scanning electron micrographs of control and irradiated trophozoites.

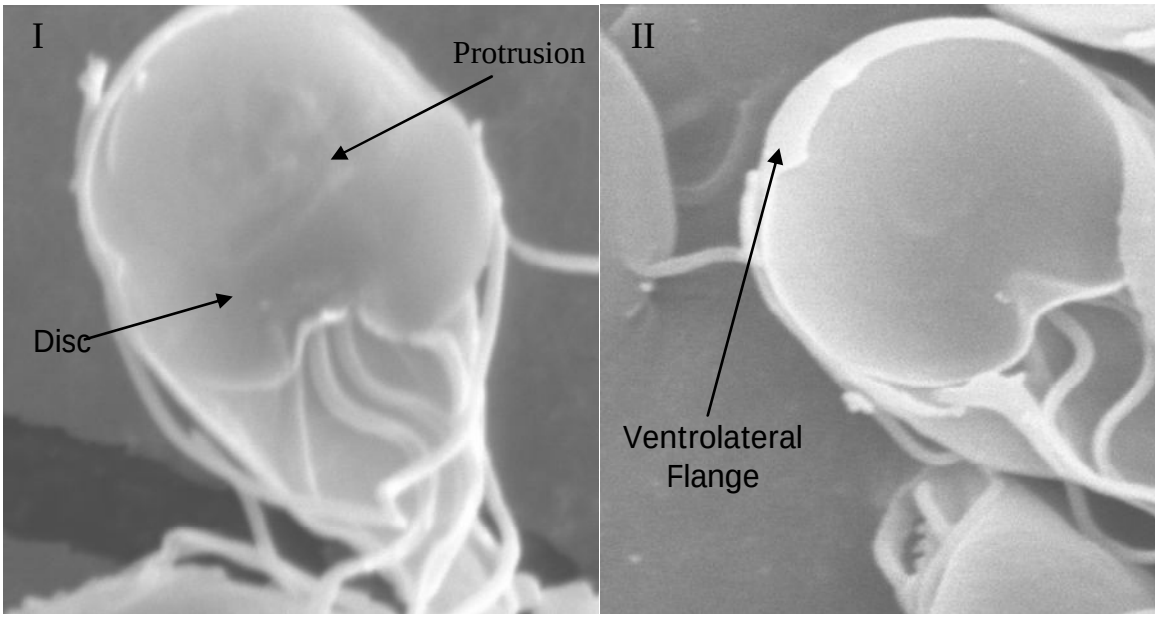
I
Protrusion
Disc
II
Ventrolateral
Flange

Figure 1. I.) Control trophozoite showing normal ultrastructure. II.) 7-kGy irradiated trophozoite demonstrating no apparent ultrastructural damage.

also showed similarity in both width and length between the recovery and control cells. Additionally, there were similar numbers of peripheral vesicles. The axonemes maintained the characteristic “9+2” microtubule arrangement, and their number and position within the cells were similar to non-irradiated controls (Figure 2). There were no discontinuities in the nuclear membrane for the recovery doses, and all maintained a more or less uniform oblong to circular shape consistent with that observed in the negative control cells. The cytoplasm retained its grainy appearance due to normal ribosomal content, although there were some slightly vacuolated areas in the recovery dose trophozoites (Figure 2).

The lethal doses resulted in several abnormalities at the ultrastructural level. There was severe degranulation due to a heavy loss of ribosomal content, a characteristic of damage by γ–radiation. There was also an increase in the peripheral vesicle size; however, there was no difference in peripheral vesicle numbers when compared to control cells (Figure 2). The structure of the adhesive disc remained consistent with that of the non-irradiated control cells. In a few trophozoites, lamellar structures resulting from membrane disruption could be seen. While peripheral vesicles were enlarged, there was no macro-vacuolarization in the cytoplasm, often evident in cells suffering from high radiation doses.

Figure 2. Transmission electron micrographs of irradiated trophozoites.

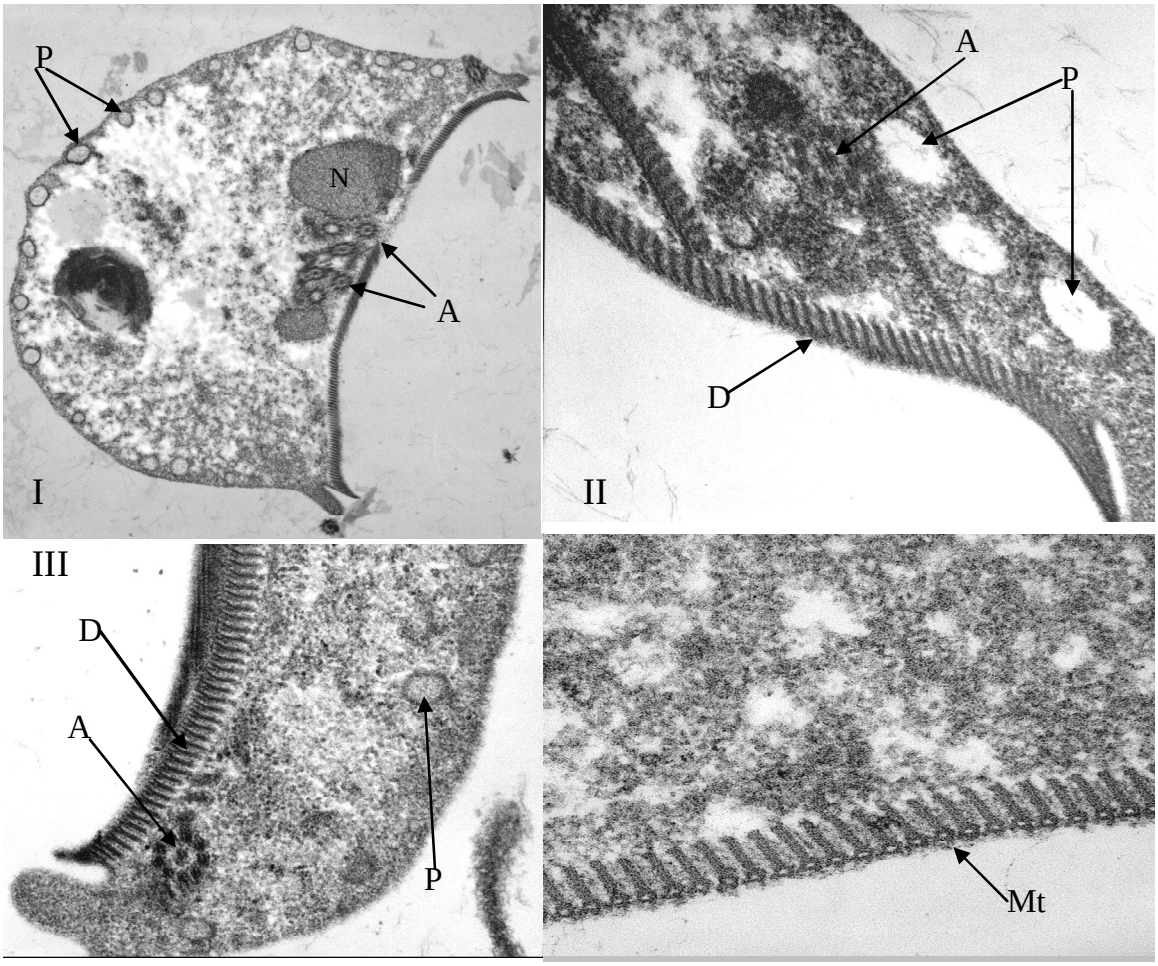

The nuclear structure of the 7-kGy-treated trophozoites did not differ from the controls, and the nuclear membrane remained intact.

γ-Irradiation Survival Curves. Dose response curves for each of the 5 *Giardia* isolates were created to determine their sensitivity to γ-irradiation (Figure 3). For all isolates, a greater dose (>250 Gy) was required for total inactivation than was observed previously for cysts (C. Sundermann, unpublished). Equations for the slopes of the survival curves, along with R^2 values are shown in Table 2. In order

Figure 2. I.) 7-kGy-irradiated trophozoite showing cytoplasmic degranulation. II.) 7-kGy irradiated trophozoite showing peripheral vesicles (P), axoneme (A), and adhesive disc. III.) Control trophozoite with axoneme, peripheral vesicle, and adhesive disc. IV.) 0.25 kGy irradiated trophozoite showing the normal adhesive disc microtubule arrangement.

to determine the sensitivity of the isolates to γ irradiation, the dose corresponding to a surviving fraction of 50, 37, and 10% (D50, D37, D10) was calculated using the equation for an exponential survival curve, $S = e^{-kD}$. In addition, the inactivation constant, k, was calculated at each of these doses (Table 2) (19).

Table 2. Dose Response Curves after γ-irradiation

Isolate	Slope	R^2	D50	D37	D10	K50	K37	K10
WB	y = 4E+06x-2.5036	0.8394	91	102	173	0.0076	0.0097	0.0133
WB-C6	y = 3E+06x-2.365	0.8303	105	119	207	0.0066	0.0084	0.0111
P-1	y = 9E+06x-2.6889	0.9534	90	101	164	0.0077	0.0098	0.014
GS-M	y = 2E+07x-2.8569	0.9402	91	101	160	0.0076	0.0098	0.0144
D3	y = 2E+06x-2.8093	0.6328	43	48	77	0.0161	0.0207	0.0299

The dose required for 50% killing for the isolates WB, P1, and GS-M ranged from 90-91 Gy and the WB-C6 isolate was less sensitive with a D50 of 101 Gy and the D3 isolate was most sensitive with a D50 of 43 Gy.

MMS sensitivity: Plate vs Tube Inactivation Methods. Dose response curves for each of the 5 isolates of *Giardia* trophozoites were created to determine the level of MMS sensitivity, as assayed by both the glass tube and 96-well plate assays (Figures 4 and 5). Equations for the survival curve slopes and R^2 values, along with D50, D37 and D10 values and inactivation constants are shown in Table 3. Similar to the γ-irradiation results, the WB, P1, and GS-M ranged from 0.01-0.012%. Unlike the γ-irradiation results, the D3 isolate was less sensitive to MMS 0.03% and the WB-C6 isolate was more sensitive at a dose of 0.008%.

Table 2. Survival after γ-irradiation. Survival curves were generated in Microsoft Excel using the trendline function. The greater the k value, the more sensitive the isolate to γ-irradiation. Radiation doses are given in Gy.

Table 3. MMS Dose Response Curve Analysis

Plate Assay

Isolate	Slope	R^2	D50	D37	D10	K50	K37	K10
WB	y = 123.59e-86.241x	0.9754	0.01	0.014	0.029	69.3	71.0	79.4
WB-C6	y = 74.745e-49.629x	0.7959	0.008	0.014	0.04	86.6	71.0	57.6
P-1	y = 84.017e-43.082x	0.9819	0.012	0.019	0.049	57.8	52.3	47
GS-M	y = 133.42e-86.603x	0.9749	0.011	0.015	0.03	63.0	66.3	76.7
D3	y = -34.096Ln(x) - 68.41	ND	0.03	0.045	0.1	23.1	22.1	23.0

Tube Assay

WB	y = 123.31e-96.751x	0.9863	0.009	0.012	0.026	77.0	82.8	88.6
WB-C6	y = 112.41e-96.676x	0.9806	0.008	0.011	0.025	86.6	90.4	92.1
P-1	y = 178.74e-82.786x	0.9843	0.015	0.019	0.035	46.2	52.3	65.8
GS-M	y = 117.66e-110.24x	0.8302	0.008	0.01	0.022	86.6	99.4	104.7
D3	y = 138.35e-99.555x	0.9757	0.01	0.013	0.026	69.3	76.5	88.6

Table 3. Dose Response survival analysis after MMS treatment. Curves were generated in Microsoft Excel using the trendline function. The greater the k value, the more sensitive the isolate was to MMS. Doses = % MMS. ND = Not determined.

Figure 3. Dose Response Curves for 5 *Giardia* isolates after γ-irradiation

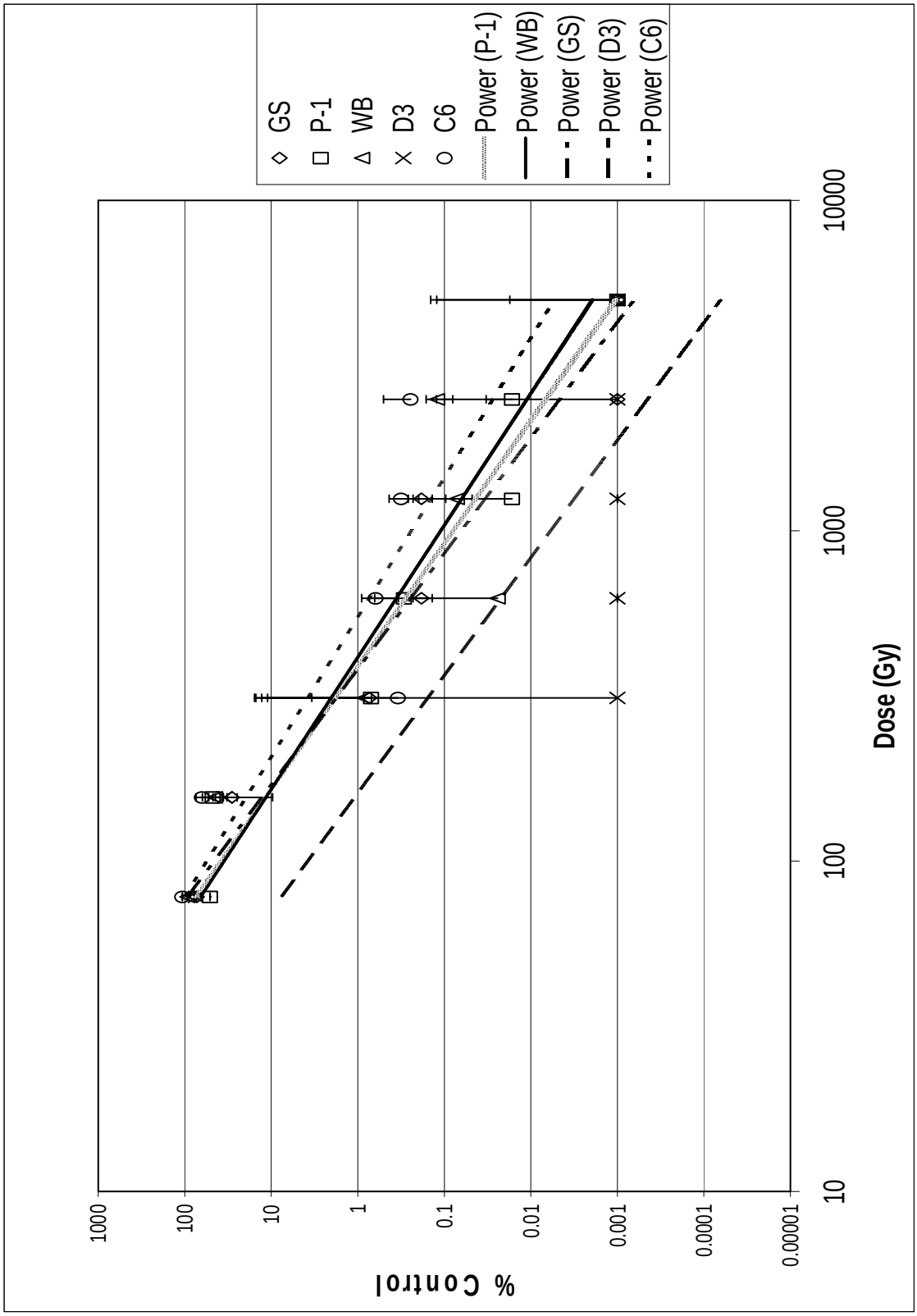

Figure 3. Dose Response curves for *Giardia* isolates to γ-irradiation. Each point is shown along with standard error bars. A trendline was calculated using Excel.

Figure 4. Dose Response Curves of 5 *Giardia* Isolates to MMS (Tube Assay)

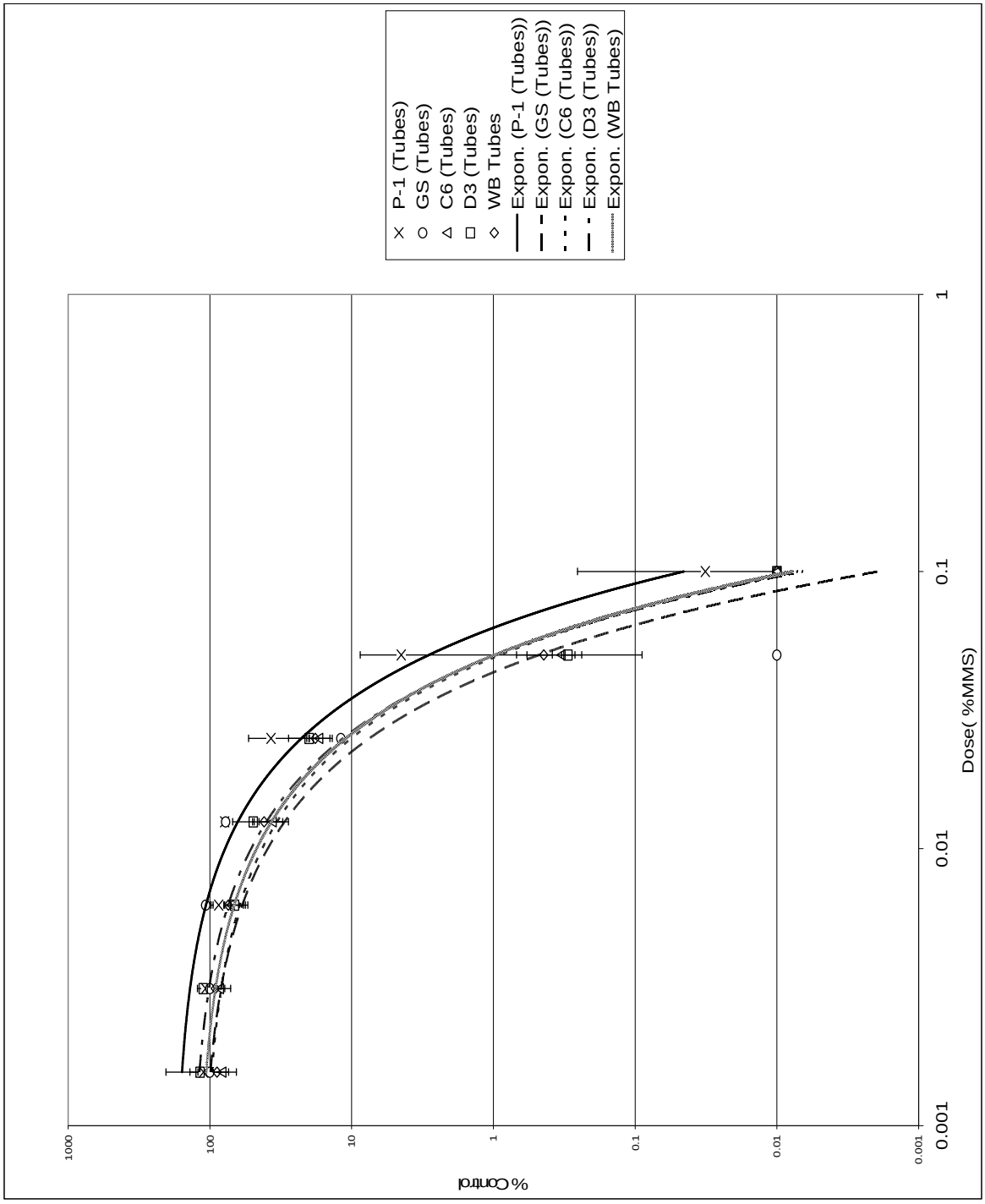

Figure 4. Dose Response Curves of 5 *Giardia* Isolates to MMS (Tube Assay). Standard error bars shown for each point. Trendline generated using Excel.

Figure 5. Dose Response Curves of 5 *Giardia* Isolates to MMS (Plate Assay)

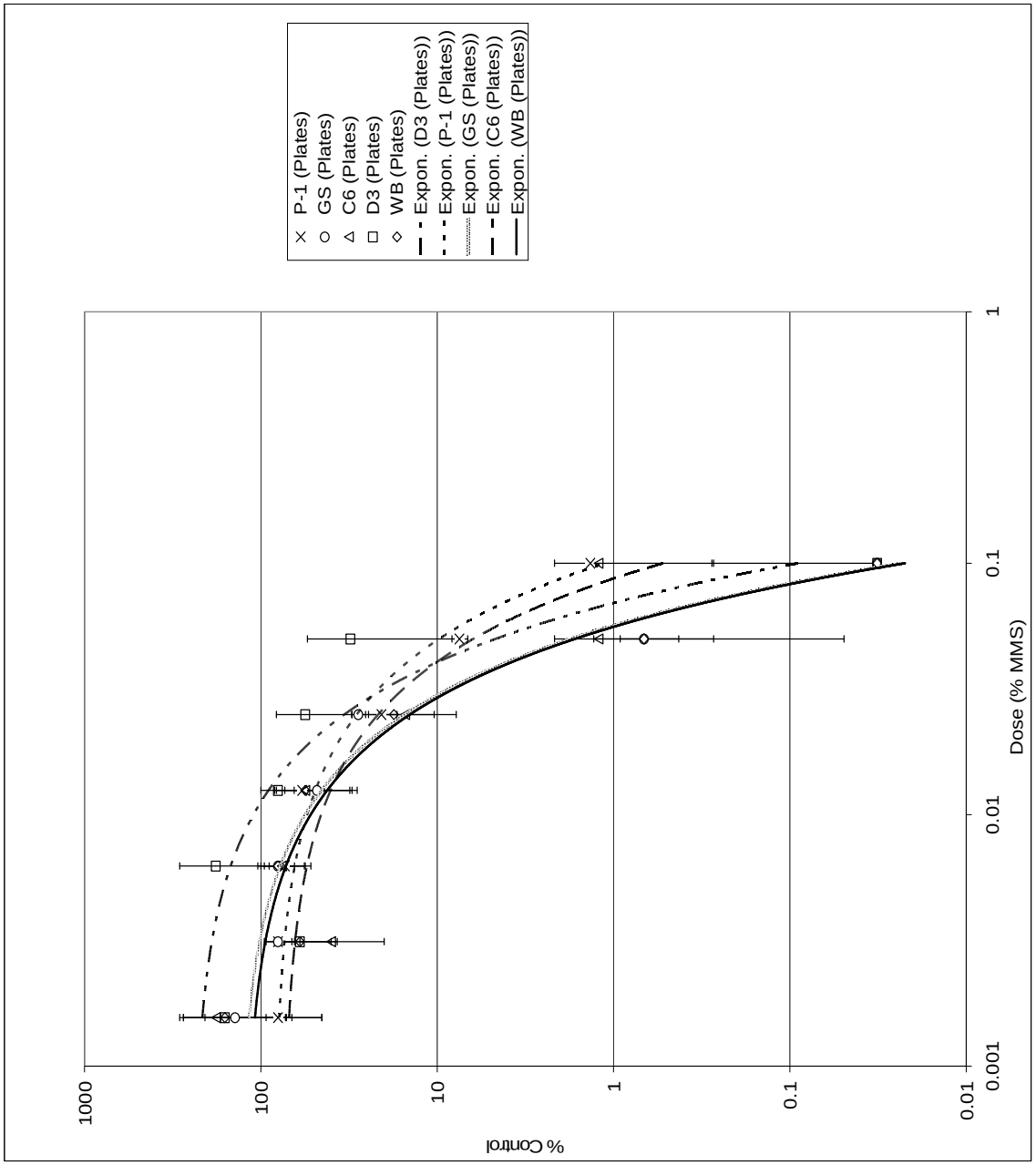

Figure 5. Dose Response Curves of 5 *Giardia* Isolates to MMS (Plate Assay). Standard error bars shown for each point. Trendline generated using Excel.

The plate assay data was compared with the tube assay data for determining the survival curves. The average % sensitivity relative to WB for all of the isolates, was 22.6% for the plate assay and 20.5% for the tube assay. The largest differences were observed in the order of sensitivity as assessed by the two assays. In the tube assay, the GS isolate was determined to be the most MMS sensitive and was 18% more sensitive than WB; however, in the plate assay, GS was determined to be 3% more MMS resistant (Figure 6).

Figure 6. Fold Sensitivity Relative to the WB Isolate

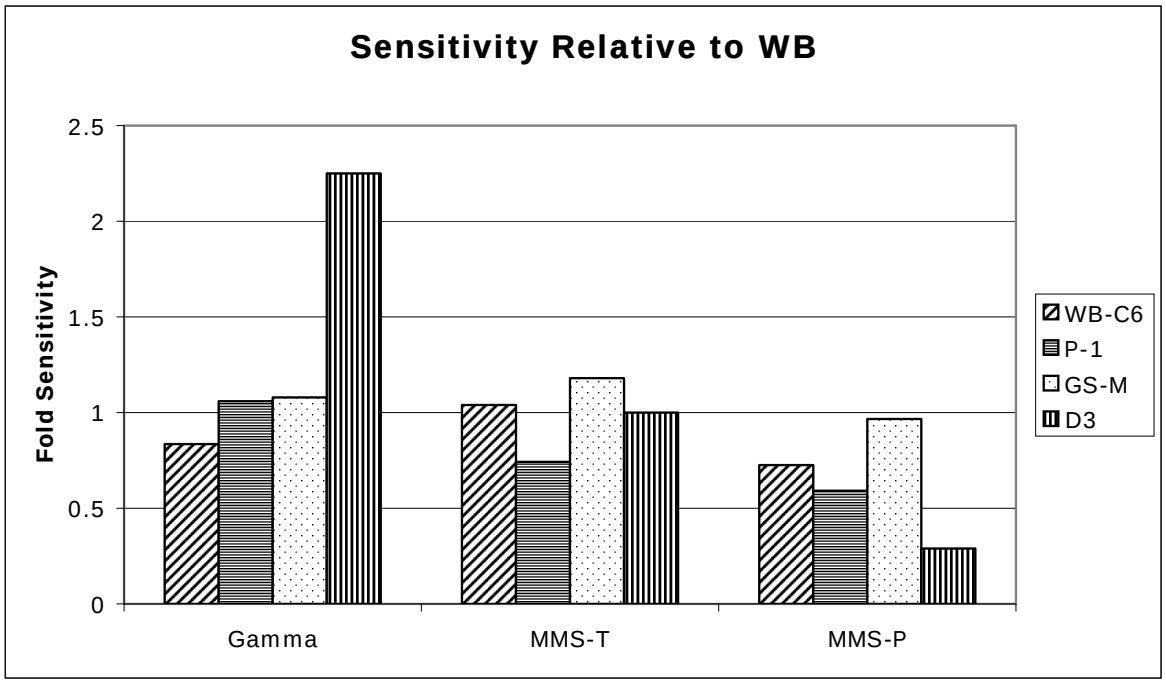

In general, the trend data indicates that the plate assay results gave an overall higher value of resistance as compared to the tube assay. The reason was a bias associated with the sensitivity of the method. The tube assay was more sensitive in measuring the inactivation level due to a larger sample size.

Figure 6. Fold sensitivity of the 5 *Giardia* isolates relative to the WB isolate. A higher number indicates greater sensitivity. MMS-T refers to the sensitivity calculated using the tube assay, while MMS-P was calculated from the plate assay.

The tubes were inoculated with $1x10^6$ trophozoites and the plates were inoculated

with $1x10^4$ trophozoites, leading to the ability of the tube assay to measure a 2 log greater killing than the plate assay. Therefore, by using a greater number of cells to seed the first well and carrying out more dilutions, the plate assay should be just as sensitive as the tube assay in determining inactivation. However, seeding the wells with that high a number of cells would lead to rapid cell death due to crowding. By the media use (10mls/plate of 4 samples in quadruplicate vs 9 mls/one sample-an 18-fold difference) and the amount of time required to make the dilutions and score the results vs direct counting in a hemacytometer, the plate assay is a far more effective way to quickly and, accurately measure inactivation in a statistically significant manner. Also, unlike other published plate assays that depend on a colorimetric measure of metabolic activity, not motility and require a standard curve for each experiment, the use of the Reed and Muench method gives a statistically direct count of the viable cells.

<u>γ irradiation vs MMS sensitivity</u>. Differing trends were observed when comparing isolate sensitivity between γ-irradiation and MMS (Table 4). While the D3 isolate was the most sensitive to γ-irradiation, GS-M was the most sensitive to MMS, as indicated by the tube assay. In addition, the most resistant isolate to γ-irradiation, WB-C6, was one of the least resistant to MMS as indicated by the tube assay. Of additional interest, when comparing sensitivity between WB, and its single cell clone, WB-C6, WB-C6 was more resistant, by 0.15 fold. In fact, this was the only

isolate that showed an increased resistance over the WB control. All other isolates were less resistant. A similar trend was seen with the P-1 isolate, as it was more resistant than the WB isolate at the measured doses of MMS by 0.4 fold (Figure 4). The GS-M isolate (assemblage B) showed very similar γ-irradiation sensitivity to the WB isolate (assemblage A) however, the D3 isolate (assemblage B) was the least resistant compared to the WB isolate. This trend was reversed for MMS, where the D3 isolate was very similar to the control, and the GS-M isolate was the least resistant.

DISCUSSION

. The first result of this study shows that morphological changes do not correlate with survival for irradiated trophozoites. So visual examination after irradiation cannot be used for survival studies. Surprisingly, the doses required to kill trophozoites were much higher than that for cysts. We hypothesize that the metabolically active trophozoites are better able to repair DNA damage and for this reason, are more resistant. In addition, because they were actively growing, in addition to DNA repair, homologous recombination pathways could also repair any DNA damage. The development of assays to evaluate recombination would be useful to providing data for this hypothesis.

Our results also indicate that the 5 isolates have fairly similar sensitivities to the two DNA damaging treatments. However, for some isolates, a significant

difference was observed. In addition, the parasites were different in their sensitivies to MMS vs γ-irradiation. The most likely explanation for the observed results is that the DNA repair systems are different among the isolates. It is well known that the first responses to DNA damaging agents are in DNA repair gene activation and cell cycle control [130]. These responses are further modulated by transcriptional effects and the relative contributions of homologous recombination and DNA end-joining repair pathways. An analysis of pathway differences would help identify the source of our observations. This would also provide additional evidence that the different isolates in addition to the assemblage designations, should be classified as different *Giardia* strains. Both γ–irradiation and MMS treatments generate free radicals [131]. DNA damage is a late effect of free radical-dependent damage [132] with protein and lipid peroxidation targeted first by the damaging agent. The genetic systems dealing with free radicals may also be altered in the various isolates and contribute to the results. A case could also be made that the membrane structures among the different isolates are different enough that the genomes have different protection levels against the DNA damaging agents. However, this is highly unlikely for the γ-irradiation results since γ particles do not have penetration differences in different substrates.

The *Giardia* anaerobic growth requirement is an additional factor to consider. It is known that a decrease in expression of DT-diaphorase confers the ability to grow equally well in aerobic or anaerobic conditions [133]. This would affect free radical formation and other cellular responses. An ability to respond

by encysting could also be a factor in the observed differences. We noticed anecdotally that both the γ-irradiation and MMS treatments did induce some encystation in all of the isolates. This is perhaps highlighted by differences seen with the WB and WB-C6 isolates. WB-C6 is a clone of WB selected for its increased frequency of *in vitro* encystation frequency [134]. An understanding of metabolic differences between these two isolates could also contribute to understanding the results.

The results from this study have a significant impact on risk considerations to *Giardia* infections from environmental sources. It is likely that further sensitivity variations would be found upon examination of other isolates. Suboptimal inactivation protocols, while effective in reducing risk to infection, would also likely select for radiation resistant parasites. Over time this might further increase environmental risks to giardiasis. In addition, since environmental samples have potentially multiple isolates, some non-pathogenic to humans, knowledge of multiple isolate sensitivies might lead to even further need for higher radiation levels in approved protocols.

The survival curves generated for the different isolates in response to the different treatments with DNA damaging agents, for the first time, show statistically relevant data when compared to previous inactivation studies. The ability to rapidly evaluate many more doses and replicates using the plate assay also provides for ease in evaluating various treatments against novel isolates. These studies could easily be expanded for studies of potential antiparasitic

agents as well as other disinfection methods. The results can then be directly compared and evaluated. If specific mutants are generated, the source of the sensitivity differences could be known and used in evaluation of environmental samples. The Reed and Muench quantitation method has long been used for other inactivation studies and is well validated. The adaptation described here for *Giardia* inactivation studies will speed future research without using laborious counting methods that have been the most statistically viable methods reported to date.

LITERATURE CITED

1. **Andrews, R. H., M. Adams, P. F. Boreham, G. Mayrhofer, and B. P. Meloni.** 1989. *Giardia intestinalis*: electrophoretic evidence for a species complex. Int J Parasitol **19:**183-90.
2. **Belosevic, M., S. A. Craik, J. L. Stafford, N. F. Neumann, J. Kruithof, and D. W. Smith.** 2001. Studies on the resistance/reactivation of *Giardia muris* cysts and *Cryptosporidium parvum* oocysts exposed to medium-pressure ultraviolet radiation. FEMS Microbiol Lett **204:**197-203.
3. **Betancourt, W. Q., and J. B. Rose.** 2004. Drinking water treatment processes for removal of *Cryptosporidium* and *Giardia*. Vet Parasitol **126:**219-34.
4. **Campbell, A. T., and P. Wallis.** 2002. The effect of UV irradiation on human-derived *Giardia lamblia* cysts. Water Res **36:**963-9.
5. **Campbell, J. D., and G. M. Faubert.** 1994. Comparative studies on *Giardia lamblia* encystation *in vitro* and *in vivo*. J Parasitol **80:**36-44.
6. **Du, J., and J. M. Gebicki.** 2004. Proteins are major initial cell targets of hydroxyl free radicals. Int J Biochem Cell Biol **36:**2334-43.
7. **Keister, D. B.** 1983. Axenic culture of *Giardia lamblia* in TYI-S-33 medium supplemented with bile. Trans R Soc Trop Med Hyg **77:**487-8.
8. **King, D. A., M. W. Sheafor, and J. K. Hurst.** 2006. Comparative toxicities of putative phagocyte-generated oxidizing radicals toward a bacterium (*Escherichia coli*) and a yeast (*Saccharomyces cerevisiae*). Free Radic Biol Med **41:**765-74.
9. **Lenaghan, S., and C. Sundermann.** 2003. Effect of varying cobalt-60 doses on survival and growth of *Giardia lamblia* trophozoites. J Eukaryot Microbiol **50 Suppl:**701.
10. **Li, D., S. A. Craik, D. W. Smith, and M. Belosevic.** 2007. Comparison of levels of inactivation of two isolates of *Giardia lamblia* cysts by UV light. Appl Environ Microbiol **73:**2218-23.
11. **Li, L., M. Story, and R. J. Legerski.** 2001. Cellular responses to ionizing radiation damage. Int J Radiat Oncol Biol Phys **49:**1157-62.
12. **Li, L., and C. C. Wang.** 2006. A likely molecular basis of the susceptibility of *Giardia lamblia* towards oxygen. Mol Microbiol **59:**202-11.
13. **Linden, K. G., G. A. Shin, G. Faubert, W. Cairns, and M. D. Sobsey.** 2002. UV disinfection of *Giardia lamblia* cysts in water. Environ Sci Technol **36:**2519-22.
14. **Mayrhofer, G., R. H. Andrews, P. L. Ey, and N. B. Chilton.** 1995. Division of *Giardia* isolates from humans into two genetically distinct assemblages by electrophoretic analysis of enzymes encoded at 27 loci and comparison with *Giardia muris*. Parasitology **111 (Pt 1):**11-7.
15. **Mofidi, A. A., E. A. Meyer, P. M. Wallis, C. I. Chou, B. P. Meyer, S. Ramalingam, and B. M. Coffey.** 2002. The effect of UV light on the

inactivation of *Giardia lamblia* and *Giardia muris* cysts as determined by animal infectivity assay (P-2951-01). Water Res **36:**2098-108.
16. **Monis, P. T., R. H. Andrews, G. Mayrhofer, and P. L. Ey.** 2003. Genetic diversity within the morphological species *Giardia intestinalis* and its relationship to host origin. Infect Genet Evol **3:**29-38.
17. **Monis, P. T., G. Mayrhofer, R. H. Andrews, W. L. Homan, L. Limper, and P. L. Ey.** 1996. Molecular genetic analysis of *Giardia intestinalis* isolates at the glutamate dehydrogenase locus. Parasitology **112 (Pt 1):**1-12.
18. **Rand, J. L., R. Hofmann, M. Z. Alam, C. Chauret, R. Cantwell, R. C. Andrews, and G. A. Gagnon.** 2007. A field study evaluation for mitigating biofouling with chlorine dioxide or chlorine integrated with UV disinfection. Water Res **41:**1939-48.
19. **Sauch, J. F., D. Flanigan, M. L. Galvin, D. Berman, and W. Jakubowski.** 1991. Propidium iodide as an indicator of *Giardia* cyst viability. Appl Environ Microbiol **57:**3243-7.
20. **Smith, A. L., and H. V. Smith.** 1989. A comparison of fluorescein diacetate and propidium iodide staining and *in vitro* excystation for determining *Giardia intestinalis* cyst viability. Parasitology **99 Pt 3:**329-31.
21. **Thompson, R. C., and P. T. Monis.** 2004. Variation in *Giardia*: implications for taxonomy and epidemiology. Adv Parasitol **58:**69-137.
22. **Wolfe, M. S.** 1992. Giardiasis. Clin Microbiol Rev **5:**93-100

CHAPTER 4

REAL-TIME REVERSE TRANSCRIPTASE POLYMERASE CHAIN REACTION (RTPCR) ANALYSIS OF REPAIR GENES FROM *GIARDIA LAMBLIA*

INTRODUCTION

Giardia lamblia (syn *intestinalis, syn duodenalis*) is one of the most common causes of waterborne diseases of humans in the U.S. according to recent CDC surveillance reports. Infection with *G. lamblia* cysts causes a gastrointestinal disease known as giardiasis. Giardiasis has been linked to food-borne illness in both the U.S. and abroad ([135]; [136]; [53, 137]). It has been shown that in developing countries, chronic giardiasis can lead to long-term growth retardation, as well as, commonly causing traveler's diarrhea ([138]; [139]; [140]; [141]). *Giardia* has a 2-stage lifecycle with an infective, environmentally resistant cyst stage and a vegetative trophozoite stage that replicates anaerobically in the host's intestinal tract. Although originally discovered by Anton von Leeuwenhoek in 1681, much remains unknown about the basic biology of *Giardia*. What is known is that *Giardia* lacks some key eukaryotic features, including mitochondria, peroxisomes, smooth endoplasmic reticulum, nucleoli, and a true golgi ([142]; [143]; [6]). While these features are lacking, trophozoites do have transcriptionally active nuclei and unique

features such as a microtubular adhesive disc for attachment to intestinal cells, and a median body of unknown function ([37]; [144]; [38]; [36]). *Giardia* was once believed to represent one of the earliest links between the bacterial and eukaryotic lineages, however evidence from molecular analysis now points to a reductionist theory. In 2000, the Giardia Database (GiardiaDB) was introduced, which represented the first completely sequenced genome of Giardia (WB isolate, clone C6) [145]. The GiardiaDB is providing a new avenue upon which to begin more in depth molecular analysis of questions that have long puzzled *Giardia* researchers.

Disinfection issues, particularly in developing countries are another area of Giardia research that has seen progress in recent years. It has long been known that Giardia cysts require relatively high levels of chlorine for inactivation, which explains why swimming pools are still common outbreak sources ([146]; [147]). Other avenues of disinfection have been explored to either complement or replace existing methods. One direction is disinfection using radiation, including both ultraviolet (UV), and gamma (γ)-irradiation. Ultraviolet light at germicidal wavelengths (254-300nm) has been shown to inactivate *Giardia* cysts 4 logs or more ([119]; [128]; [80]). It has been found that *Giardia* is not capable of photoreactivation, the reversion of the cyclobutane dimers produced by UV treatment that causes cell toxicity due to a missing photolyase , which performs this function in most organisms ([118]; [148]; [128]). γ-irradiation has been shown to be effective against both the cyst and trophozoite stages ([67], Lenaghan 2008, Sundermann submitted). The biggest advantage of radiation

methods is their lack of toxic residues. Ozonation, another method that does not result in toxic residues has also become a popular means of disinfection, and in combination with other chemical methods, inactivates *Giardia* cysts at levels nontoxic to humans ([149]; [150]; [49]; [151]). As these various disinfection methods become more popular, it becomes necessary to reevaluate the biological methods used to evaluate *Giardia* disinfection effectiveness. Quantitative evaluation of survival was not determined for most earlier studies, which reported only a qualitative answer to whether or not treated cysts produced diseases in animals. This approach cannot evaluate subtle responses to the disinfection treatments. A method that quantitatively correlates survival between *in vitro* and *in vivo* is needed.

In a previous study we found the optimal levels of both γ-irradiation and methyl methane sulfonate (MMS) that inactivate the trophozoites from 5 *G. lamblia* isolates (Lenaghan 2008). We also determined the UV doses required to inactivate trophozoites for the 5 isolates. These studies showed that significant differences in radiation sensitivity were seen among the isolates. Since these treatments cause DNA damage as their main mechanism of action, an understanding of how DNA damage is processed in *Giardia* is essential to understanding how the different isolates have different sensitivities. Such an understanding is important for determining how to optimize these treatments for disinfection. As a first step, a method to evaluate the *Giardia* DNA repair system response to DNA damage was developed. We then evaluated gene expression differences between control, γ-irradiation, or MMS treated trophozoites.

Representative genes from each major DNA repair pathway were tested along with controls of housekeeping genes and structural genes. The response of each DNA repair pathway after UV and γ-irradiation is evaluated here.

MATERIALS AND METHODS

Trophozoite Cultivation

Giardia lamblia isolate WB trophozoites (ATCC 30957) were used in this study. Trophozoites were cultured as described previously (Lenaghan 2008).

γ-Irradiation

Late logarithmic stage cultures were placed in PBS at a concentration of $1x10^6$ cells/ml, aliquoted into sterile 1.5 ml microfuge tubes and placed on ice. A Cobalt 60 (Co60) source was used to deliver various γ-irradiation doses. The output at the distance used for this work was 7,000 Rad/min or 70 Grey(GY)/min. Doses were determined based on the time exposed to the source. Doses of 78, 156 GY were chosen based on data from a previous study [67]. Trophozoites were kept on ice during irradiation and until all doses were completed. The samples were then added to 8 ml of fresh culture media in glass tubes and placed in a 37^oC incubator. Samples were incubated for 0, 4, 8, 12, 18, 24, 30, and 36 hours before placing on ice to detach viable parasites. Viable cell numbers were determined by hemacytometer counting before the sample was centrifuged at 3,000 X g for 10 minutes and the supernatant removed with a

pipet. 1 ml of Trizol® reagent was then added to the cell pellet and the samples were stored at -20^{o}C until RNA extraction.

MMS treatment.

Parasites grown to a density of approximately 1 X 10^6 cells/ml were incubated on ice to detach the parasites and then centrifuged at 2,000 X g for 10 minutes. The medium was removed with a pipet and the trophozoites resuspended in sterile phosphate buffered saline (PBS) to a final density of 1x10^6 cells/ml and placed on ice. MMS was added to a sterile 1.5 ml microfuge tube to create an initial dilution of 1% in 100 µl PBS and then serially diluted 2-fold in PBS with a final volume of 100 µl in each dilution tube. After warming the tubes to 37^{o}C, 900 µl of the trophozoite suspension was added to create the final concentrations of 0.0125 and 0.00156% MMS respectively, concentrations that give 50 and 10% killing. The tubes were then incubated for 10 minutes at 37^{o}C. Sterile 5% sodium thiosulfate (1/10 dilution) was added to the tubes and incubated for 10 minutes at room temperature to inactivate the MMS. Samples were then diluted into to fresh media and incubated at 37^{o}C. Samples were removed at various times and treated as described above for γ-irradiation.

Primer Design

Oligonucleotides were created for known DNA repair genes found in Giardia by probing Genbank and designing primers using Macvector® (Invitrogen). Table 1 includes forward and reverse primers for each gene tested, as well as, the accession number of the gene. Primers were designed to anneal

at 48^0C and were tested by PCR to ensure that no primer-dimers were present and that primers generated bands of the correct molecular weight.

Table 1. Primers used for rtPCR analysis of DNA repair genes.

Gene Name:	Amplicon:	Forward Primer:	Reverse Primer:	Accession Number:
DMC1b:	(122-397)	TGGCAGATGTCACTCAAAC	TGGATAGTCGCTTCACCTG	XM_001709949
MRE11:	(98-321)	CTACCTGCTTCTTGAGGAG	CTTATCGTTGTTGTCGTGG	AY295093
RAD51:	(141-384)	CCAAGAACAGTATGTCCTCTC	ATCCACTTTTGCCTCTGAC	XM_001709373
MSH2:	(298-564)	TTTGAGGAAAGGAGCGACGG	AGGCGTGTCAGTGAGAATACAGC	AY295098
RAD50:	(651-913)	CGGAGGCGAACTCAAAGACAATAG	GGATAACTCAGGAGAATCGGGTG	XM_001707248
PMS1:	(211-482)	GGATGTGGACTGGACTTATC	CTTTGACGAACAGGGATTG	AY295095
RAD52:	(469-761)	ACTTCAAGGGGCAGTGTTCTTTC	TGTGCTGGCAGATTACCAATGG	XM_001706528
Gamma-Tubulin	(1-250)	ATGTGCGTTTATATTGAAAA	ACATCCTTCCTGTCATTGAA	XM_766625
Ferredoxin		GTTGAGAACCACCCAACAAC	CGCTTGTACGTCTTTTTTGT	XM_001705479.1
FeOut		GTCTCTACTATCGTCAATAA		

Table 1. Primers used for rtPCR analysis of DNA repair genes. Amplicon indicates the region of the target gene that was expressed by the primers. The accession number for each gene was listed and corresponds to Genbank.

Synthesis of cDNA and rtPCR

Total RNA was extracted using the Trizol® Reagent following the manufacturer's protocol. cDNA was synthesized by adding according to the manufacturer's recommendations, ~2 µg to a reaction mixture containing Murine Maloney Leukemia Virus reverse transcriptase (MMLV-RT) (USB) and incubating at 42^{o}C for 1 hour. Fresh MMLV-RT was added after 30 minutes to insure efficient production of cDNA. Equal concentrations of 12-18 oligo(dT) and random hexamer primers (0.5 µg) were used for cDNA synthesis. The concentration of cDNA in each tube was determined with a Nanodrop 1000 spectrophotometer. To ensure that there was no contaminating genomic DNA, primers were designed for the ferredoxin gene (*accession* # XM_001705479.1) that selectively amplified genomic DNA and not cDNA. Ferredoxin is one of the few genes with introns found so far in *Giardia***.** Genomic DNA amplifies with both forward primers, the one starting at the intron, and the one that preceded the intron, whereas cDNA was only amplifies with the forward primer located outside the intron. Real-time polymerase chain reaction (rtPCR) was conducted using the Hotstart-IT^{TM} SYBR® Green qPCR Master Mix (2X) kit (USB), 10nM Fluorescein passive reference dye (USB), 1.0µM primer, and 300 ng cDNA. rtPCR reactions were performed in a iCycler (Biorad) with an initial 95^{o}C for 5 minutes denaturation, followed by 35 cycles of 95^{o}C for 30s, 48^{o}C for 1 min, and 72^{o}C for 30s, and a final 72^{o}C for 5 minutes elongation. Melting curves were generated for each reaction to ensure that only the correct band was amplified.

Levels of genomic DNA in each cDNA sample were quantified in each rtPCR using the ferredoxin primers, and any genomic DNA was subtracted from the cDNA. The α–giardin gene was also used in every plate as a housekeeping gene positive control. The fold induction was calculated using the equation ((cDNA Tx Experimental/cDNA Tx housekeeping)/(cDNA T_0 experimental/cDNA T_0 housekeeping)), where Tx is the experimental timepoint.

RESULTS

MMS and γ-radiation Survival.

Doses response curves for the WB isolate of *Giardia* were generated for both γ-radiation and MMS in a previous study (Lenaghan 2008). Doses leading to 10 and 50% killing were chosen for rtPCR experiments. It was determined that doses greater than 50% were not useful for gene induction studies.

Gene expression after γ-radiation

At the lowest dose of γ-radiation tested, 78 Gy, there was very little induction of DNA repair gene expression. *RAD51* was not induced at any of the experimental time points and levels remained below the housekeeping gene. *MRE11* expression was reduced for the entire time course with a 10 fold decrease at 24 hours. *RAD52* was the only gene expressed above 2.5 fold, gradually increasing from 1.5 to 2.97 fold from 18 to 30 hours. *DMC1b* remained at low levels, but was induced 2.17 fold at 24 hours. All other genes tested remained below a 2 fold induction, *RAD50* 1.33 fold at 18 hours, *PMS1* 1.62 fold

at 18 to 24 hours, *FEN1* 1.48 fold at 24 hours and *MSH2* remained around 1.8 fold for the entire time course (Figure 1). The expression profile of the higher dose of γ-radiation tested, 156 Gy, varied greatly from the lower dose. *PMS1*, *RAD51*, *DMC1b*, and *MRE11* were all expressed below the level of the housekeeping gene. *FEN1* was expressed at the same level as the housekeeping gene and there was a slight induction of *RAD50*, 1.47 fold at 18 hours, and *MSH2*, 1.79 fold at 30 hours. The highest expression induction was seen for the *RAD52* gene, induced 4.85 fold at 4 hours and increased to 7.8 fold at 18 hours before gradually decreasing (Figure 2).

Figure 1. DNA repair gene expression after 78 Gy γ-radiation exposure.

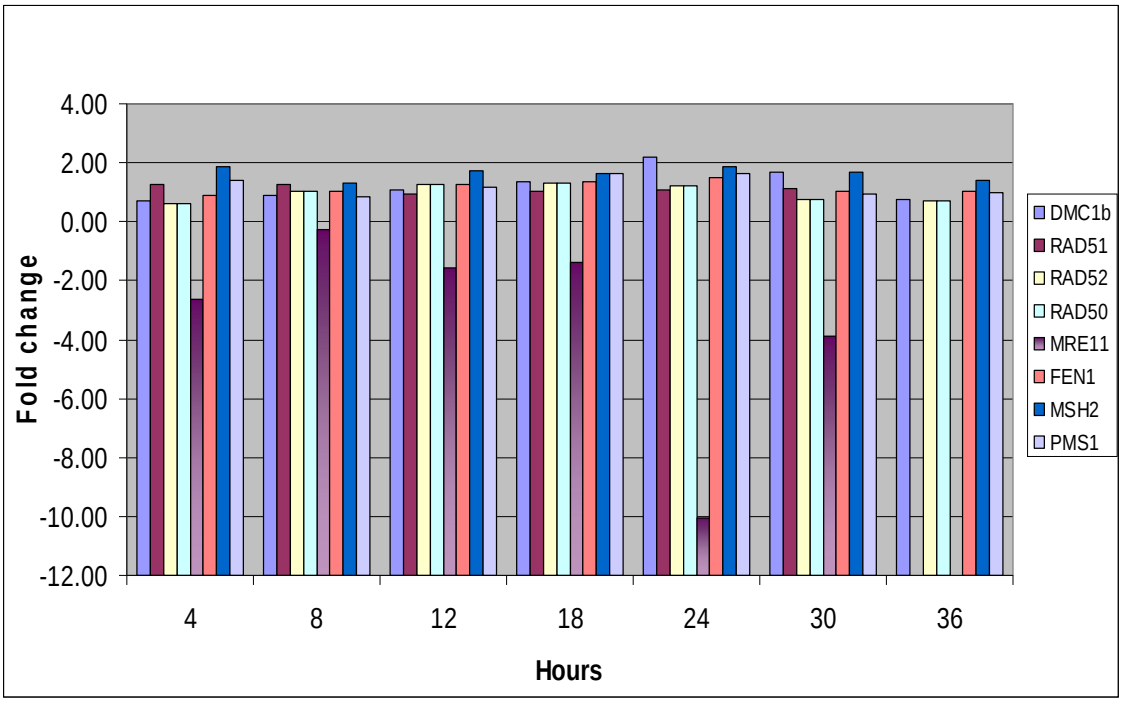

Figure 1. Expression of repair genes after exposure to 78 Gy of γ-radiation. Bars indicate fold change relative to the housekeeping control gene. The 0 time point was omitted since standardization set all genes to 1.0.

Figure 2. DNA repair gene expression after 156 Gy γ-radiation exposure.

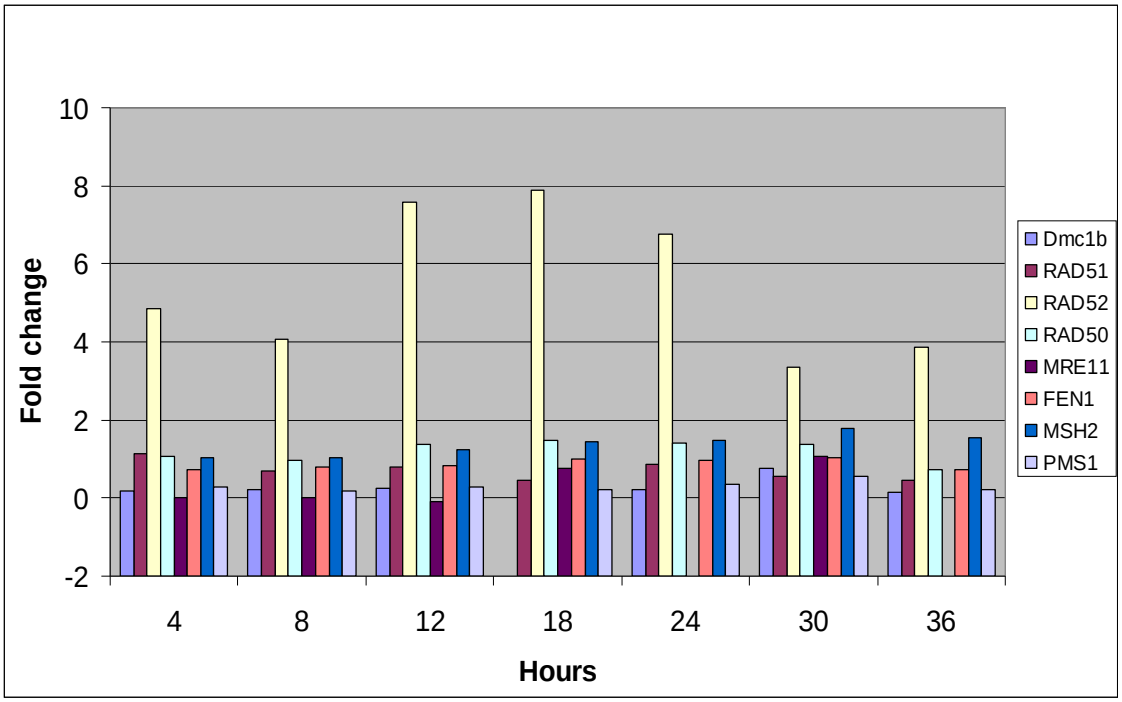

MMS induction

At the lowest dose of MMS, 0.00156%, little induction was seen in the homologous recombination DNA repair genes, *RAD51*, *DMC1b*, and *RAD52* with the highest induction of 1.27 fold. *FEN1* was similarly induced to a maximum of 1.5 fold at 18 hours, but remained lower at all other time points. *MRE11* showed reduced expression to the housekeeping gene at all doses tested and showed a minimal level of -1.3 fold at 36 hours. *MSH2* showed gradual induction from 2.5 to 4.7 fold from 4 to 18 hours, and again from 1.88 to 6.18 fold from 24 to 36 hours. *PMS1* was expressed at a maximum of 2.42 at 36 hours, while *RAD50* gradually increased from

Figure 2. Expression of repair genes after exposure to 156 Gy of γ-radiation. Bars indicate fold change relative to the housekeeping control gene. The 0 time point was omitted since standardization set all genes to 1.0.

2.0 to 3.7 fold from 4 to 18 hours (Figure 3). The higher dose of MMS, 0.0125%, had a different expression profile. Both *DMC1b* and *RAD51* showed decreased expression levels, -9 to -35 fold from 4 to 30 hours for *DMC1b* and -16 fold for *RAD51* at 8 hours, although *RAD51* returned to baseline levels after this time point. All other genes tested were induced above 2 fold. *RAD50*, *FEN1*, *MSH2*, and *PMS1* were all induced at the 24 hours time point to 2.9, 2.95, 2.72, and 3.07 fold respectively. *MRE11* was expressed at levels similar to the housekeeping gene with the exception of the 18 hours time point, which showed a 2.0 fold induction. *RAD52* induction reached a maximum of 2.4 fold at 8 hours and then gradually decreased after this point (Figure 4).

Figure 3. DNA repair gene expression after exposure to 0.00156% MMS

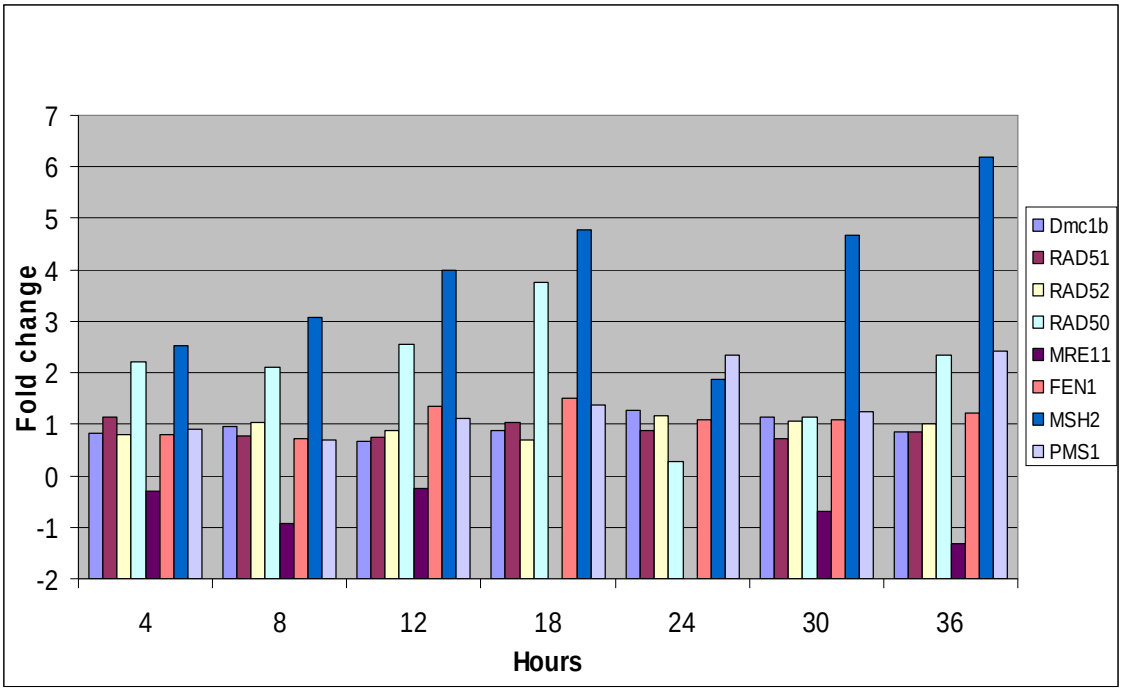

Figure 3. Expression of repair genes after exposure to 0.00156% MMS. Bars indicate fold change relative to the housekeeping control gene. The 0 time point was omitted since standardization set all genes to 1.0.

Figure 4. DNA repair gene expression after exposure to 0.0125% MMS

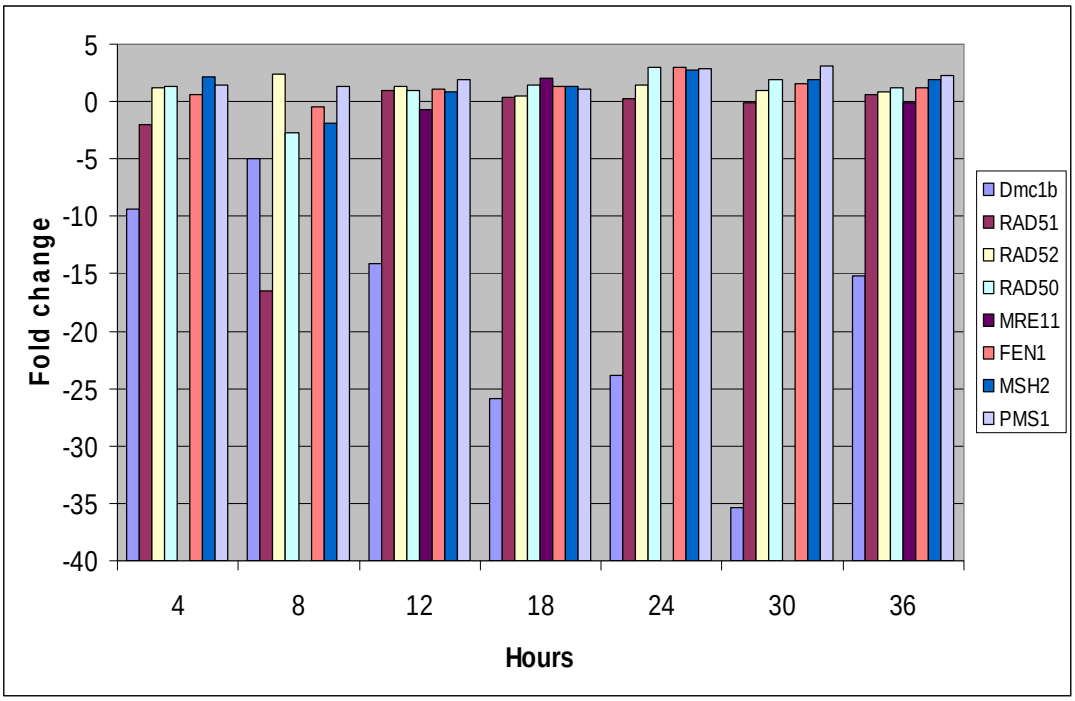

DISCUSSION

As expected, the low doses of both γ-radiation and MMS had very low levels of DNA repair gene induction. This was not surprising, since these doses were equivalent with a low level of killing, ~10%. The higher dose of γ-radiation tested represented ~ 50% killing and stimulated elevated expression of several genes including *RAD52*, which is known to be induced in other eukaryotic organisms. *RAD52* is a key initiator of homologous recombinational DNA repair and the high level of induction, 7.6 fold, may indicate that this repair pathway is active in *Giardia*.

Figure 4. Expression of repair genes after exposure to 0.0125% MMS. Bars indicate fold change relative to the housekeeping control gene. The 0 time point was omitted since standardization set all genes to 1.0.

While *RAD51*, highly inducible homologous recombination DNA repair gene in other model systems, was not induced in either treatment, this can be explained by the debate as to whether this gene is actually a *DMC1* homolog in *Giardia* [152]. It has been reported that *Giardia* does not have a functional *RAD51* and that the gene labeled as such in Genbank may be more closely related to *DMC1*. Since *DMC1* is not inducible in other eukaryotic model systems, the data from this study seems to support a theory that *Giardia* does not have a functional *RAD51* gene. The absence of RAD51 activity would make *Giardia* very unique among eukaryotes, as all other known eukaryotes have one or several copies of the *RAD51* gene. Further studies need to be conducted to determine how homologous recombination DNA repair functions in *Giardia* to determine if another gene may fill the role of the missing *RAD51*.

Both 78 GY and 0.00156% MMS, 10% killing levels, had very low levels of induction with a 2.97 fold induction of *RAD52* for γ-radiation and a 6.18 fold induction of *MSH2* for MMS. This may indicate that different pathways are involved in the repair of γ-radiation and MMS. It appears that the homologous recombination DNA repair pathway is activated the most in response to low levels of γ-radiation and that the mismatch DNA repair pathway is activated the most in response to low levels of MMS. Further evidence for this is the induction of *PMS1* to 2.42 fold after the lowest level of MMS. This pattern is repeated in the higher doses of both γ-radiation and MMS, where *RAD52* is induced to a much higher level, 7.6 fold, in response to γ-radiation, but is not induced beyond 2.4 fold with MMS. *MSH2* and *PMS1* are again induced in response to MMS at

the higher dose, but not in a dose dependant manner. Of further interest is the decrease in levels of both *DMC1b* and *RAD51,* 35 fold and 16 fold, respectively. These genes are both involved in the homologous recombination DNA repair pathway and remain at baseline levels in response to γ-radiation. Another gene induced in response to the highest dose of MMS and not γ-radiation was *FEN1*, which was induced at a constant level of ~2 fold with the greatest induction at 24 hours to 2.95 fold. Based on this data, it appears that different DNA repair pathways are involved in repair of γ-radiation and MMS damage, despite the fact that MMS has been shown to mimic damage from γ-radiation in other eukaryotic organisms. Further testing of a larger population of genes will provide more information as to the mechanisms that *Giardia* uses to repair DNA damage from both γ-radiation and alkylating agents.

LITERATURE CITED

1. Peterson, D.G., B.W. Larson, and J.F. Barlow, *Thirteen month old Caucasian male admitted with extreme pallor.* S D J Med, 1984. **37**(10): p. 15-9.
2. Porter, J.D., et al., *Food-borne outbreak of Giardia lamblia.* Am J Public Health, 1990. **80**(10): p. 1259-60.
3. Robinson, R.D., et al., *Gastrointestinal parasitic infection in healthy Jamaican carriers of HTLV-I.* J Trop Med Hyg, 1991. **94**(6): p. 411-5.
4. Slifko, T.R., H.V. Smith, and J.B. Rose, *Emerging parasite zoonoses associated with water and food.* Int J Parasitol, 2000. **30**(12-13): p. 1379-93.
5. Fraser, D., *Epidemiology of Giardia lamblia and Cryptosporidium infections in childhood.* Isr J Med Sci, 1994. **30**(5-6): p. 356-61.
6. Brodsky, R.E., H.C. Spencer, Jr., and M.G. Schultz, *Giardiasis in American travelers to the Soviet Union.* J Infect Dis, 1974. **130**(3): p. 319-23.
7. Black, R.E., *Epidemiology of travelers' diarrhea and relative importance of various pathogens.* Rev Infect Dis, 1990. **12 Suppl 1**: p. S73-9.
8. Okhuysen, P.C., *Traveler's diarrhea due to intestinal protozoa.* Clin Infect Dis, 2001. **33**(1): p. 110-4.
9. Lujan, H.D., et al., *Developmental induction of Golgi structure and function in the primitive eukaryote Giardia lamblia.* J Biol Chem, 1995. **270**(9): p. 4612-8.
10. Marti, M., et al., *The secretory apparatus of an ancient eukaryote: protein sorting to separate export pathways occurs before formation of transient Golgi-like compartments.* Mol Biol Cell, 2003. **14**(4): p. 1433-47.
11. Xin, D.D., et al., *Identification of a Giardia krr1 homolog gene and the secondarily anucleolate condition of Giaridia lamblia.* Mol Biol Evol, 2005. **22**(3): p. 391-4.
12. Kabnick, K.S. and D.A. Peattie, *In situ analyses reveal that the two nuclei of Giardia lamblia are equivalent.* J Cell Sci, 1990. **95 (Pt 3)**: p. 353-60.
13. Ghosh, S., et al., *How Giardia swim and divide.* Infect Immun, 2001. **69**(12): p. 7866-72.
14. Yu, L.Z., C.W. Birky, Jr., and R.D. Adam, *The two nuclei of Giardia each have complete copies of the genome and are partitioned equationally at cytokinesis.* Eukaryot Cell, 2002. **1**(2): p. 191-9.
15. Bernander, R., J.E. Palm, and S.G. Svard, *Genome ploidy in different stages of the Giardia lamblia life cycle.* Cell Microbiol, 2001. **3**(1): p. 55-62.
16. McArthur, A.G., et al., *The Giardia genome project database.* FEMS Microbiol Lett, 2000. **189**(2): p. 271-3.
17. Jarroll, E.L., A.K. Bingham, and E.A. Meyer, *Effect of chlorine on Giardia lamblia cyst viability.* Appl Environ Microbiol, 1981. **41**(2): p. 483-7.
18. Leahy, J.G., A.J. Rubin, and O.J. Sproul, *Inactivation of Giardia muris cysts by free chlorine.* Appl Environ Microbiol, 1987. **53**(7): p. 1448-53.
19. Linden, K.G., et al., *UV disinfection of Giardia lamblia cysts in water.* Environ Sci Technol, 2002. **36**(11): p. 2519-22.
20. Li, D., et al., *Comparison of levels of inactivation of two isolates of Giardia lamblia cysts by UV light.* Appl Environ Microbiol, 2007. **73**(7): p. 2218-23.

21. Mofidi, A.A., et al., *The effect of UV light on the inactivation of Giardia lamblia and Giardia muris cysts as determined by animal infectivity assay (P-2951-01).* Water Res, 2002. **36**(8): p. 2098-108.
22. Belosevic, M., et al., *Studies on the resistance/reactivation of Giardia muris cysts and Cryptosporidium parvum oocysts exposed to medium-pressure ultraviolet radiation.* FEMS Microbiol Lett, 2001. **204**(1): p. 197-203.
23. Li, D., et al., *Survival of Giardia lamblia trophozoites after exposure to UV light.* FEMS Microbiol Lett, 2008. **278**(1): p. 56-61.
24. Lenaghan, S. and C. Sundermann, *Effect of varying cobalt-60 doses on survival and growth of Giardia lamblia trophozoites.* J Eukaryot Microbiol, 2003. **50 Suppl**: p. 701.
25. Labatiuk, C.W., et al., *Comparison of animal infectivity, excystation, and fluorogenic dye as measures of Giardia muris cyst inactivation by ozone.* Appl Environ Microbiol, 1991. **57**(11): p. 3187-92.
26. Wickramanayake, G.B., A.J. Rubin, and O.J. Sproul, *Inactivation of Giardia lamblia cysts with ozone.* Appl Environ Microbiol, 1984. **48**(3): p. 671-2.
27. Wolfe, M.S., *Giardiasis.* Clin Microbiol Rev, 1992. **5**(1): p. 93-100.
28. Haas, C.N. and B. Kaymak, *Effect of initial microbial density on inactivation of Giardia muris by ozone.* Water Res, 2003. **37**(12): p. 2980-8.
29. Ramesh, M.A., S.B. Malik, and J.M. Logsdon, Jr., *A phylogenomic inventory of meiotic genes; evidence for sex in Giardia and an early eukaryotic origin of meiosis.* Curr Biol, 2005. **15**(2): p. 185-91.

CONCLUSION

The main objective of this dissertation was to determine the feasibility of using γ-radiation as a means of disinfecting *Giardia* for the control of fruits and vegetables. It was determined that a dose of 7 kGy was required to completely inactivate the organism, and lead to complete cellular lethality. At doses below this level, some trophozoites would survive and have the potential to repair. As most disinfection studies focus not on complete lethality, but instead a 2 log or greater inactivation, dose/response curves were generated for 5 isolates of *Giardia* to determine log inactivation. It was observed that all tested isolates from both assemblage A and B had similar levels of inactivation at the log scale, and that in the most resistant cells, a dose of greater than 156 Gy was necessary to achieve 2 log inactivation. MMS was used to compare inactivation from a chemical agent that induces damage in the same manner as γ-radiation. Doses of MMS required to achieve 2 log inactivation were greater than 0.05% MMS demonstrated by both the standard test tube assay, and the novel 96 well plate assay developed in this dissertation as a high-throughput method to determine inactivation.

To determine the mechanism of damage from γ-radiation, ultrastructural observations using a variety of microscopic techniques were employed. It was determined by NIC microscopy that there was no observable damage to trophozoites at doses of less than 7 kGy, and the majority of these trophozoites were motile and retained the ability to attach to glass. Similar results were obtained with scanning electron microscopy, demonstrating no damage at doses below 7 kGy. Through transmission electron microscopy, damage to the cytoplasm in the form of degranulation was observed, along with increased size of peripheral vesicles, and the presence of lamellar bodies in doses of 7 kGy. Although these cells retained there normal shape it was concluded that damage was occurring within the cell. As it was previously known that γ-radiation causes damage to DNA, a variety of genes involved in DNA repair were tested to determine if these genes were inducible in *Giardia*. It was found that several genes including RAD52 and MSH2 were induced as a result of insult from γ-radiation and that the dose received had a direct effect on the levels of induction. Different patterns of induction were seen when compared with MMS treated trophozoites at similar levels of killing. This may indicate that the pathways involved in repair differ between MMS and γ-radiation induced damage.

Research is ongoing to compare the repair pathways of multiple isolates of *Giardia* and determine if differences in these key genes could lead to differences in pathogenesis. Comparisons between UV repair pathways and γ-radiation has also been undertaken in order to determine major repair pathways

in *Giardia*. Elucidation of these key pathways may lead to the creation of more effective drugs, or better means of disinfection.